

# **DEVELOPMENT OF A REPEATABLE DIP MOULDING PROCESS FOR MANUFACTURING POLYMER ARTIFICIAL HEART VALVES**

**LEBOHANG REGINALD MASHEANE**

Dissertation submitted in fulfilment of the requirements of the degree

## **MASTER OF ENGINEERING IN MECHANICAL ENGINEERING**

in the

Department of Mechanical and Mechatronics Engineering  
Faculty of Engineering and Information Technology

at the

Central University of Technology, Free State

Supervisor: Prof. W B du Preez (PhD, Pr Sci Nat)  
Co-supervisor: Mr J Combrinck (MTech: Mech Eng)

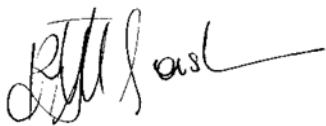
BLOEMFONTEIN

October 2017

## Declaration of Independent Work

---

I, LEBOHANG REGINALD MASHEANE, identity number \_\_\_\_\_ and student number \_\_\_\_\_, do hereby declare that this research project submitted to the Central University of Technology, Free State for the MASTER OF ENGINEERING IN MECHANICAL ENGINEERING, is my own independent work; and complies with the Code of Academic Integrity, as well as other relevant policies, procedures, rules and regulations of Central University of Technology, Free State; and has not been submitted before to any institution by myself or any other person in fulfilment (or partial fulfilment) of the requirements for the attainment of any qualification.



---

**SIGNATURE OF STUDENT**

**23/10/2017**

**DATE**

## Acknowledgements

---

First of all, I would like to give thanks to God Almighty from whom every good and perfect gift comes. He granted me the strength to complete this research project.

I also wish to express my sincere gratitude to my supervisors, Prof. Willie du Preez and Mr Jacques Combrinck for their endless support, guidance and time during this research project. I am privileged to learn from their vast knowledge of product development.

Without the support of the Centre for Rapid Prototyping and Manufacturing (CRPM), the Product Development Technology Station (PDTS), Robert WM Frater Cardiovascular Research Centre, Department of Cardiothoracic Surgery, University of the Free State (UFS), Central University of Technology (CUT), Technology Innovation Agency (TIA) and Lubrizol Europe Coordination Centre, the success of this research project would not been possible. Thanks to these centres and institutions. I would personally like to thank Mr Gerrie Booysen for his continual support and readiness to assist.

Finally, I thank the love of my life, Pelonomi Leeuw, my brother Ronald Masheane and my parents for their patience and support during this study.

## Summary

---

Polyurethane heart valves have been widely studied as possible replacements for mechanical and biological heart valves. To function optimally, these valves have to be free from calcification, require no anticoagulation, function silently and have longevities exceeding those of biological heart valves. The potential widespread use of such valves certainly exists and modern materials and fabrication methods place it within reach. However, polymer heart valves that are available at present are unaffordable for large parts of the population. Therefore, the development of an inexpensive routine production technique for manufacturing of polyurethane heart valves will greatly benefit a very large number of patients in developing and emerging countries. Polyurethane heart valves show favourable physical properties and flow dynamics compared to human heart valves; however, the successful outcome of producing a polyurethane heart valve with the required flexibility, durability and hemodynamic function is often difficult to predict. The design of the mould, the selection of the material and the fabrication method used are key factors that influence the achievement of an acceptable heart valve for use in the human body.

In this study, a repeatable, semi-automated dip moulding process for producing tri-leaflet polyurethane heart valves was developed. An experimental facility was designed and established, as well as an experimental dip-moulding mould, which allowed the selection of an appropriate set of dip-moulding process parameters and mould properties for the routine production of polyurethane valve leaflets with the required physical and mechanical properties. The results obtained from the experimental facility were evaluated with regard to compliance of the relevant properties, namely leaflet thickness, surface topography and mechanical strength, with the requirements of polymer heart valves.

Additive manufacturing of Ti6Al4V (ELI) was used for producing the heart valve frame, sewing ring and mould. By applying the experimentally developed dip-moulding process and using the mould assembly, the valve leaflets were moulded directly onto the valve frame. The first prototype polyurethane heart valves were tested in the pulse duplicator machine of the Robert WM Frater Cardiovascular Research Centre of the University of the Free State. The valves displayed good opening and closing performance, mimicking the behaviour of natural heart valves during the pulse duplicator tests. Although these prototype valves did not meet all the minimum specifications of the ISO 5840 standard, it was clearly demonstrated that with further design improvements it would be possible to produce tri-leaflet valves through dip moulding, which would provide an attractive alternative to the tissue and mechanical heart valves currently used.

## Publications Resulting from this Research

---

1. W.B. du Preez, L. Masheane, J. Combrinck & G. Booysen, Developing a process for manufacturing of a polymer heart valve, 16th Annual RAPDASA International Conference, Roodevallei, Pretoria, 4 – 6 November 2015
2. L. Masheane, W.B. du Preez, J. Combrinck, 2016. Assessment of manufacturability and performance of polyurethane heart valves produced through a locally developed dip-moulding process, Proceedings of the 17th RAPDASA Annual International Conference, VUT Southern Gauteng Science and Technology Park, South Africa, 2 - 4 Nov 2016, ISBN 978-0-620-72061-8

# Table of Contents

Declaration of Independent Work.....	i
Acknowledgements .....	ii
Summary.....	iii
Publications Resulting from this Research .....	v
List of Figures.....	ix
List of Tables.....	xiii
List of Acronyms and Abbreviations .....	xiv
<b>CHAPTER 1: INTRODUCTION.....</b>	<b>1</b>
1.1. Artificial Heart Valves .....	1
1.2. Problem Statement .....	3
1.3. Aim of the Study.....	3
1.4. Objectives .....	4
1.5. Research Methodology .....	4
1.6. The Overview of the Dissertation Layout .....	6
<b>CHAPTER 2: LITERATURE REVIEW .....</b>	<b>8</b>
2.1. Brief Anatomy of Heart Valves .....	8
2.2. Heart Valve Diseases.....	9
2.3. History of Surgical Valve Replacement .....	10
2.3.1. Mechanical heart valves .....	10
2.3.2. Biological heart valves .....	14
2.3.3. Polymeric heart valves.....	17
2.4. Development of Polymeric Heart Valves.....	18
2.4.1. Polymer materials for heart valves .....	21
2.4.2. Fabrication process of PU heart valves .....	24
2.5. Dip Moulding Process .....	27
2.6. Design of Polyurethane Heart Valves .....	29

2.7. Additive Manufacturing.....	31
2.8. Thickness Measurement .....	33
CHAPTER 3: METHODOLOGY .....	34
3.1. Overview of Research Methodology .....	34
3.2. Phase 1: Experimental Dip Moulding Facility .....	36
3.3. Phase 2: Determination of Dip Moulding Process Parameters.....	37
3.3.1. Polymer solution preparation .....	38
3.3.2. Design and manufacturing of an experimental mould.....	40
3.3.3. Measuring the surface roughness of the square moulds .....	41
3.3.4. Manufacture of PCU films through the dip moulding process .....	43
3.4. Characterization of the Films Produced during Phase 2 .....	46
3.4.1. Film thickness measurement .....	46
3.4.2. Mechanical tests.....	47
3.4.3. Optical microscopy .....	50
3.4.4. Scanning electron microscopy .....	51
3.5. Phase 3: Manufacturing of Prototype Polyurethane Heart Valves.....	54
3.5.1. Computer-aided design model of tri-leaflet valve.....	55
3.5.2. Additive Manufacturing of the mould assembly .....	58
3.5.3. Surface finish of the tri-leaflet mould .....	58
3.5.4. Tri-leaflet mould assembly.....	60
3.5.5. Dip moulding of the PCU heart valve.....	61
3.6. Characterization of Dip Moulded Prototype Heart Valves .....	62
3.6.1. Thickness measurement of PCU heart valve.....	62
3.6.2. Surface topography of the PCU heart valve .....	63
3.6.3. Testing of prototype PCU valve in pulse duplicator .....	63
CHAPTER 4: RESULTS AND DISCUSSION.....	66
4.1. Introduction .....	66
4.2. Presentation and Discussion of Phase 2 Results.....	66
4.2.1. Surface roughness measurement of the experimental square mould.....	66



4.2.2. Film thickness measurement .....	68
4.2.3. Optical microscopy observations .....	72
4.2.4. Scanning electron microscopy .....	73
4.2.5. Mechanical properties of PCU film samples .....	76
4.2.6. Recommended dip-moulding parameter set.....	77
4.3. Observation and Analysis of Phase 3 Results.....	77
4.3.1. Surface roughness measurement of the tri-leaflet mould .....	77
4.3.2. Optimisation of dip moulding process parameters.....	79
4.3.3. Measurement of valve leaflet thickness .....	81
4.3.4. Surface topography of the valve leaflet .....	82
4.3.5. Assessment of prototype PCU heart valves in a pulse duplicator machine	84
CHAPTER 5: CONCLUSIONS AND FUTURE WORK.....	89
5.1. Conclusions.....	89
5.2. Future Work .....	90
LIST OF REFERENCES .....	92

## List of Figures


Figure 1.1:	Types of heart valve replacement. (A): Mechanical ball cage valve, (B): Mechanical tilt disc valve, (C): Polymer valve, (D): Tissue valve.....	2
Figure 1.2:	The schematic of research methodology for the study.....	6
Figure 1.3:	Schematic overview of the dissertation.....	7
Figure 2.1:	Cross-section of the heart, showing the location of the four valves of the heart [1].....	9
Figure 2.2:	The first concepts of caged ball valves. (A): Charles Hufnagel valve, (B): Starr–Edwards valve.....	11
Figure 2.3:	Tilting disc design valves. (A): Mono-leaflet (Medtronic-Hall), (B): Bi-leaflet valve (St Jude).....	11
Figure 2.4:	Mechanical valves explanted for severe dysfunction. (A): Pannus ingrowth interacting with leaflet opening, (B): Combination of thrombus formation and pannus tissue growth on the valve, (C): Obstructive thrombosis of a valve.....	13
Figure 2.5:	Biological valves. (A): Hancock porcine valve, (B): Carpentier-Edwards pericardium.....	15
Figure 2.6:	Clinical biological valves failure. (A): Leaflet failed due to wear and tear, (B): Calcification degeneration, (C): Pannus, (D): Endocarditis, (E): Thrombus.....	16
Figure 2.7:	Tri-leaflet polymer heart valve developed by Reul-Ghista.....	19
Figure 2.8:	Description of dip moulding process.....	28
Figure 2.9:	Schematic drawing of Direct Metal Laser Sintering process.....	32
Figure 3.1:	Diagrammatic representation of the full polyurethane heart valve research programme.  Phase 1, Phase 2, Phase 3 and Phase 4.....	34

Figure 3.2:	Schematic layout of the experimental facility used during the dip moulding process.....	36
Figure 3.3:	A diagrammatic representation of the Phase 2 research methodology aimed at determining suitable dip moulding parameters for heart valve production.....	38
Figure 3.4:	Bosch MSM66110 hand blender used in mixing the PC3595A-clear with N, N-dimethylacetamide solvent.....	39
Figure 3.5:	Line drawing of the mould used for producing experimental samples.....	41
Figure 3.6:	The clamping of the mould and surface roughness measurement setup.....	42
Figure 3.7:	Experimental set up for dipping stage consisting of square mould fixed in collet and PCU solution in position for dip moulding.....	44
Figure 3.8:	Shows the FMP40 measurement instrument, FD10 probe and the stand to clamp the mould.....	47
Figure 3.9:	Lloyds LS 100 Plus electromechanical universal testing machine.	48
Figure 3.10:	Samples mounted on nominal gauge and two steel grips.....	49
Figure 3.11:	ZEISS Axio Scope.A1 Optical Microscope.....	50
Figure 3.12:	Preparation of film samples for SEM: (A) Film clamped with two hemostat forceps straight curved stainless steel with locking clamp, (B) Film samples dipped into liquid nitrogen.....	51
Figure 3.13:	PCU film samples prepared for SEM. (A) Film mounted on aluminium pin stubs, (B) Film samples sputter-coated with gold...	52
Figure 3.14:	Scanning Electron Microscopy (Shimadzu SSX 550).....	53
Figure 3.15:	A diagrammatic presentation of the Phase 3 research methodology.....	54
Figure 3.16:	Carpentier-Edwards perimount Magna 19 mm valve.....	55
Figure 3.17:	Technical significant specifications of Carpentier-Edwards perimount Magna 19 mm valve.....	56

Figure 3.18:	Reverse engineering process. (A): Renishaw Cyclone 2 scanner device, (B): Wolf and Beck OTM3M laser scanning on cyclone, (C): Negative silicone halve of the heart valve.....	56
Figure 3.19:	CAD model of exploded view of tri-leaflet mould assembly.....	57
Figure 3.20:	Schematic prediction of stair steps effect on DMLS surface finish model.....	58
Figure 3.21:	Ti6Al4V tri-leaflet mould manufactured with DMLS.....	59
Figure 3.22:	Tri-leaflet mould assembly.....	60
Figure 3.23:	Representation of the thickness measurement sites across a single leaflet.....	62
Figure 3.24:	The ViVitro Labs Model Left Heart pulse duplicator machine.....	64
Figure 4.1:	Surface roughness measurements on square moulds before and after polishing.....	67
Figure 4.2:	Variation of the PCU film thickness for the different measurement points on each face of the mould dipped in a 15% PCU solution...	69
Figure 4.3:	Variation of the PCU film thickness along the measurement points after one, two and three dips in the three PCU solutions....	71
Figure 4.4:	Micrographs of surface structural features produced by a CNC finish experimental mould are observed on the films through OM. (A): Surface facing towards the mould (B): Surface facing away from the mould.....	73
Figure 4.5:	SEM micrographs of the polyurethane film surface topography for the different PCU solutions. (A): 15% solution, film surface facing away from the mould, (B): 20% solution, film surface facing away from the mould, (C): 35% solution, film surface facing away from the mould, (D): 15% solution, film surface facing towards the mould; (E): 20% solution, film surface facing towards the mould, (F): 35% solution, film surface facing towards the mould.....	74

Figure 4.6:	SEM micrographs showing the variation of the surface topography of polyurethane films produced with two moulds of differing surface finish values. (A): Ra = 0.853 $\mu\text{m}$ , (B): Ra = 0.158 $\mu\text{m}$ .....	75
Figure 4.7:	SEM micrographs of the fracture surfaces of films produced with the three different PCU solutions. (A): 35% solution, two dips, (B): 20% solution, three dips, (C): 15% solution, three dips.....	75
Figure 4.8:	Surface roughness measurements on tri-leaflet mould after DMLS finish and MMP technology.....	78
Figure 4.9:	Sample of the valves produced with different dip mould parameters.....	79
Figure 4.10:	Tri-leaflet PU valve produced with dip moulding process without final trimming. (A): Side view of the valve, (B): Top view of the valve.....	80
Figure 4.11:	The SEM micrograph of the leaflet fracture surface.....	81
Figure 4.12:	SEM micrographs of polyurethane leaflet surface topography for different faces. (A): Flat surface of the mould facing away from the mould, (B): Flat surface of the mould facing towards the mould, (C): Curved surface of the mould facing away from the mould, (D): Curved surface of the mould facing towards the mould.....	83
Figure 4.13:	SEM micrograph of the fracture surface of a leaflet produced with a single dip PCU solution.....	84
Figure 4.14:	Polyurethane heart valve captured from the fatigue testing video, (A): Valve fully closed, (B): Valve fully opened.....	84
Figure 4.15:	Percentage regurgitation of three prototypes valves for different beats per minute.....	86
Figure 4.16:	Effective Orifice Area.....	88

## List of Tables

---

Table 2.1:	Summary of polymeric heart valve development.....	19
Table 2.2:	Summary of polymer materials for heart valves.....	22
Table 2.3:	Summary of advantages and disadvantages of fabrication processes.....	26
Table 3.1:	Measuring parameters and conditions.....	41
Table 3.2:	Technical specifications of the MT694 Dual Laser Infrared Thermometer.....	45
Table 4.1:	Measurements of surface finish of the square mould flat surface	66
Table 4.2:	Results of the thickness measurements of the PCU films at the different points on the four faces of the mould dipped in a 15% PCU solution.....	68
Table 4.3:	The recorded thicknesses of the PCU films at the different points on the moulds dipped in the different PCU solutions and for different numbers of dips.....	70
Table 4.4:	Mechanical properties determined for the films produced with the different PCU solutions and different numbers of dips.....	76
Table 4.5:	Surface roughness of tri-leaflet mould before and after MMP technique applied.....	78
Table 4.6:	Thicknesses of the polyurethane leaflets in a high concentrated polymer solvent solution.....	81
Table 4.7:	Pulse duplicator results obtained at different test conditions from three sets of PCU heart valves.....	85

## List of Acronyms and Abbreviations

---

2D	Two Dimensional
3D	Three Dimensional
AS	Aortic Stenosis
AM	Additive Manufacturing
ASTM	American Society for Testing Materials
AV	Aortic Valves
BPM	Beats Per Minute
BHV	Biological Heart Valves
CUT	Central University of Technology, Free State
CRPM	Centre for Rapid Prototyping and Manufacturing
CAD	Computer-Aided Design
CNC	Computer Numerical Control
DMLS	Direct Metal Laser Sintering
DMAc	N, N-dimethylacetamide
EOA	Effective Orifice Area
FDA	Food and Drug Administration
HV	Heart Valve
INR	International Normalized Ratio
ISO	International Organization for Standardization
LS	Laser Sintering
LCD	Liquid Crystal Display
NURBS	Non-Uniform Rational Basis Spline
PCU	Polycarbonateurethane
PDMS	Polydimethylsiloxane
PDTS	Product Development Technology Station
PEU	Polyetherurethane

PHMO	Polyhexamethyleneoxide
POSS	Polyhedral Oligomer Silsesquioxane
PTFE	Polytetrafluoroethylene
PU	Polyurethane
PVA	Polyvinyl Alcohol
SEM	Scanning Electron Microscopy
SIBS	Poly(styrene-block-isobutylene-block-styrene)
STL	Standard Triangulation Language
SV	Stroke Volume
TIA	Technology Innovation Agency
TPU	Thermoplastic Polyurethane
UFS	University of the Free State



# CHAPTER 1: INTRODUCTION

---

## 1.1. Artificial Heart Valves

Heart valve implants are prosthetic devices designed to replicate the function of the natural valves of the human heart [1]. The human heart contains four valves, namely the tricuspid valve, pulmonic valve, mitral valve and aortic valve [2][3]. Their main purpose is to maintain unimpeded forward blood flow through the heart and from the heart into the major blood vessels connected to the heart, into the pulmonary artery and into the aorta [4]. As a result of a number of diseases, both acquired and congenital, any one of the four heart valves may malfunction due to a number of acquired and/or congenital diseases, resulting in either impeded forward flow (stenosis) or backward flow (regurgitation) [2][4]. These heart diseases burden the heart and may lead to serious problems that could result in a heart failure [5][6].

Artificial heart valves have been developed over more than six decades. Nowadays, they represent the most widely used cardiovascular devices. Heart valves manufactured from polyurethane (PU), which is a biocompatible material, have shown good performance in terms of resistance to thromboembolism and structural deterioration. However, there still exists a need to further improve the material properties, design of the valve and manufacturing process so that even more acceptable and affordable PU heart valves can be produced.

Artificial heart valves are classified into three categories based on their mechanism or the material of fabrication, as shown in Figure 1.1:

- Mechanical heart valves

Modern mechanical valves can last over 25 years in an accelerated valve wear tester. However, all current mechanical heart valves require lifelong treatment with blood-thinning anticoagulants which requires monthly monitoring blood tests [7].

- Polymer heart valves

In contrast to mechanical heart valves, polymer heart valves do not require the use of anticoagulant drugs due to the improved blood flow dynamics, resulting in less red cell damage and hence less clot formation. Their weakness, however, is their limited lifespan [7][8].

- Natural tissue heart valves

Traditional tissue valves made from pig heart valves, will last 15 years on average before they require replacement, but will typically have a shorter lifespan in younger patients [5][9].

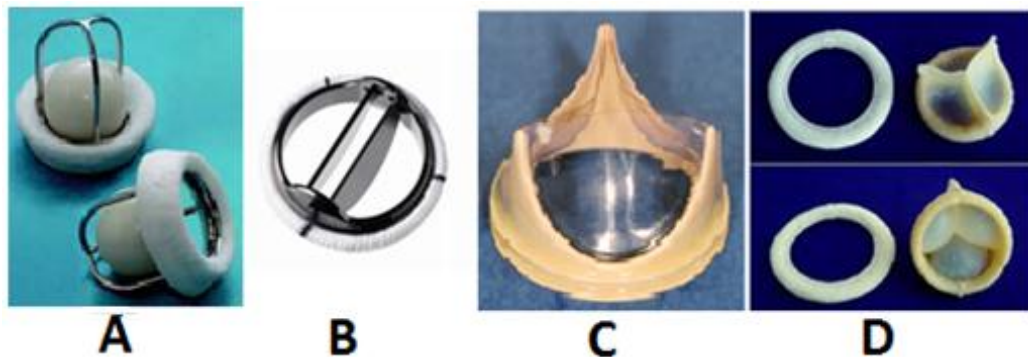


**Figure 1.1: Types of heart valve replacement. (A): Mechanical ball-cage valve, (B): Mechanical tilt-disc valve, (C): Polymer valve, (D): Tissue valve.**

Polymer heart valves have been used over the past 60 years since the first stages of cardiac prosthesis development and advances have been made along with the development of biological and mechanical heart valves [1][5]. Their durability and biocompatibility have been the major limitations that hindered the acceptance of polymer heart valves. However, progress in materials and manufacturing techniques has been leading the way to a better future for these devices and their huge potential [5].

Following on unsuccessful attempts by the Robert WM Frater Cardiovascular Research Centre in the Department of Cardiothoracic Surgery of the University of the Free State, they approached the Centre for Rapid Prototyping and Manufacturing of the Central University of Technology, Free State to develop a reliable and repeatable process for producing polymer heart valves.

## **1.2. Problem Statement**

There is a great demand for heart valve implants [10]. It is estimated that more than 300 000 replacement heart valves are implanted annually worldwide [7]. However, there is still a need for a locally manufactured, cost effective and affordable prosthetic heart valve for patients in developing economies. Such a heart valve should mimic the hemodynamic performance of a native heart valve, which does not require anti-coagulation medication and has a long enough fatigue life to avoid further replacement surgeries. To ensure the durability of polymer heart valves, the thickness (typically 100  $\mu\text{m}$ ) should be very well controlled during fabrication, to avoid thinner weaker sections in the valve leaflets, and the surface finish of the processing mould should result in surface finish of the leaflets that would avoid the negative impact of blood coagulation. A successful development of such a fabrication process would contribute to improve the quality of life for cardiovascular patients in emerging and developing countries through the manufacturing of affordable heart valves.

## **1.3. Aim of the Study**

The aim of this study is to establish a controllable experimental facility, expertise and a proven procedure that will result in a fabrication process for repeatable and reliable production of polyurethane heart valves.

## 1.4. Objectives

- To establish local competence in designing experimental equipment and facilities to manufacture polymer heart valves through additive manufacturing and dip moulding technologies.
- To determine dip moulding parameters and develop a procedure that would enable the production of experimental prototype polymer heart valves.
- To apply the dip moulding procedure for the production of functional prototype polyurethane heart valves that would perform well when submitted to pulse duplicator tests.

## 1.5. Overview of Research Approach

The overview of the research approach can be summarised as follows:

### ➤ Literature survey on designs of artificial heart valves

A literature survey on the existing artificial heart valve designs was performed to select an appropriate heart valve design.

### ➤ Identification of fabrication methods of polymer heart valves

Several types of fabrication methods and materials used for the manufacturing of polymer heart valves were reviewed. An appropriate production method and a suitable material was identified for the fabrication of the polymer heart valves with leaflets meeting the required biomechanical properties.

➤ **Manufacturing and testing of polyurethane films**

Using the selected dip moulding method and a polyurethane material, thin films were produced on an experimental dip moulding mould in an experimental facility. The thicknesses of the manufactured polyurethane films were measured and their mechanical properties were determined by using a tensile testing system. The surface topography of the polyurethane films was evaluated through optical and scanning electron microscopy. Based on these results, a set of parameters for dip moulding of polyurethane heart valves was selected.

➤ **Manufacturing of prototype polyurethane heart valves**

Using the recommended set of dip moulding procedures established for the fabrication of polyurethane films, a tri-leaflet polyurethane heart valve was manufactured. Thicknesses of the moulded leaflets were determined and analysed on scanning electron microscopy.

➤ **Assessment of the performance of the prototype polyurethane heart valves**

The dynamic functioning of the polyurethane heart valves was assessed through pulse duplicator tests to determine the extent to which they met the specifications for such valves.

Figure 1.2 provides a schematic overview of this research approach.

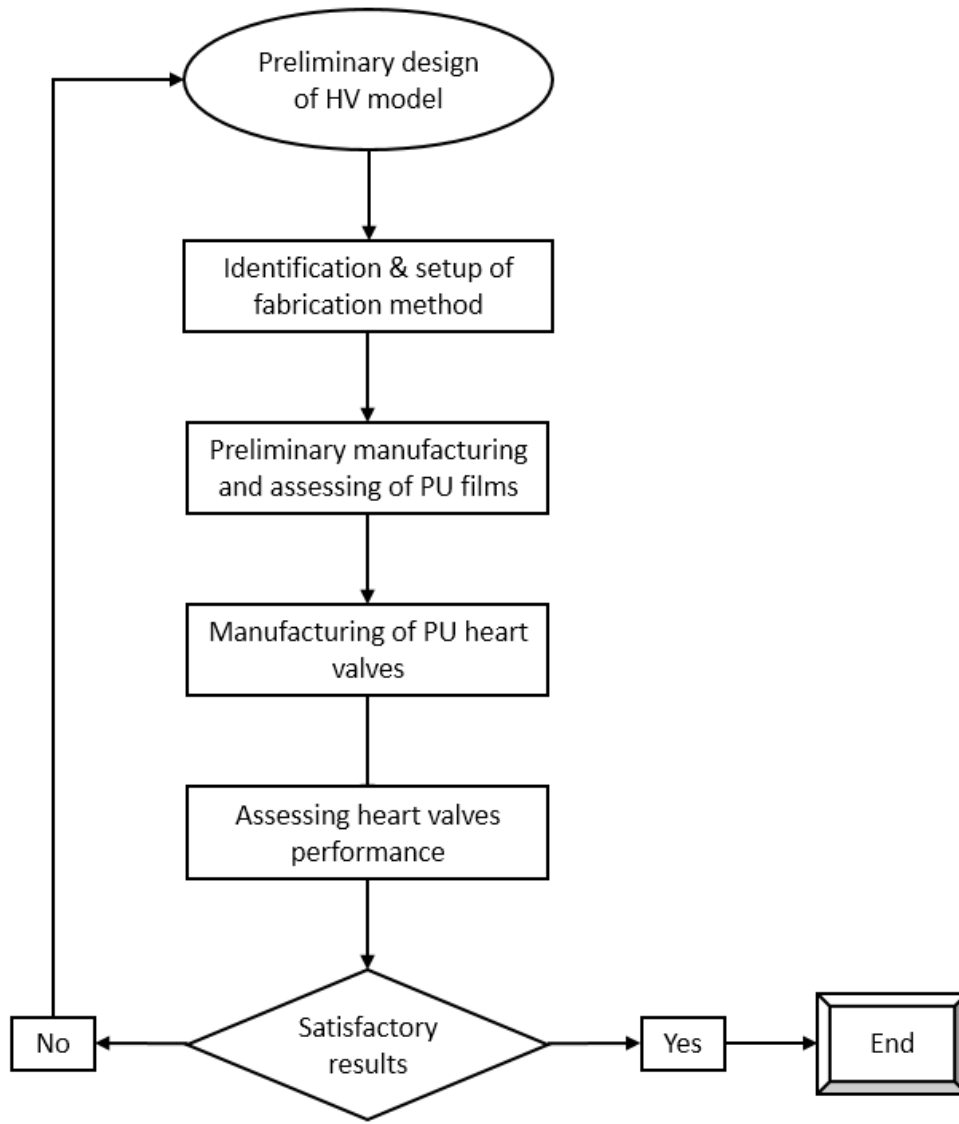


**Figure 1.2: Schematic of the research approach for the study.**

## 1.6. The Overview of the Dissertation Layout

The dissertation layout is summarized in the schematic diagram in Figure 1.3.

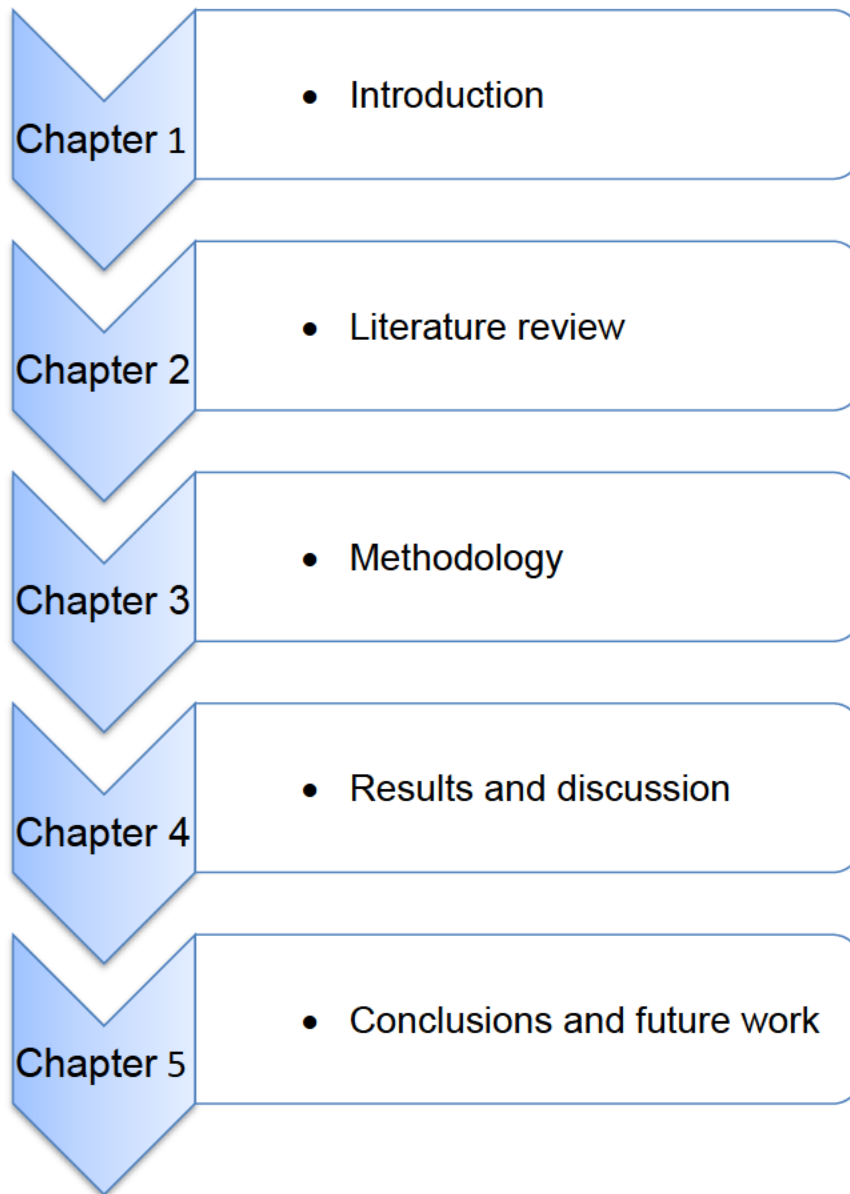


**Figure 1.3: Schematic overview of the dissertation.**

## CHAPTER 2: LITERATURE REVIEW

---

### 2.1. Brief Anatomy of Heart Valves

There are four fluidic control components in the human heart which are responsible for maintaining a unidirectional blood flow during the cardiac cycle. These components were historically considered as passive tissues known as heart valves. The heart valve was believed to perform the function of closing and opening due to inertial forces exerted by the surrounding blood [7]. However, this description does not adequately describe the biomechanical complication of their function as their mechanics are multi-modal and their loading cycle is repeated every second [6][7][11][12].

The mitral and tricuspid heart valves are atrioventricular valves which set out blood from the atria to the ventricles and the two semilunar valves (aortic and pulmonary) ensure blood flows into the arteries leaving the heart (see Figure 2.1) [11]. These heart valves consist of three leaflets which demonstrate distinct biomechanical features at each length-scale and have various functions at different biological levels (such as cell-, tissue- and organ levels, etc.). Each leaflet is a complex and multi-layered structure [6][12].



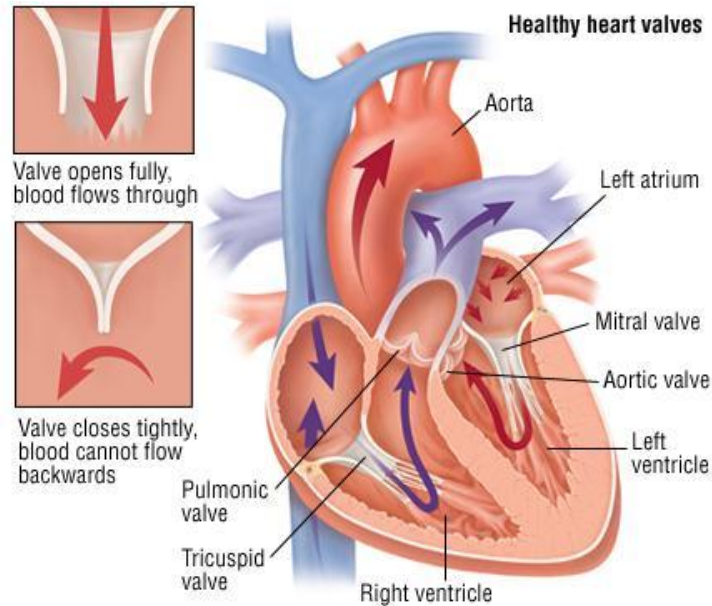


**Figure 2.1: Cross-section of the heart, showing the location of the four valves of the heart [1].**

## 2.2. Heart Valve Diseases

Heart diseases may originate from the malformation in the womb of the cardiovascular organs and/or be acquired along the active lifespan of a person. Any of the valves may malfunction due to a variety of diseases, leading to a possible narrowing, leaking or the valve not closing properly. Such a defect will compromise the normal functioning of a valve, resulting in complications such as potential congestive heart failure and eventual death of the patient if the disease is not treated in due time [7].

In 2015 to 2016, the American Heart Association [13] conducted research on heart diseases. It was found that about 360 000 people died of heart disease in the United States every year. Already in 2003, 19 989 death cases were directly generated by heart valve disease and contributed as the cause of 42 590 deaths [14]. This included 12 471 cases of aortic valve diseases which was found to be the most common cause of the mortality and contributed to 26 336 cases. It was found that 2 759 deaths were caused

by mitral valve disease and it contributed to 6 600 deaths. Pulmonary valve diseases (right side valve) resulted in 11 deaths and 35 contributory deaths, which were significantly less than the tricuspid valve diseases causing 16 deaths and 69 contributory deaths.

The survey indicate that the estimated number of patients worldwide that are in need of heart valves would triple from 290 000 in 2003 to over 850 000 by 2050, based on the population growth and ageing alone [15][16]. It was also reported that in sub-Saharan Africa, parts of Asia and South American, developing and emerging countries, very young individuals suffer from similar diseases leading to premature death when they are still relatively young [15]. These statistics vividly show that heart diseases are threatening the longevity of people all over the world [6]. Heart valve abnormalities are usually treated with medication but in severe cases it may be imperative to proceed with heart valve repair and/or heart valve replacement [7][15][16].

## **2.3. History of Surgical Valve Replacement**

A heart valve can be replaced with either a biological or an artificial valve. These prosthetics are designed to replicate the function of the natural valves of the human heart. Commercially available artificial valves are those that are manufactured entirely from strong durable artificial materials. Biological valves are primarily produced from living tissue and include three porcine aortic heart valve leaflets and bovine pericardium. The biological valves can also be transplanted from donors and from the patients themselves [7].

### **2.3.1. Mechanical heart valves**

There are three basic types of mechanical valve designs: (i) a caged-ball, (ii) a tilting-disc or mono-leaflet and (iii) bi-leaflet design valves, as shown in Figures 2.2 and 2.3 respectively. These valves are commonly manufactured from different artificial

biomaterial such as titanium, cobalt, low-temperature isotropic carbon alloys, Delrin, Teflon, Dacron, etc. [11].

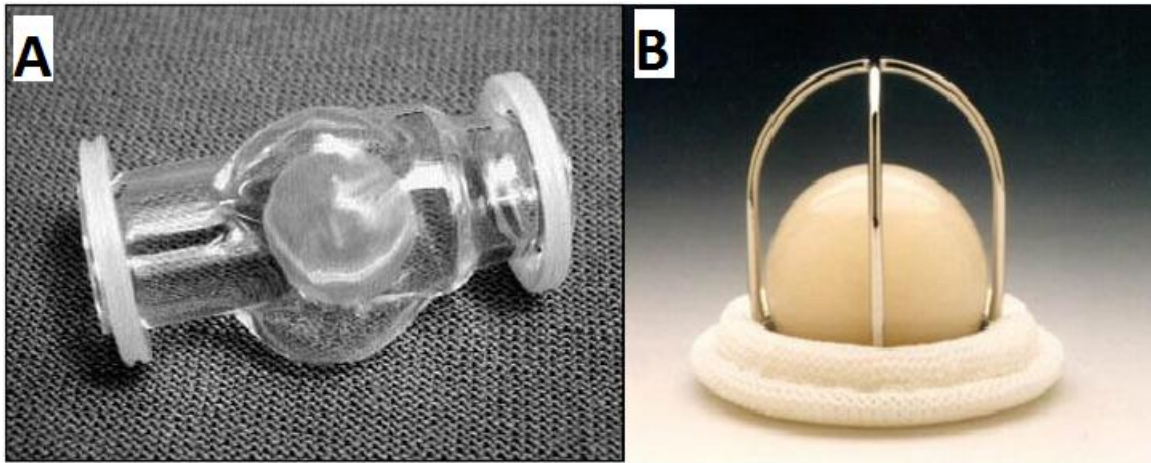


**Figure 2.2: The first concepts of caged-ball valves. (A): Charles Hufnagel valve, (B): Starr–Edwards valve.**

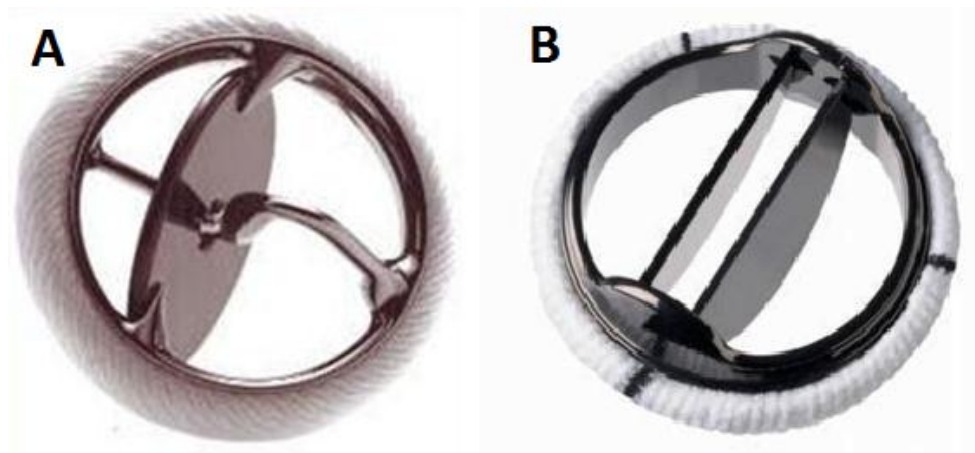


**Figure 2.3: Tilting-disc design valves. (A): Mono-leaflet (Medtronic-Hall), (B): Bi-leaflet valve (St Jude).**

The first mechanical valve in the form of a ball surrounded by a cage was developed by Charles Hufnagel in 1952 [17]. The valve consisted of a Plexiglass (methyl methacrylate) cage containing a ball occlude which was inserted into the descending thoracic aorta

(Figure 2.2 A) [7]. The caged-ball valve shown in Figure 2.2 B was the first mechanical heart valve used as a replacement implant of a mitral valve in 1960. The valve was designed by Starr–Edwards and consisted of a silastic ball with a circular sewing ring and a cage formed by three metal arches (Figure 2.2 B) [7][17]. Ball-cage valves operate similarly to industrial non-return valves allowing fluid to flow only in one direction. When pressure is exerted by the heart onto the blood, exceeding the pressure in the aorta, the ball is ultimately pushed away from the heart. This is the open position of the valve and blood flows into the artery. Similarly, when the heart ejects blood, the pressure inside is significantly reduced which then draws the ball backwards to a closed position of the valve [18].

The caged-ball valves displayed a good durability; however, the blood encountered an obstruction as it pushed against the ball resulting in an extra workload for the heart. This type of valve experienced a larger pressure drop across it in the open position and thus higher mechanical stresses on the valve [7]. The valve also suffered from slow hemodynamic performance and continuous thromboembolism (formation of a blood clot in a blood vessel, called a thrombus that breaks loose and is carried by the bloodstream to plug another vessel). Due to these shortcomings, this type of valves is no longer implanted [17][18][19].

Further studies on developing commercialized valves were conducted to address the poor hemodynamic performance of ball-cage valves. These studies resulted in a tilting-disk valve design. The tilting-disc valves typically comprises of a single- or double-disk secured by an annular metal ring (Figure 2.3). The opening angle of the disk relative to the valve annulus ranges from  $60^\circ$  to  $80^\circ$  and  $75^\circ$  to  $90^\circ$  for mono-leaflet and bi-leaflet design valves respectively, resulting in two and three distinct orifices of different sizes [11][18]. Although these valves resulted in a better hemodynamic performance compared to the caged-ball valves, their main drawback is stent fracture and related complications [20].

Generally, it has been reported that commercially available mechanical heart valves can last indefinitely (the equivalent of over 25 years in an accelerated valve wear tester). However, current mechanical heart valves suffer from thromboembolism and require lifelong treatment with anticoagulation drugs (blood thinners) [11][7]. Figure 2.4 shows mechanical heart valves suffering from thrombosis and pannus tissue overgrowth, often occurring at the base of the valve or at the apex of the cage, leading to stenosis or blockage of the valve.

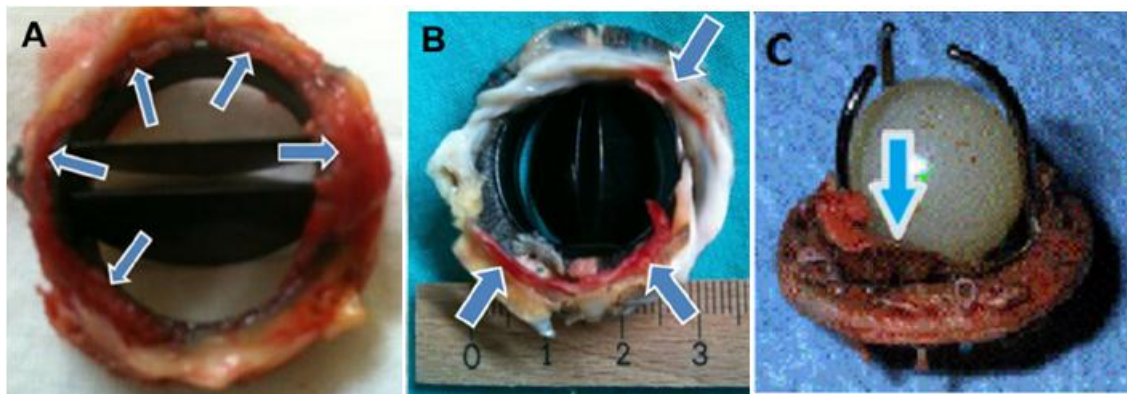


**Figure 2.4: Mechanical valves explanted for severe dysfunction. (A): Pannus ingrowth interacting with leaflet opening, (B): Combination of thrombus formation and pannus tissue growth on the valve, (C): Obstructive thrombosis of a valve.**

According to the literature, the pannus alone (Figure 2.4 A) may be encountered as a slowly progressive obstruction by a subvalvular annulus, which is often difficult to visualize and thus distinguish from progressive structural valve deterioration [20]. Thromboembolism complications are an important cause of morbidity and mortality in patients with mechanical heart valves as shown in Figure 2.4 B and C. In other cases, the thrombosis and pannus are observed in combination and this causes subacute valve obstruction. In the ball-caged valve shown in Figure 2.4 C, the silastic ball sometimes changes colour and dimensions due to lipids insudation leading to a decreased poppet excursion and consequent valve incompetence and thrombus [11][17][20].

It is not always possible to accurately monitor the level of anticoagulation in replacement heart valves since international normalized ratio (INR) clinics are not always in close proximity to patients, especially in developing- and emerging countries, and an uncontrolled anticoagulation process can lead to internal bleeding within the heart [21][22][23]. From medical reports it is clear that these valves are not free from the problems associated with mechanical prostheses in general, that is, lifelong anticoagulation is necessary. In addition, mechanical heart valves have characteristic operating sounds which can disturb patients and constantly remind them of their implant, lowering their quality of life.

### **2.3.2. Biological heart valves**

Biological heart valves (BHV) have been used since the early 1960s, when aortic valves obtained fresh from human cadavers were transplanted to other individuals [18][24]. This type of heart valve is also created from animal donor valves or other animal tissue that is strong and flexible. Most commercially produced BHVs are mounted on and supported by a metal- or plastic stent, typically with three posts (sometimes referred to as struts) surrounded by a sewing cuff at the base. Stents vary in structural design, flexibility and composition [24], as shown in Figure 2.5, which shows different innovations of biological valves. (A): Hancock porcine valve, (B): Carpentier-Edwards pericardium.

Similar to natural valves, BHVs function due to a pressure gradient across the valve. When the blood pressure below the valve is greater than the pressure above, the leaflets are pushed outwards, reversing the curvature and causing the valve to open. When the blood pressure above the valve is greater than the pressure below, the valve closes by pushing the leaflets towards the centre. As the total surface area of the leaflets exceeds that of the orifice, the leaflets overlap in the centre and allow for complete closure of the valve, without leakage [7][15].



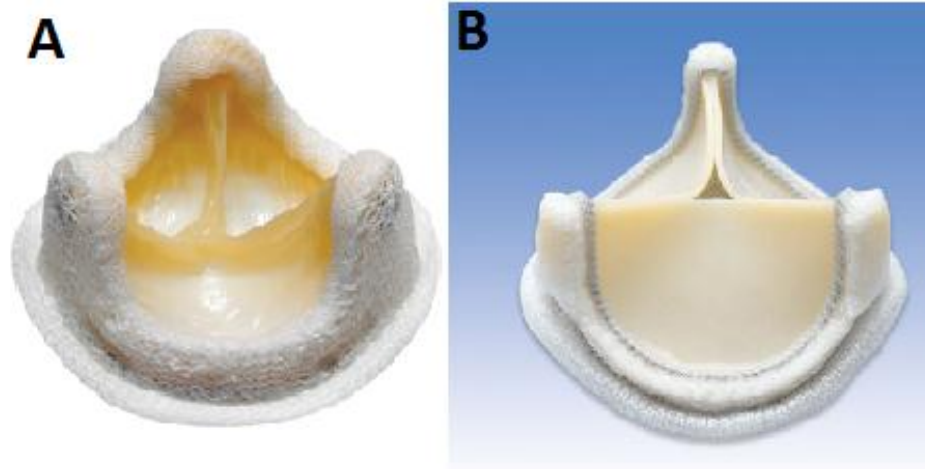


**Figure 2.5: Biological valves. (A): Hancock porcine valve, (B): Carpentier-Edwards pericardium.**

These valves function quite effectively for an average of 12 to 15 years before they require replacement, although typically for shorter periods in younger patients, and usually do not require lifelong anticoagulation treatment. Compared to mechanical valves, they have better hemodynamic properties and resistance to thrombosis due to their similarity to native flexible leaflet valves [25][26].

The main drawback of biological valves is their lifespan. Structural valve dysfunction is caused by progressive valve leaflet wear and tear (Figure 2.6 A), eventuating in regurgitation or stenosis. Pathological specimens showing the most common reasons for biological valve failure as a result of wear and tear, pannus overgrowth, calcification (especially in the young patient), thrombosis, endocarditis and structural valve deterioration are illustrated in Figure 2.6 [27].

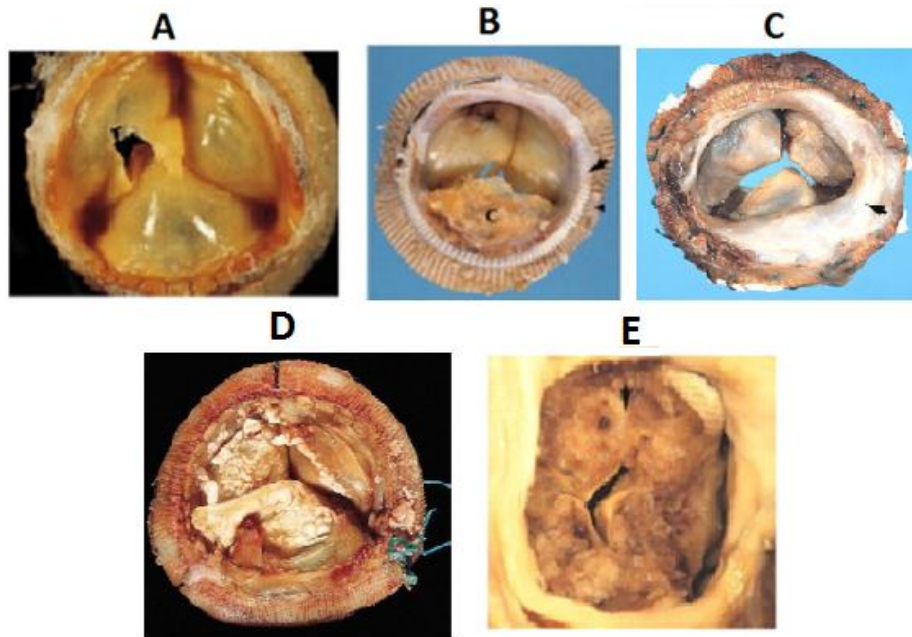


**Figure 2.6: Clinical biological valve failure. (A): Leaflet failed due to wear and tear, (B): Calcification degeneration, (C): Pannus, (D): Endocarditis, (E): Thrombus.**

These valves calcify progressively and rapidly in immature animals, analogous to the accelerated rate of calcification in young patients, and typically develop within the substance of the leaflet flexion where deformation is maximal. Calcification deposits predominate at the commissural tissue adjacent to the stent posts, as shown in Figure 2.6 B [7]. Early pannus (Figure 2.6 C) is composed of myofibroblasts, fibroblasts and capillary endothelial cells and over time pannus calcifies. It has been reported that some pannus formation over the suture is normally expected and functions to form a non-thrombogenic surface. Meanwhile endocarditis and thrombosis occur less frequently than the aforementioned modes of biological failure, occurring at a rate of 1.2% per year and 0.2% per year, as shown in Figure 2.6 D and E, respectively [27][28][29][30][31].

These trends indicate that the majority of implanted valves would have to be explanted after 15 years [28]. A young person with a biological valve would require multiple surgeries to replace the heart valve. This could lead to significant morbidity, such as blood



transfusions, renal failure, wound infection, postoperative pain, delayed recovery and multiple surgeries, which are expensive [32].

During the past 50 years, improvements have been made in the properties of mechanical and biological valves, but it was reported that no significant change in their clinical application had been achieved. The main complications of these valves, such as inefficient functioning and limited long-term durability with the need for anticoagulation and without the ability to be accepted in different types of patients, are still problematic [15]. Consequently, the search for an alternative solution has attracted the attention of many researchers.

### **2.3.3. Polymeric heart valves**

A flexible polymer heart valve design first appeared in 1960. Nina Star Braunwald [15][33] conducted groundbreaking research focusing primarily upon the development of a flexible polyurethane mitral valve. She designed and fabricated a valve using Teflon chordae tendinea, which was implanted initially into dogs. During this time, problems with durability and biocompatibility hindered the acceptance of polymer valves. Despite this early effort, utilization of polymer valves did not emerge at the time due to the success of the Starr-Edwards valve and later prosthetic valves, as well as the subsequent development of safer and effective open surgical and minimally invasive mitral valve repair techniques.

Nevertheless, polymer heart valves have been extensively investigated as possible replacement for mechanical and biological heart valves. Progress in materials and manufacturing techniques of polymer valves has improved the usage of these devices and their potential [10]. A polymer heart valve shows favourable physical properties and flow dynamics compared to human heart valves, however, the outcome of efforts to produce a polymer heart valve with the required flexibility, durability and hemodynamic function is often difficult to predict [7][34][18][35].

This study focused on the development of a polymeric heart valve.

## **2.4. Development of Polymeric Heart Valves**

Polyurethane heart valves have a long history and it has been proven by many researchers that it is difficult to manufacture a flexible polymer valve which is able to withstand the rigours experienced by a prosthetic valve. Polymer heart valves offer the potential to avoid the drawbacks of both mechanical and biological valves. Because of its potential, much research has been conducted on the development and improvement of polymer heart valves. This includes finding a suitable polymer and developing a reproducible and affordable manufacturing process of leaflets with the correct thickness to obtain a durable heart valve which is biocompatible and maintains a satisfactory blood flow [36][16][37].

Different designs of polymer heart valves, primarily comprised of polymers, were tested over the years and were mostly unsuccessful due to material degradation, thrombosis and calcification. Figure 2.7 shows a flexible tri-leaflet heart valve developed by Reul-Ghista using a polymer material that was unsuccessful due to the occurrence of calcification and regurgitation [38].



**Figure 2.7: Tri-leaflet polymer heart valve developed by Reul-Ghista.**

The University of Glasgow, based in Scotland, developed a polyurethane polymer heart valve which was tested extensively up to in vivo sheep trials during 2001 [15]. Even though the valves were implanted to replace the mitral valve, they were reported to have displayed good results. In 2005, the Aortech Polyurethane valves were manufactured, but demonstrated poor hydrodynamics [15][39]. The development of polymer heart valves is summarized in Table 2.1, with the focus on in vivo performance from their emergence in 1960 through the advent of new biostable polymers.

**Table 2.1: Summary of polymeric heart valve development [5][40].**

Valve material	Trial conducted	Clinical results	Location implanted	Reason for failure
PU bi-leaflet	1960	One human implantation resulting in death	Mitral	Arrhythmia
Composite silicon rubber-	1967-1973	20 patient deaths associated with device failure	Aortic	Degradation, fatigue failure and thrombosis

<b>polypropylene fabric tri-leaflet</b>				
<b>Expanded PTFE tri-leaflet</b>	1987	28 dogs, 15 months, experimented with different leaflet thicknesses	Tricuspid	Leaflet stiffening, suture ring dehiscence, strut entrapment
<b>ABIOMED PU tri-leaflet</b>	1983-1993	In vitro test revealed stenotic turbulent flow worse than a THV		Stiff leaflets, narrow orifice
<b>PU tri-leaflet</b>	1987	17 – 21 week sheep studies	Mitral	Calcification, thrombosis, stenosis and regurgitation
<b>PTFE tri-leaflet</b>	1990	12 sheep, 8 – 10 weeks	Tricuspid	Leaflet stiffening, calcification and thrombosis
<b>Leeds PU tri-leaflet valve</b>	1996	In vitro hemodynamics comparison of dip casting versus film fabrication		Method of manufacturing had significant effect on results
<b>AorTech MDI siloxane – PU tri-leaflet</b>	2002	12 sheep, 6 – 9 months	Mitral	No evidence of degradation, thrombosis or calcification
<b>PCU tri-leaflet</b>	2004	14 growing calves, 20 weeks	Seven mitral and seven aortic	Two AV animals died from pannus overgrowth causing severe AS, degradation and calcification observed to a greater degree in AVs but comparably less than in HVs

<b>Innovia SIBS – Dacron composite tri-leaflet</b>	2010	Six sheep	Aortic	Viscoelastic creep in SIBS, Dacron fatigue and calcification, no evidence of SIBS degradation
--	------	-----------	--------	---

The steady lifespan improvements of biological valves resulted in an increased lifespan demand for polymer heart valves. If a polymer valve cannot meet or exceed the performance of biological valves currently on the market, then there would be a limited drive to approve their use in humans. The selection of the material and the fabrication method used to manufacture polymer valves are important factors that influence the implementation of a heart valve for use in the human body. Over the years, a number of researchers developed different polymeric materials and improved on the manufacturing processes for polymer heart valves.

The material and new polymer valve concepts are discussed in the next section.

#### **2.4.1. Polymer materials for heart valves**

The choice of material is a crucial parameter in polymer heart valve development [11]. Extensive research has been conducted to improve clinical results of polymer heart valves. For a polymer heart valve to become a viable alternative in heart valve replacement therapy, the chosen polymer should not only have acceptable characteristics of biostability, anti-thrombogenicity, resistance to degradation and calcification, but also display good endothelial cell affinity. These crucial properties restrict the possible materials for biomedical applications. However, remarkable progress has been made and this has resulted in emerging new materials with improved properties [11][12].

During the past 20 years, new developments of several polymers such as silicone, polyolefin, polytetrafluoroethylene (PTFE) and polyurethanes (PUs) have been tested as

leaflet materials. Silicone was pre-eminently used in the early development of polymer valves due to its biostability, biocompatibility and fatigue resistance. However, valves developed by Mohri et al. from this material showed inadequate durability under prolonged stress with tearing of leaflets [5].

PTFE is a highly crystalline fluorinated homochain polymer with a good biocompatibility. Clinical reports indicated that these valves suffered from thrombosis and leaflets tended to become stiff due to calcification. Regurgitation was observed through holes in some of the valve leaflets [40].

Historically, PUs have been a popular choice of material. Their segmented structure allows for the alteration of the polymer bonds resulting in a material with flexibility and good mechanical properties. Most PUs are thermosetting polymers that do not melt when heated, which restrict the manufacturing techniques, however, elastic melt-processable thermoplastic polyurethanes are also available.

The types of PUs used in heart valve leaflets vary by research group, design and manufacturing process, as shown in Table 2.2.

**Table 2.2: Summary of polymer materials for heart valves [40].**

<b>HV Material</b>	<b>Advantages</b>	<b>Drawbacks</b>	<b>Outcome/comments</b>
<b>Silicone</b>	Good flexibility and biocompatibility	Short durability; distorted and thickened leaflets; tearing; thrombosis formation	Suffered from structural failure and impaired hemodynamic performance and durability
<b>PTFE</b>	Good hemodynamic properties	Low resistance to thromboembolism and calcification; free edge inversion and stiffening of the leaflet	PTFE was found to be unsuitable for developing HVs because of its major complications
<b>PU</b>			
<b>- Polyester urethane</b>	Good viscoelasticity	Susceptible to hydrolysis	Biodegradation and calcification have been the

<b>- PEU</b>	Good resistance to hydrolysis	Low resistance to oxidation	main problems in several in vitro and in vivo studies
<b>- PCU</b>	Good resistance to hydrolysis and oxidation	Prone to calcification	
<b>PVA</b>	Good mechanical properties	Not suitable for dip casting	Mechanical properties were satisfactory but PVA needs to be assessed further for other characteristics
<b>SIBS</b>	Enhanced resistance to hydrolysis, oxidation	Causes platelet activation and thrombogenicity	Having resistance to oxidation and acid hydrolysis, biostability and minimized thrombus, it is a potential material of choice for developing HVs
<b>PDMS–PHMO -PU</b>	Mechanical properties; good resistance to oxidation and calcification	Difficult to manufacture	Showed better long-term stability than PDMS based PU but needs more studies to show the real advantage of this structural modification
<b>POSS–PCU nanocomposite</b>	Excellent resistance to oxidation, hydrolysis and calcification; excellent biocompatibility; anti-thrombogenicity	Not detected yet	Based on potentially improved biocompatibility and biostability, the development of POSS–PCU HVs is currently under investigation

The most widely used types of PU are polyetherurethanes (PEUs) and polycarbonateurethanes (PCUs). Wheatley designed and manufactured a heart valve using PEU with a durability of more than 300 million cycles obtained during accelerated testing [41]. The disadvantage of PEU leaflets for in vivo long-term application is its low biostability, which is mainly caused by its susceptibility to degradation [15].

Jansen and Reul used an aliphatic PCU material, in which the leaflets were formed on a stretched stent in the half-open position for minimizing stresses during both opening and



closing [41]. These valves had low energy losses, and lifetimes (400 and 650 million cycles in vitro durability testing). ADIAM Life Science AG in Germany also developed a valve using the same material for the mitral position [42]. In vitro durability cycles of 600 to a 1000 were achieved, which is equivalent to a life span of 16 to 26 years. However, calcification was localised only at tears and wear-induced defects in the material during in vitro fatigue.

It has been proven that PU-based material has excellent blood compatibility, biostability, hydrodynamic function and durability [5][9][11][42]. However, there have been problems associated with long-term implants, with material degradation, particularly due to oxidation or hydrolysis, causing premature failure of heart valves. PCU has emerged as the recommended material for polymer heart valves and is also being used by the team from Cardiothoracic Surgery at UFS [5][13]. Based on this, polyurethane material was selected for this project.

The physical properties of polyurethanes also depend largely on the process that is used to manufacture the leaflets. These factors include residual stresses which affect the longevity of the leaflets and could cause premature failure and chain degradation [39].

#### **2.4.2. Fabrication process of PU heart valves**

There are several types of fabrication techniques that could potentially be used for producing PU heart valves, such as dip moulding, injection moulding, film fabrication or compression moulding. Several studies have evaluated the impact of different fabrication techniques on the function and durability of the manufactured valves [6][15][35][36]. The dip moulding process involves the use of a specifically designed mould. This mould undergoes a repeatable cycle of being dipped into a polymer solution for moulding a part that can be removed from the mould after the polymer solution has cooled down [14]. Usually this process of manufacturing involves multiple dips into a less concentrated solution.



Heart valves can also be manufactured through the injection moulding process. During the injection moulding process, the granular polymer feedstock is heated until it is soft enough to be injected under pressure into a mould cavity to fill it completely. The valve leaflets are fabricated in the partially open position in a mould. The partially open position permits the leaflets to open easily to a wider angle resulting in an increased effective orifice area (EOA) for a polymer material [15][43].

Thermoforming is a manufacturing process where a plastic sheet is heated to a forming temperature at which it becomes pliable. The sheet is then formed to a specific shape in a mould and trimmed to create a usable product [16]. During the film fabrication technique, the leaflets are produced by solvent-bonding a polymeric film to the valve frame which is fabricated separately. After the leaflets are glued to the frame, the assembly is subjected to a forming process to obtain the desired geometry of the valve [17].

In compression moulding, the process consists of a static assembly (female component) and moving assembly (male component). When these components are closed, hot polymer is injected into the mould cavity to produce the whole geometry of the heart valve. Pressure is applied to force the material into contact with all mould areas and the process is maintained until the moulding material has cured. Table 2.3 provides a summary of advantages and disadvantages of the different fabrication processes used to manufacturing polymer heart valves.

**Table 2.3: Summary of advantages and disadvantages of fabrication processes.**

<b>Fabrication process</b>	<b>Advantages</b>	<b>Disadvantages</b>
<b>Dip moulding</b> [34][44]	<ul style="list-style-type: none"> <li>● Low tooling costs</li> <li>● Short lead times</li> <li>● Ability to vary surface texture without the need for new tooling</li> <li>● Ability to mould complex hollow shapes</li> </ul>	<ul style="list-style-type: none"> <li>● Unable to withstand high temperatures</li> <li>● Large parts are difficult to dip mould</li> <li>● Difficult to control the dimensions of outer surfaces</li> </ul>
<b>Injection moulding</b> [45][46]	<ul style="list-style-type: none"> <li>● Can form complex shapes and fine details</li> <li>● Excellent surface finish</li> <li>● Good dimensional accuracy</li> <li>● High production rate</li> <li>● Low labour cost</li> </ul>	<ul style="list-style-type: none"> <li>● Limited to thin-walled parts</li> <li>● High tooling and equipment cost</li> <li>● Long lead time</li> </ul>
<b>Thermoforming</b> [45][47]	<ul style="list-style-type: none"> <li>● Can produce very large parts</li> <li>● High production rate</li> <li>● Low cost</li> </ul>	<ul style="list-style-type: none"> <li>● Limited shape complexity</li> <li>● Limited to thin-walled parts</li> <li>● Scrap cannot be recycled</li> <li>● Trimming is required</li> </ul>
<b>Film fabrication</b> [48]	<ul style="list-style-type: none"> <li>● Less processing time</li> <li>● Potentially lower cost</li> <li>● High resin mechanical properties due to solid state of initial polymer material and elevated temperature cure</li> </ul>	<ul style="list-style-type: none"> <li>● Expensive to manufacture and install the mould</li> <li>● Difficult to clean and maintain</li> </ul>
<b>Compression moulding</b> [43]	<ul style="list-style-type: none"> <li>● Smoother cavity surface permits easier flow of solution and better surface finish</li> <li>● Lower tooling cost</li> <li>● Good for small production runs</li> </ul>	<ul style="list-style-type: none"> <li>● Difficult to justify for small quantities</li> <li>● Poor product consistency</li> <li>● Difficult in controlling flashing</li> <li>● Slower process times</li> <li>● Mould can be damaged</li> </ul>

- |  |   |  |
|--|---|--|
|  | <ul style="list-style-type: none"><li>• No gates, sprues or runners</li></ul> |  |
|--|---|--|

Corden et al. showed valves manufactured using the dip moulding process resulted in a 31 % reduction of open leaflet bending strain compared to valves manufactured from solvent or polyurethane cast sheets [48]. The increased durability of dip moulded valves compared to thermally formed film fabricated leaflets was also verified by Leat and Fisher, although no significant difference was found in the hydrodynamic functioning of the valves between the two manufacturing methods [40][49][50].

The dip moulding process was found to produce heart valves with improved leaflets in comparison to valves manufactured from film fabrication, injection moulding, compression moulding and thermoforming [16][51]. However, low reproducibility, long- term manufacturing time and undesirable thickness distribution in the leaflets may limit the practicability of this method.

## 2.5. Dip Moulding Process

This is one of the oldest commercially applied coating processes which operates by the thin film deposition of various liquid chemical solutions [52][53]. The dip moulding process produces a part with internal dimensions and shape identical to the external dimensions of the mould. Because there is no shrinkage during the process, extremely accurate internal dimensions are produced with free flow dimensions on the exterior surface [52]. At first glance, this dip moulding process is rather simple; however, deeper understanding of the process parameters needed for heart valve production is required. This will enable a better tailoring of the final films since it is the coating process that serves as an important link between the structure and the liquid solution [8].

During the dip moulding process, illustrated in Figure 2.8, the product is formed over a metal mould fabricated to the desired shape. The mould and liquid (polyurethane) solution

are preheated in an oven to the required temperature (Figure 2.8 stage 1). The mould is then immersed into a liquid solution (stage 2) at a controlled dipping speed. This is followed by a retention time to allow sufficient interaction time for the mould to wet completely with the liquid solution.

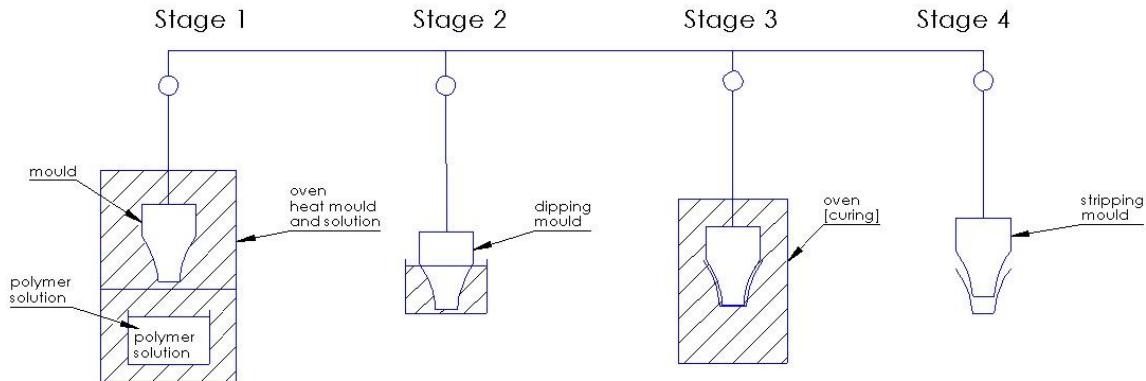


**Figure 2.8: Illustration of the dip moulding process.**

The mould is then withdrawn from the solution at a controlled speed with a thin layer of liquid solution coated or deposited onto it. Excess liquid is allowed to drain from the surface of the mould. After dipping, the mould is placed in an oven (stage 3) to allow the solvent to evaporate from the liquid solution. During the curing process the material cross-links to complete the forming process. This process can be repeated depending on the thickness of material required. The final product is removed from the mould manually, or with compressed air (stage 4).

During the curing process the excess liquid flows across the mould surface under the influence of gravity and ultimately accumulates as a thicker film at the lowest areas. Other factors that can have an influence on the final film thickness distribution that need to be controlled include [34][54]:

- the liquid solution concentration of the particular polymer;
- temperatures of the mould and polymer solution;
- dipping and withdrawal speed;
- retention time;
- curing time and temperature of the polymer solution;
- repeatability of dipping cycles.

The limitations of the dip moulding process are that large parts are difficult to dip mould and it is difficult to control the outer surface thickness of the moulded product [4][41]. Automated dip moulding processes provide high productivity and improved quality due to the accurate control of temperatures and dipping movements [52][53].

## **2.6. Design of Polyurethane Heart Valves**

The valve design is another key factor influencing the haemodynamic performance of a polymer valve; while synthetic material offers the potential to control physical, mechanical and chemical properties to an extent not possible with biological material. The first step for the design of a polyurethane valve is to have the geometry of the natural valve. However, it has been reported that creating a synthetic leaflet valve with similar structure to the native valve does not essentially result in optimum function. In contrast to polymeric valves, the native valves are comprised of different layers of biological tissue with different degrees of anisotropy and mechanical response [34].

There are different types of polymer valve design configurations, however the tri-leaflet structure has superior stress distribution characteristics compared to bio- or quatro- leaflet valves [3][7][9]. The central flow of a the tri-leaflet valve also results in improved mechanical efficiency, hydraulic characteristics and flow patterns that cause much less

blood trauma than mechanical valves. Other important parameters that have a significant effect on the valve performance are [7][41][55]:

- the leaflet geometry, especially the thickness of the leaflet (which is found not to be necessarily uniform);
- diameter of the valve;
- width and height of the posts;
- thickness and flexibility of the stent;
- material properties of the leaflet and the stent.

Intensive research through incorporating very thin leaflets have been conducted by a number of researchers [43][50][56]. A polyurethane valve leaflet with a thickness of between 100 – 150  $\mu\text{m}$  improved the trans-valvular pressure gradient characteristics of the valve, resulting in less energy losses [15][57]. A better hydrodynamic function can be obtained by reducing the leaflet's thickness; however, this can result in a valve with a shorter lifespan and durability. Generally, the results from accelerated fatigue tests have been unsatisfactory, with leaflet tears developing within a few tens of millions of cycles. Valves constructed by the Helmholtz Institute located in Aachen, survived over 400 million cycles in durability tests, which is equivalent to approximately 10 years cycling at physiological rates [15][36][41].

Most tri-leaflet valve designs require a supporting frame or stent. The frame may be titanium or titanium-alloy, although any implantable metal material may be appropriate, such as stainless steel or cobalt-chromium alloys. Additive manufacturing is a suitable manufacturing process for the manufacture of the frame or stent.

## 2.7. Additive Manufacturing

Additive manufacturing (AM) is defined by both the ASTM and ISO as a process of joining materials to make parts or objects from 3D model data, usually layer upon layer [58]. The part is produced by selective melting of material in the x-y plane to create a layer. In the z-plane the layers are stacked on top of one another, which results in a stair-step effect on inclined or curved surfaces of the product. The surface finish can be improved if the build settings are adjusted to a finer resolution [59]. AM differs from conventional manufacturing processes such as turning, milling, grinding, etc., which are subtractive, meaning that material is removed in the form of shavings from the stock material.

AM technologies offer the following advantages:

- reduced lead-times to produce prototype products;
- product visualization in its physical state;
- early detection and reduction of design errors;
- waste elimination and avoidance of costly late design changes;
- ability to plan for assemblies [60].

The AM processes use the following five basic steps to make a prototype or product [61][62].

- i. Design a digital 3D model using a CAD package.
- ii. Convert the CAD model into Standard Triangulation Language (STL) file format. This format converts a CAD part drawing to a set of triangles by tessellating it. The disadvantage is that the part loses some resolution as only triangles, and not true arcs, splines, etc. represent it. However, the errors introduced by these approximations are acceptable as long as they are less than the inaccuracy inherent in the manufacturing process.
- iii. Slicing of the STL file into 2D cross-sectional layers with a typical thickness of 75 to 250  $\mu\text{m}$ , depending upon the AM process. These 2D layers are stacked upon one another resulting in a 3D part. This sectioning approach is common to all

currently available AM processes. Obviously, the thinner the sections, the more accurate the part and longer the time required to build the part.

- iv. Production of the prototype part.
- v. Post processing. This involves removing the part from the machine and detaching any supports depending on the process.

A schematic diagram of the Direct Metal Laser Sintering (DMLS) process is shown in Figure 2.9.

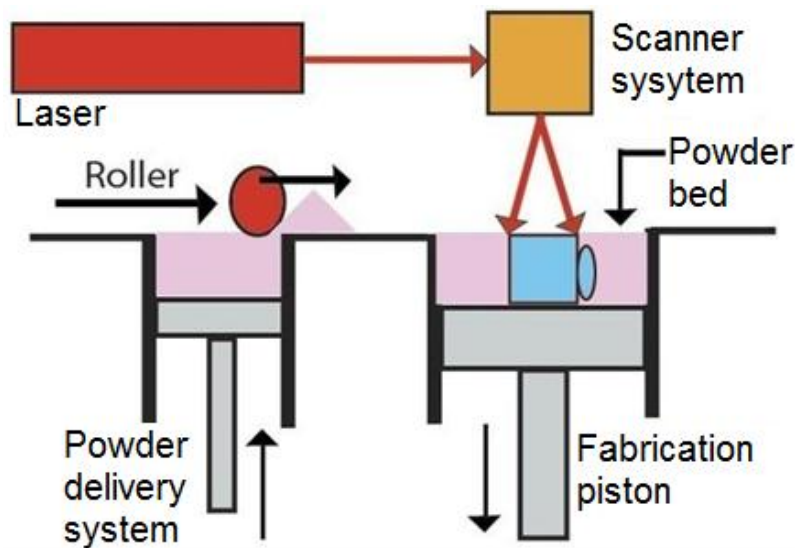


**Figure 2.9: Schematic drawing of the Direct Metal Laser Sintering process.**

This process was used to manufacture the stent, frame and tri-leaflet mould due to its ability to manufacture complex geometries. To produce the valve frame, selective laser melting was used to fuse titanium alloy (Ti6Al4V (ELI)) powder particles into solid layers. Ti6Al4V (ELI) was selected due to its high strength and fatigue resistance and its biocompatibility.



## 2.8. Thickness Measurement

Precise control of leaflet thickness is a critical parameter in development of polyurethane artificial heart valves. Several measuring processes, including microscopy and reflectivity methods, such as profilometry, atomic force microscopy, and X-ray reflectivity, have been developed to measure the thicknesses of thin films in the nanometre regime. However, often measurements should be rapid and non-destructive to determine film thicknesses prior to further surface characterization [63]. This also applies to the current study.

Ellipsometry is a rapid, non-contact, and non-destructive method for probing thickness and refractive index in nanoscale polymer coatings through changes in polarization due to the reflection of light from a surface. This technique is applicable for both ex-situ measurements in air and in-situ experiments in a liquid media. However, like other reflectivity techniques, thickness determinations via ellipsometry are determined by the film's optical properties [63]. Accurate thickness measuring techniques using a mechanical probe (a sharp tip) of either a contact profiler or a scanning probe microscope are also available for this kind of work [64].

## CHAPTER 3: METHODOLOGY

### 3.1. Overview of Research Methodology

In collaboration with the Robert WM Frater Cardiovascular Research Centre in the Department of Cardiothoracic Surgery of the University of the Free State (UFS), a long-term research and development programme was initiated to establish local competence in designing, manufacturing and testing of polyurethane heart valves at a competitive cost with regard to current commercial alternatives. A four-phased approach was adopted for this long-term programme. Figure 3.1 illustrates the research methodology of the complete programme.

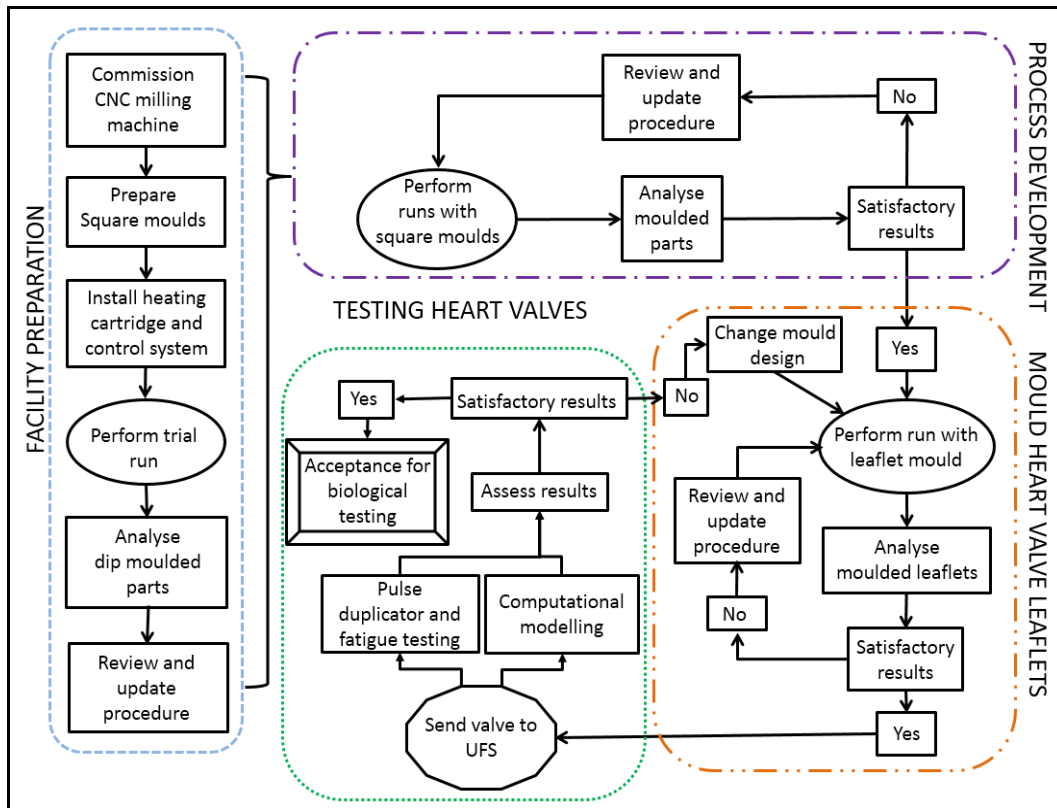


**Figure 3.1: Diagrammatic representation of the full polyurethane heart valve research programme. — — — — Phase 1, — · — · — Phase 2, — · · — · — Phase 3 and · · · · · Phase 4.**

The following outline defines the four-phased approach that was adopted.

- Phase 1 consists of the design and establishment of an experimental dip moulding facility for the determination of the dip moulding process variables.
- Phase 2 focuses on determining a set of dip moulding process parameters and procedures with an experimental mould that would result in controllable and reproducible polymer films with the potential to be used for heart valves.
- In Phase 3, the set of dip moulding parameters and procedures determined during Phase 2 was applied to the actual mould to produce the first functional PCU heart valve prototypes for testing in a pulse duplicator.
- Phase 4 entails producing further prototype PCU heart valves to be tested for functionality and durability in a pulse duplicator and fatigue tester at the UFS. Successful outcome of the testing will lead to the production of PCU heart valve prototypes that will be used for clinical and biological compatibility tests in animals. The Robert WM Frater Cardiovascular Research Centre in the Department of Cardiothoracic Surgery of the UFS will be responsible for conducting these animal trials.

In this study, the project plan was followed through to Phase 3 where the first prototype PCU heart valves were produced and tested in a pulse duplicator at the UFS.

The four phases of the programme are described in detail in the following sections.

### 3.2. Phase 1: Experimental Dip Moulding Facility

For the experimental dip moulding facility, a Computer Numerical Control (CNC) milling machine was converted to function as an automated dip moulding machine. With the spindle of the CNC machine moving in the vertical direction (z-axis), together with the collet holding the mould, the dipping process can be accurately controlled. Experimental moulds with square cross-sections were manufactured and numbered according to the number of dips required per mould. A controllable heating system was developed to preheat these moulds to specified temperatures to influence the viscosity of the PCU liquid material that flows over the four faces of the mould. Figure 3.2 shows the experimental facility used during the dip moulding process.

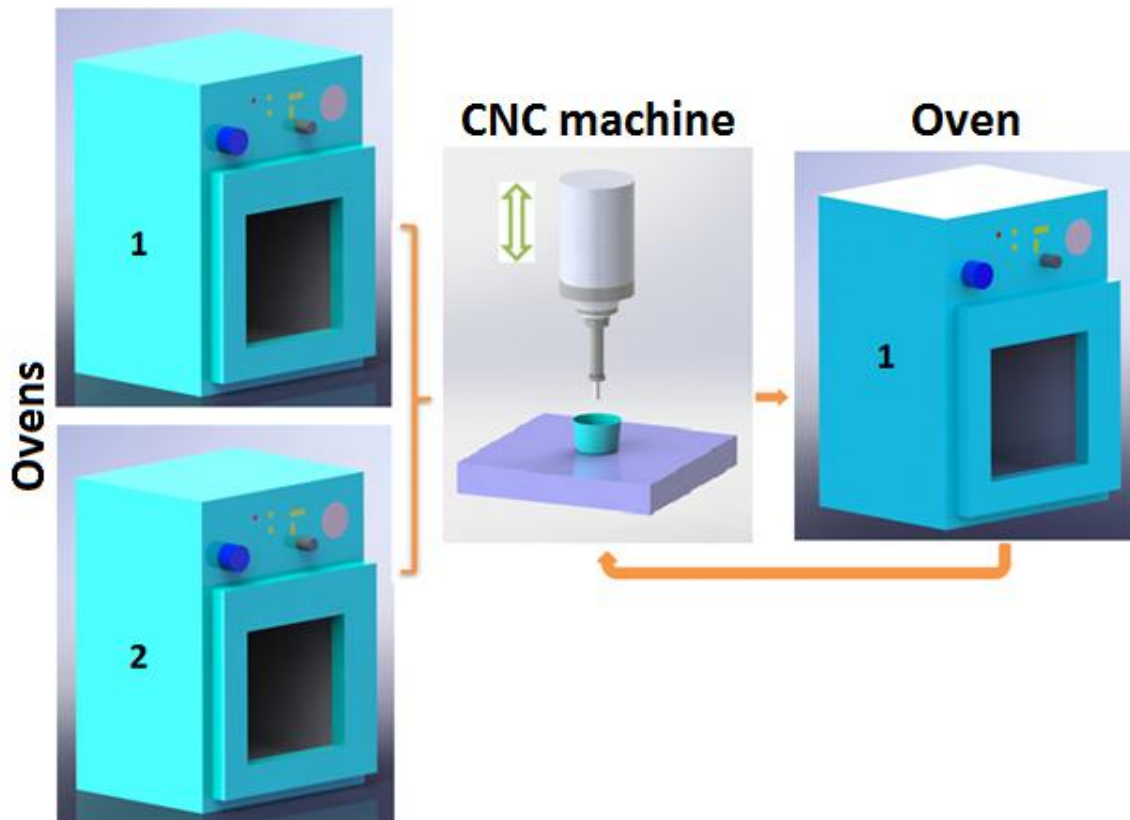


**Figure 3.2: Schematic layout of the experimental facility used during the dip moulding process.**

The mould is placed in the heating oven 1 shown in Figure 3.2 for different periods of time to investigate the mould heating temperature that will provide an optimal viscosity of the PCU solution when the mould is dipped into it. Solutions with the required concentrations are heated in the second oven (oven 2) to dissolve PCU into the liquid solvent completely, allowing solutions with varying viscosities to be prepared. During a dip moulding cycle, the heated mould is placed into the collet of the CNC machine and is dipped into the solution contained in a glass container on the bed of the CNC machine, as shown in Figure 3.2. The entry and extraction speeds during the dipping are controlled by a CNC program. After the dipping process, the mould with the excess solution on its surface is transferred back to oven 1 for curing at a specified temperature. This allows for the evaporation of excess liquid solvent, allowing the PCU to cure. To increase the thickness of the film, the mould with a solidified PCU film, is again clamped in the collet of the CNC machine for a second dipping cycle. This process is repeated until a satisfactory thickness of the film is achieved.

### **3.3. Phase 2: Determination of Dip Moulding Process Parameters**

This phase of the study entailed trials to optimize the dip moulding procedure by using experimental square moulds. Tests were conducted to analyse the effect of different sets of dip moulding parameters. The number of dips was varied to determine the difference in thickness of the moulded material. Tensile tests were conducted on the moulded films to determine their mechanical properties and compare these with the mechanical properties of natural heart valve leaflets. Scanning electron microscopy (SEM) studies were performed on some samples to verify the wall thickness measured using thickness measuring equipment and also to evaluate the surface topography of the film surfaces facing towards and away from the mould.

Figure 3.3 shows a diagrammatic representation of the research methodology used during Phase 2, to determine a set of process parameters suitable for the dip moulding of heart valve leaflets.

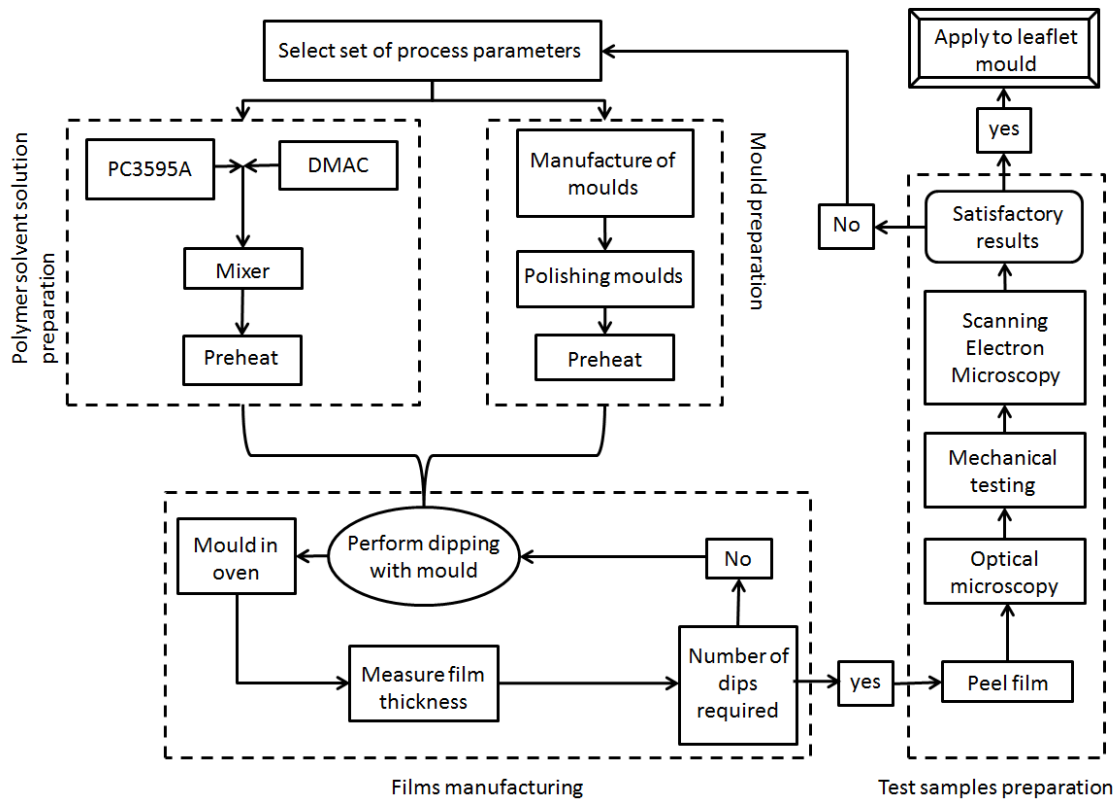


**Figure 3.3: A diagrammatic representation of the Phase 2 research methodology aimed at determining suitable dip moulding parameters for heart valve production.**

Trial runs were performed, the trial samples were analysed and the dip moulding procedure was modified. Once satisfactory results were obtained and an optimised procedure was established, the development proceeded to Phase 3.

### 3.3.1. Polymer solution preparation

Polyurethane is a Food and Drug Administration (FDA) approved thermoplastic polymer for cardiovascular devices. Thermoplastic polyurethane is a biocompatible polymer material with relatively good mechanical properties and good hydrodynamic function. The commercial trademark polyurethane, known as PC3595A-clear, is one of the series of PCUs, which is a family of aliphatic and aromatic polycarbonate-based thermoplastic. In

this study, PC3595A granules were supplied by the Lubrizol Europe Coordination Centre, which is part of the Lubrizol Life Science Group. The granules were dissolved in an N, N-dimethylacetamide (DMAc) solvent to obtain a solution that was used to fabricate polyurethane samples through the dip-moulding process.

The PCU and DMAc constituents were mixed at room temperature in a glass container (Figure 3.4) to obtain a PCU solution with concentrations of 15%, 20% and 35% (w/w). An AWTC 2000 precision balance scale was used to accurately determine the weights of the solution constituents. A blender (Bosch MSM66110 shown in Figure 3.4) with four sharpened winged blades and variable speed settings was used to obtain a homogeneous solution of PC3595A in DMAc.



**Figure 3.4: Bosch MSM66110 hand blender used in mixing the PC3595A-clear with N, N-dimethylacetamide solvent.**

Because the PC3595A-clear does not dissolve quickly in the DMAc solvent, the mixing process was performed for a period of 5 minutes followed by a 30 minutes break to allow quiescent conditions to set in before repeating the stirring of the solution. The process was repeated four times. The homogeneous mixture was stored at room temperature for 12 hours and stirred again before it was placed into an oven at 50<sup>0</sup>C for two hours to obtain the required viscosity for the dip-moulding process.

### **3.3.2. Design and manufacturing of an experimental mould**

For the initial experimental work aimed at determining the optimum dip moulding parameters, an experimental square mould consist of a 20 x 20 mm<sup>2</sup> cross-section and a height of 80 mm was designed, as shown in Figure 3.5. The geometry and dimensions of the mould were determined by the technical specifications of the mechanical testing machine. A 25 mm cylindrical mild steel rod was used for the manufacturing of the experimental square mould. Milling to produce the 60 mm long flat surfaces of the mould was performed along the longitudinal direction (x-axis) of the mould. This practice was beneficial when conducting mechanical tests, since the cutter marks were along the x-axis of the mould. The slot in the mould allowed a cartridge heater to be inserted into the mould to improve the effective viscosity of the moulded material by heating the mould. The four faces of the mould were numbered 1 to 4 and the mould was numbered according to the number of dips required. Figure 3.5 illustrates the CAD design of the experimental square mould used to determine the mechanical properties of the experimental samples.



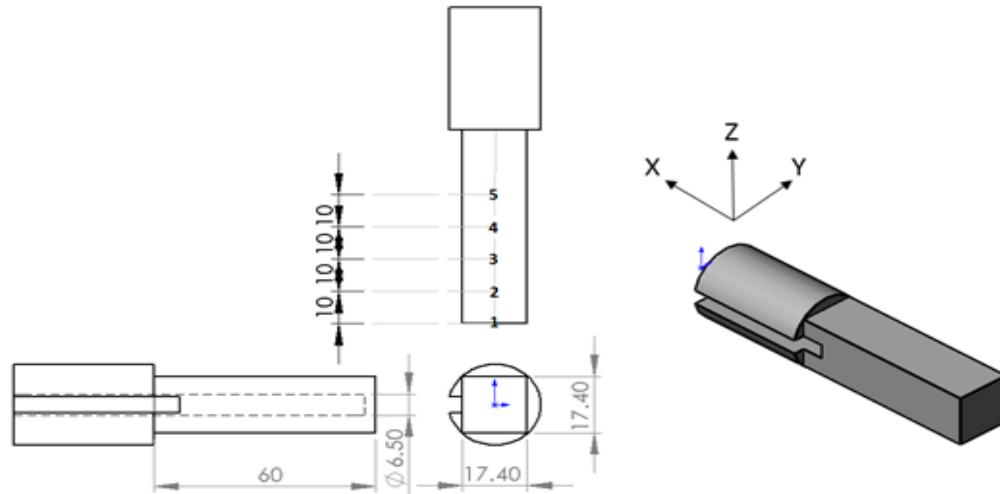


**Figure 3.5: Line drawing of the mould used for producing experimental samples.**

The mould was fixed in a vice for precision and uniform polishing of all four flat surfaces, removing the cutter marks produced during the manufacturing of the mould. A 280- and 600 grit aluminium-oxide polishing stone, bathed in paraffin as lubrication, was respectively applied longitudinally to the mould. When the stone and paraffin rubbed on the surface of the mould, a slurry was formed, which cut and smoothed the surface. For further improvement of the surface finish, 800 grit water sandpaper bathed in paraffin was applied to the polished surfaces. The mould was cleaned with paraffin, sprayed with ethanol to dissolve and remove any dirt and then positioned upright in the oven for preheating at 25°C.

### 3.3.3. Measuring the surface roughness of the square moulds

Surface roughness measurements of the polished moulds were performed using a Mitutoyo SURFTEST SJ-210 surface roughness measuring instrument. The SURFTEST SJ-210 (Figure 3.6) is a portable surface roughness measuring instrument, which traces the surfaces of parts, calculates their surface roughness based on roughness standards and displays the results on a LCD screen.

Because the mould consisted of four flat surfaces, a supporting stand (see Figure 3.6) was manufactured to obtain accurate roughness measurements of the different surfaces. Each surface of the mould was positioned such that it was parallel to the axis of movement of the stylus of the surface roughness measuring instrument. This enabled the stylus to make proper contact with the measured surface while it was tracing across the surface. The surface roughness was measured at three locations on each surface of the mould, i.e. left, middle and right.



**Figure 3.6: The clamping of the mould and surface roughness measurement setup.**

After setting of the desired measurement parameters, such as the cut-off length  $\lambda_c$ , the number of samplings  $N$  and the traversal measuring speed, the measuring instrument was positioned on the stand. The flat surface of the square mould was positioned slightly lower than the detector to bring the surface that must be measured smoothly in contact with the stylus. After the stylus was in contact with the surface flat surface of the mould, the START/STOP button on the control board of the display unit was pressed. The stylus

started to traverse over the surface while an image in a wave form, indicating the irregularities of the surface, was displayed on the LCD screen. When the set traversal length of the stylus was reached, the stylus with the detector returned back to the original position and the results of the measurement were digitally displayed on the LCD screen. Table 3.1 shows the measuring parameters used to obtain the surface roughness values.

**Table 3.1: Measuring parameters and conditions.**

Measuring parameters	Values
Roughness measurement parameter	R <sub>a</sub>
Cut-off value or sampling length, $\lambda_c$ (mm)	2.5
Number of sampling lengths, N	2, 3, 4 and 5
Evaluation length range $l_n = \lambda_c \times N$ (mm)	5 to 12.5
Measurement traversal speed (mm/s)	0.5

#### 3.3.4. Manufacture of PCU films through the dip moulding process

To perform the dip moulding under repeatable controlled conditions, a CNC milling machine was converted to function as an automated dip moulding machine. A DAHLIH MCV 720 CNC machine (shown in Figure 3.7) allowed control of the experimental parameters, such as the vertical travelling speeds and retention time of the mould in the PCU solution. Figure 3.7 shows the experimental set up of the dipping stage.

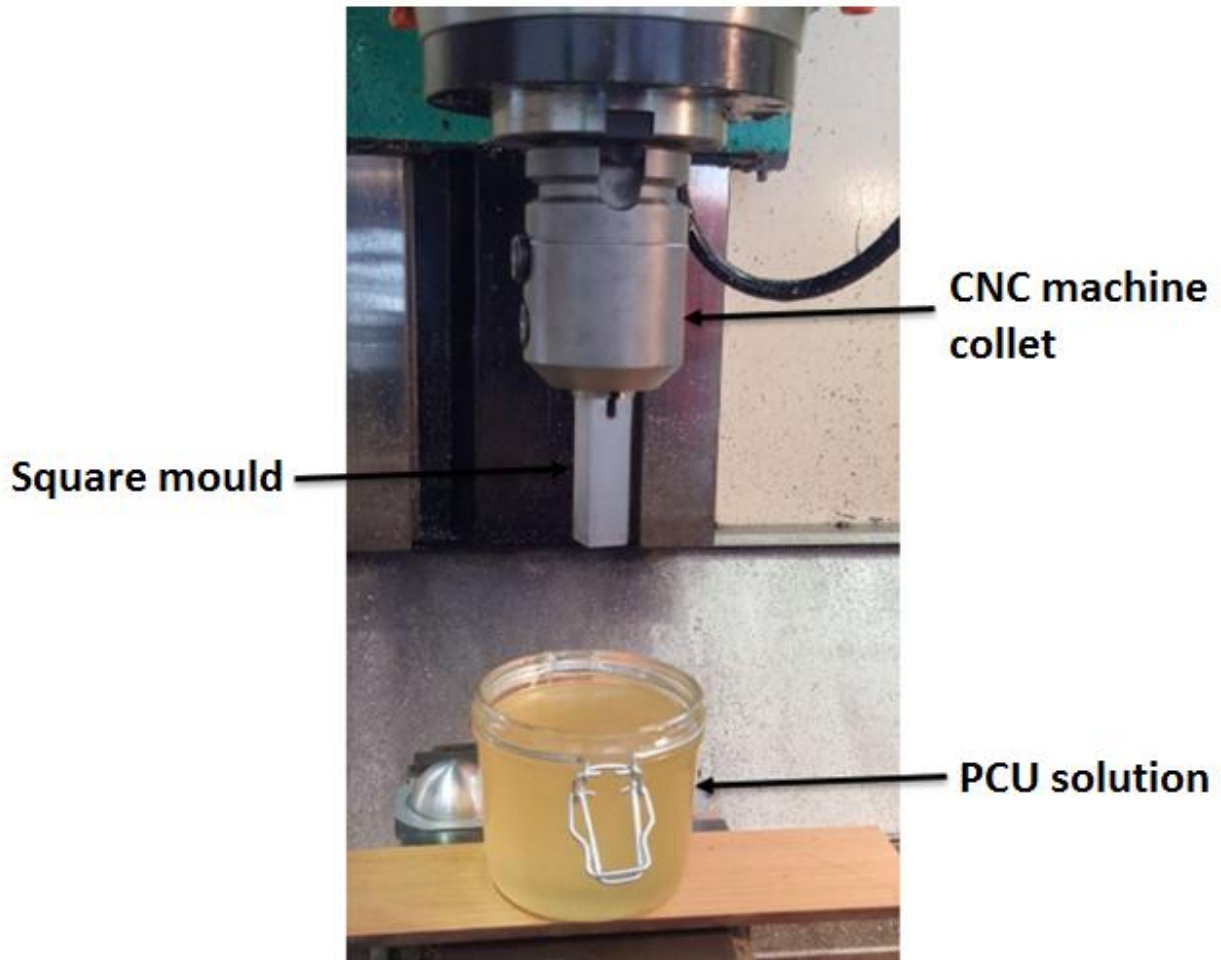


**Figure 3.7: Experimental set up for the dipping stage consisting of a square mould fixed into a collet of the CNC machine and the PCU solution in position for dip moulding.**

The mould and PCU solution were placed in two different ovens at controlled temperatures for preheating. After the mould and solution reached the required temperatures, the mould was inserted into a collet of the CNC machine. The heat loss of the liquid solution to the surroundings was reduced by placing a sheet of wood between the PCU solution and the steel bed of the CNC machine

The temperature of both the mould and the PCU solution were measured with a non-contact (MT694) infrared thermometer before lowering the mould to a predetermined

depth into the PCU liquid solution. The MT694 infrared thermometer has a dual laser thermometer that provides a super-fast sampling rate of 150 milliseconds and accurate read-out of measurements. An IR sensor automatically compensated for temperature deviation due to ambient conditions. The thermometer was switched to degrees Celsius, the built-in laser pointer was aimed on the area of interest and then scanned across with an up-and-down motion until the maximum temperature was obtained. Table 3.2 displays the technical specifications of the MT694 infrared thermometer used to measure the temperatures of the mould and the liquid solution.

**Table 3.2: Technical specifications of the MT694 Dual Laser Infrared Thermometer.**

<b>Temperature range</b>	<b>-50°C to 650°C</b>
Temperature resolution	0,1°C
Emissivity	0,1 to 1
Basic accuracy	±2%
Laser pointer	Dual, Class 2, Output <1 mW, Wavelength 630-670 nm
Spectral response	6~14 µm

The travelling distance and speeds and the retention time were controlled in the CNC program of the milling machine. After positioning the liquid solution on a sheet of wood, the start button on the CNC machine was pressed and the square mould was dipped slowly into the PCU solution at a controlled speed to limit disruption of the solution. The mould was kept in the solution for the programmed retention time and then withdrawn at constant speed. After each coating, the excess PCU liquid solution was allowed to drain. Thereafter, the experimental square mould was removed from the CNC machine and placed upright inside the heating oven. This process allowed the polymer films to be solidified by evaporation of the excess solvent at the predetermined temperature in the oven for 1 to 12 hours. The mould was removed from the oven and kept at room temperature to allow complete evaporation of the DMAc and curing of the material. This process was repeated to produce samples from one, two and three dips. After each dip the film thicknesses were measured on all the faces of the mould.

### **3.4. Characterization of the Films Produced during Phase 2**

The thicknesses of PCU film samples produced from different solution concentrations and different numbers of dips were measured. Tensile tests were performed on the films to determine their mechanical properties. The surface topography of these film samples were assessed using optical and scanning electron microscopy. The homogeneity of the material was also determined by investigating fracture surfaces prepared as described in section 3.4.4.

#### **3.4.1. Film thickness measurement**

A Fisher Dual Scope FMP40 Compact handheld instrument for non-destructive coating thickness measurement, according to the magnetic induction method or the Eddy current method for all metal substrates, was used during the thickness measurements. The FMP40 instrument automatically recognises the substrate material and integrates both measurement methods. The instrument is capable of measuring numerous coatings both on steel and iron and on non-ferromagnetic metals.

The quality of the thickness measurement depends on several key factors. These include the proper probe selection and the quality of the probe itself. Important aspects for probe selection are the thicknesses of the coating and the substrate material, the measurement area dimensions as well as the shape and the surface condition of the specimen. An FD10 probe (see Figure 3.8) was selected because it can recognize the base material under a coating, has a small probe tip and can detect smooth surfaces and thin coatings by making use of the Eddy current test method, which is activated automatically for the patented conductivity compensation. Figure 3.8 shows the thickness measuring assembly of the experimental square mould clamped in the stand, the Fisher Dual Scope FMP40 with the FD10 probe applying the Eddy current measurement principle and the measuring ruler.



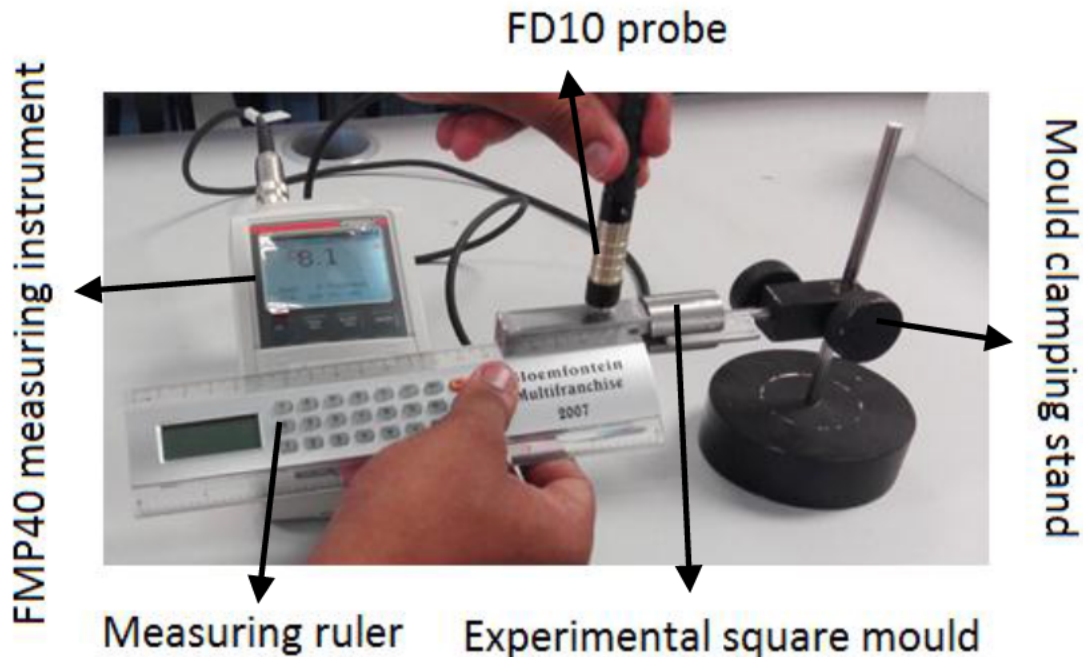


**Figure 3.8: Shows the FMP40 measurement instrument, FD10 probe and the stand to clamp the mould.**

The thickness measurements of the produced films were taken along the centre line of each face of the mould with increments of 10 mm between the five different points on each face of the mould, as shown in Figure 3.5.

### 3.4.2. Mechanical tests

The Young's modulus, tensile strength and elongation of the film test samples were experimentally determined on a LS100 Plus Lloyd Instruments material testing machine using NEXYGEN Plus software. Figure 3.9 shows the LS100 Plus Lloyd Instruments electromechanical universal testing machine. The machine consists of a moveable cross-head which applies a fixed rate of deformation, a load cell for detecting the forces within the specimen and a chart recorder which records the test results. For additional flexibility, the LS100 Plus Lloyd can be connected to a personal computer with an optional NEXYGEN Plus software. The software interacts with Excel and Word, offering automatic transfer of the test results directly into these programmes.

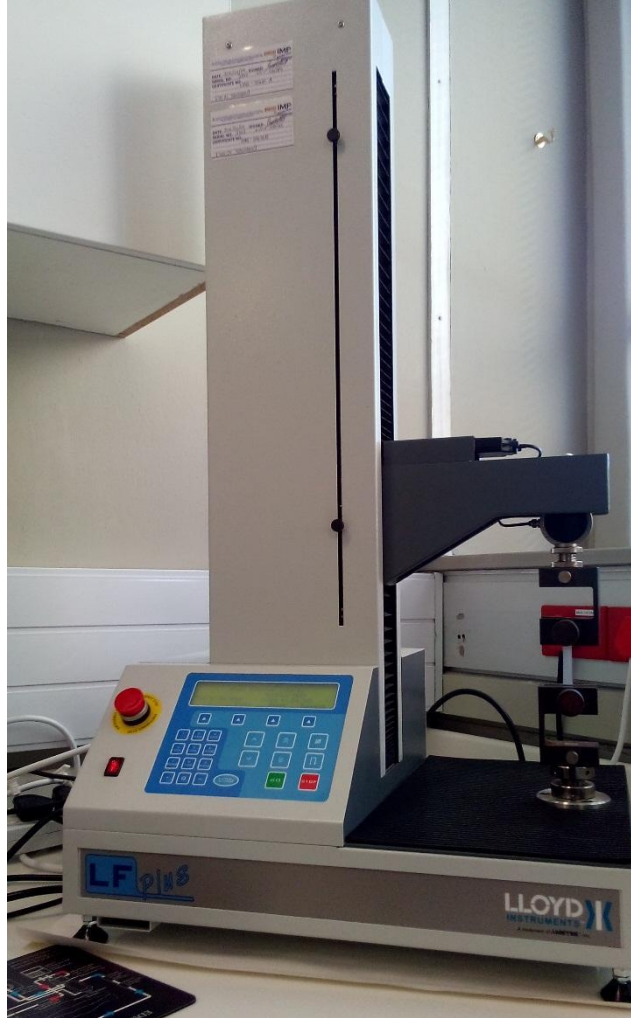


**Figure 3.9: Lloyds LS 100 Plus electromechanical universal testing machine.**

Each experimental square mould produced four PCU film samples, one on each of the faces of the mould (see Figure 3.5), which were stripped off the mould after curing. Three of the samples from each mould were investigated by optical microscopy before they were used for mechanical testing; while one sample from each mould was used for SEM. Samples were cut from the moulds to obtain consistent sample dimensions of  $40\pm 1$  mm long and  $14\pm 1$  mm wide.



Three samples of each type of film produced through dipping the mould once, twice and three times in PCU solutions with concentrations of 15, 25 and 35% (w/w) were used for the mechanical tests. The thickness, height and width of each sample was measured with a Mitutoyo Digimatic calliper with an accuracy of 0,02 mm. Straight curved stainless steel hemostat forceps with locking clamp were used to fix both ends of the film sample into the machine clamps. The PCU film sample was mounted at a nominal gauge length of 6 mm and held between two manually tightened steel grips lined with P120 waterproof sandpaper to prevent slippage, as illustrated in Figure 3.10.



**Figure 3.10: PCU film sample mounted on nominal gauge and two steel grips.**

The upper grip was attached to the 500 N cross-head load cell. The width and thickness of the PCU samples were measured and entered into the programmable test set-up (NEXYGEN Plus). A cross-head speed of 10 mm/min and a pre-load of 0,1 N were used. Constant tension was applied on both ends of the PCU film sample with an extension rate of 3 mm/min. The data were recorded on a personal computer.

### 3.4.3. Optical microscopy

Optical microscopy in reflected and transmitted mode was performed to investigate the surface topography of the samples. A polarised light (ZEISS Axio Scope.A1) equipped with a camera (resolution 5 megapixel) and dedicated image analysis software (AxioVision SE64) for evaluating the surface topography of the samples was used. Figure 3.11 displays ZEISS Axio Scope.A1 used for all the optical microscopy analysis.

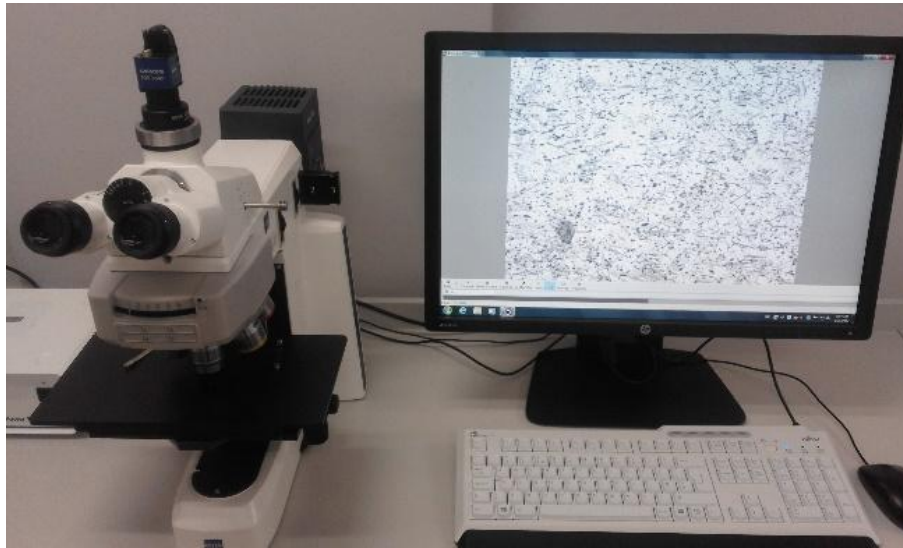


**Figure 3.11: ZEISS Axio Scope.A1 optical microscope used during the optical microscopy analysis.**

Two surfaces were inspected on each prepared sample, one on the surface facing towards the mould and the other on the surface facing away from the mould. The aim was to investigate the possible irregular surface finish of the films. Images of thin films sections were captured at different magnification levels and positions on the surface.

### 3.4.4. Scanning electron microscopy

To obtain further detailed information about the samples, SEM analyses were conducted on the samples. SEM is an instrument that produces a large magnified image by using a focused beam of electrons as opposed to light. The surfaces of a specimen from the square mould were examined through SEM. Each specimen was divided into three samples, with dimensions of about 10 x 14 mm and one sample with a dimension of 20 x 14 mm. The two 10 x 14 mm samples were used to observe the surface topography facing towards- and away from the mould respectively. The third sample was clamped with two hemostat forceps, straight curved stainless steel, with locking clamp (Figure 3.12. A) and dipped in liquid nitrogen and then broken into two pieces (Figure 3.12. B). This allowed the fracture surfaces to be imaged in the SEM and to subsequently determine the film thickness from the cross-sectional views.

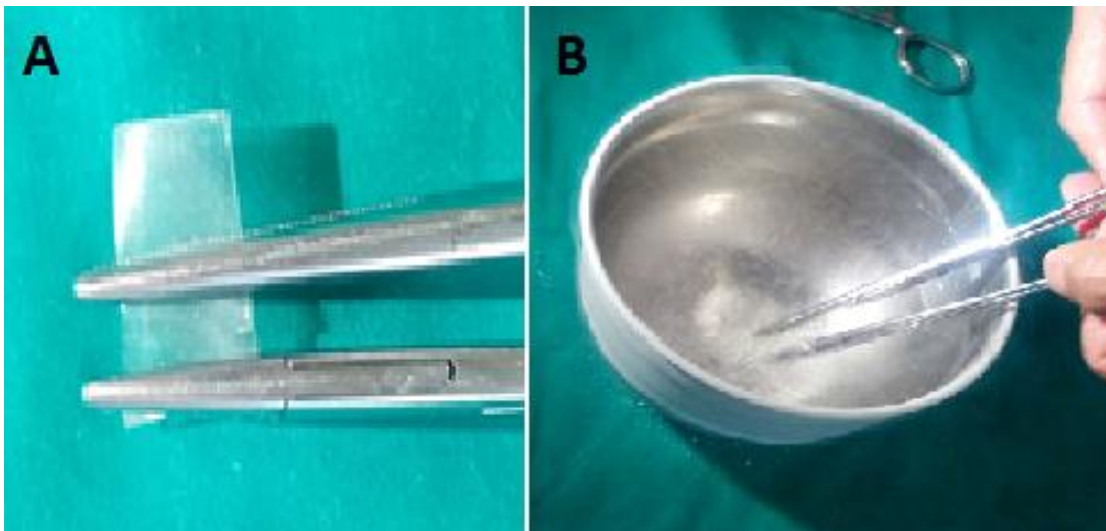


**Figure 3.12: Preparation of film samples for SEM. (A): Film clamped with two hemostat forceps, straight curved stainless steel, with locking clamp, (B): Film samples dipped into liquid nitrogen.**

The processed specimens were mounted on the aluminium pin stubs (SPI suppliers, Rick Loveland & Associates cc, Halfway House, South Africa) using a high strength, hand mouldable, putty-like adhesive (Pratley Steel Quickset) and left for six hours to cure (see Figure 3.13. A). Figure 3.13. B shows the samples which were sputter-coated with gold to obtain a conductive surface required for the electron microscopy process.

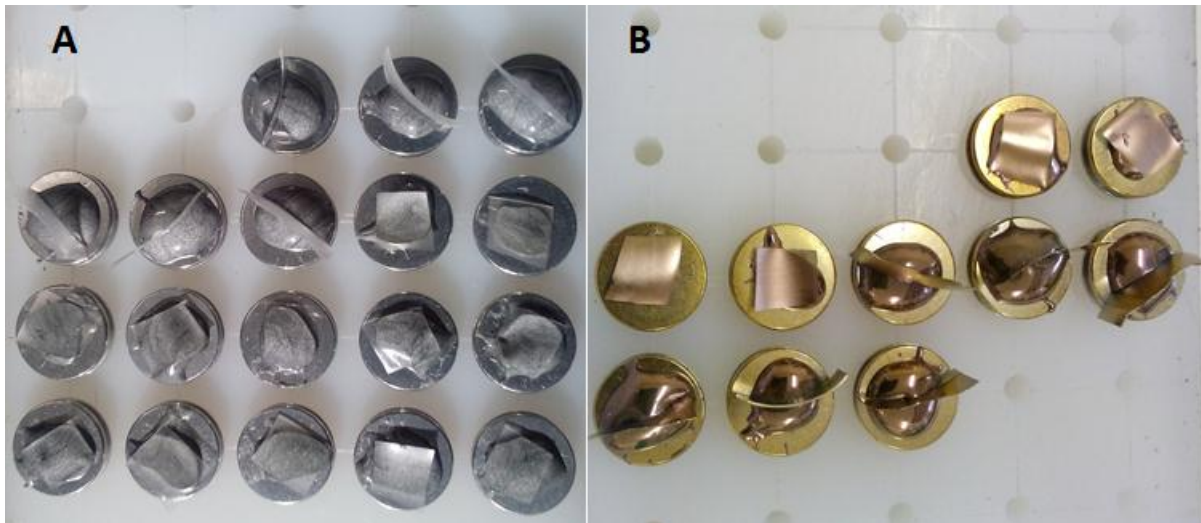


**Figure 3.13: PCU film samples prepared for SEM. (A): Film mounted on aluminium pin stubs, (B): Film samples sputter-coated with gold.**

During these processes, the specimens were stored in an airtight container until studied in a SEM (Shimadzu SSX 550), shown in Figure 3.14. The operating parameters/settings of the SEM on the following scanning modes were used to photograph the samples:

- Accelerating voltage: 5kV
- Probe size: 150 nm
- Working distance:  $\pm 15$  mm
- Magnification: between x140 and x1200.



**Figure 3.14: Scanning Electron Microscopy (Shimadzu SSX 550).**

### 3.5. Phase 3: Manufacturing of Prototype Polyurethane Heart Valves

During this phase the dip moulding procedure developed in Phase 2 was applied to the actual mould designed to produce the tri-leaflet PCU heart valve. Thicknesses of the moulded leaflets were measured and SEM analysis was done on the leaflets. The dip-moulding procedure was reviewed and altered until the results were satisfactory. Figure 3.15 illustrates the layout of the research methodology followed during Phase 3, aimed at manufacturing prototype tri-leaflet PCU heart valves.

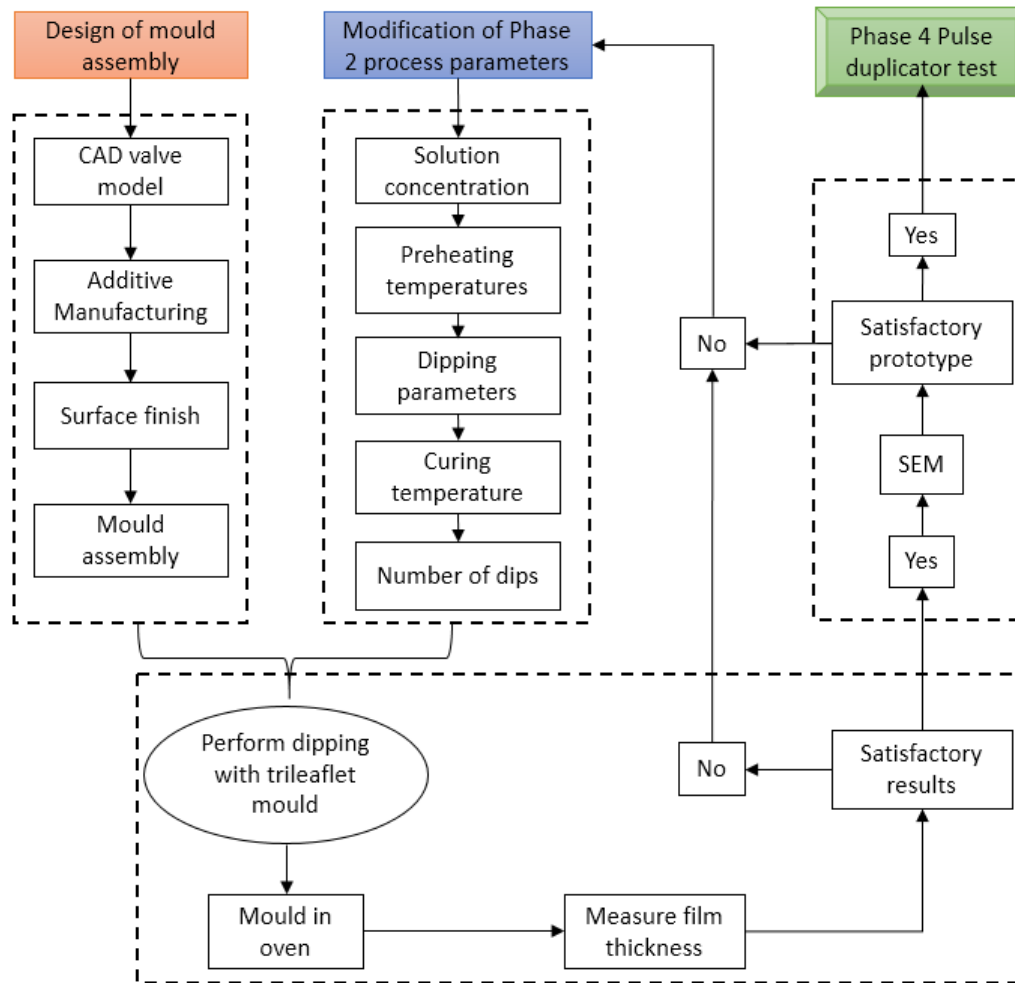


Figure 3.15: A diagrammatic presentation of the Phase 3 research methodology.

### 3.5.1. Computer-aided design model of tri-leaflet valve

A CAD model of a natural heart valve did not exist. An extensive effort was required to obtain a CAD model of the valve leaflet geometry. The process of duplicating an existing component without the aid of drawing is known as reverse-engineering. Through the application of this technique, an existing model is recreated by acquiring its surface or geometrical data using contact or non-contact digitizing or measuring devices.

The Carpentier-Edwards Perimount Magna 19 mm valve (Figure 3.16), as recommended by the Robert WM Frater Cardiovascular Research Centre in the Department of Cardiothoracic Surgery of the University of the Free State, was reverse-engineered to obtain the baseline geometry. The valve typically comprises three thin leaflets attached to a cylindrical support frame, referred to as the stent that incorporates a sewing ring. The stent has three posts to support the flexible leaflets. The sewing ring has three arch saddles to ensure conformity with the aortic annulus.



**Figure 3.16: Carpentier-Edwards Perimount Magna 19 mm valve.**

Figure 3.17 displays the technical specifications of the Carpentier-Edwards Perimount Magna 19 mm valve.



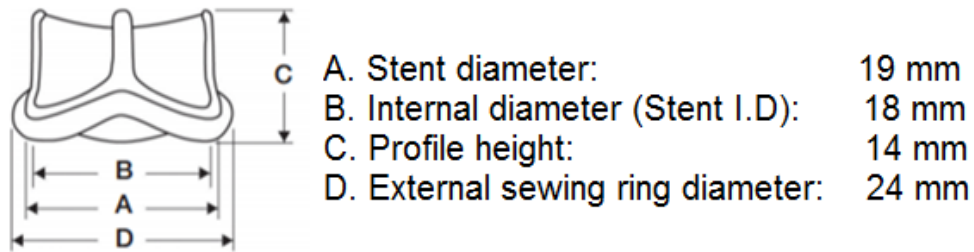


**Figure 3.17: Technical specifications of the Carpentier-Edwards Perimount Magna 19 mm valve.**

A Carpentier-Edwards Perimount Magna 19 mm valve was fixed in a sewing cuff and silicone was cast onto both sides of the valve and allowed to cure, as shown in Figure 3.18 C. The two negative silicone halves were laser-scanned using a Renishaw® Cyclone 2 Coordinate Measuring Machine (Figure 3.18 A).

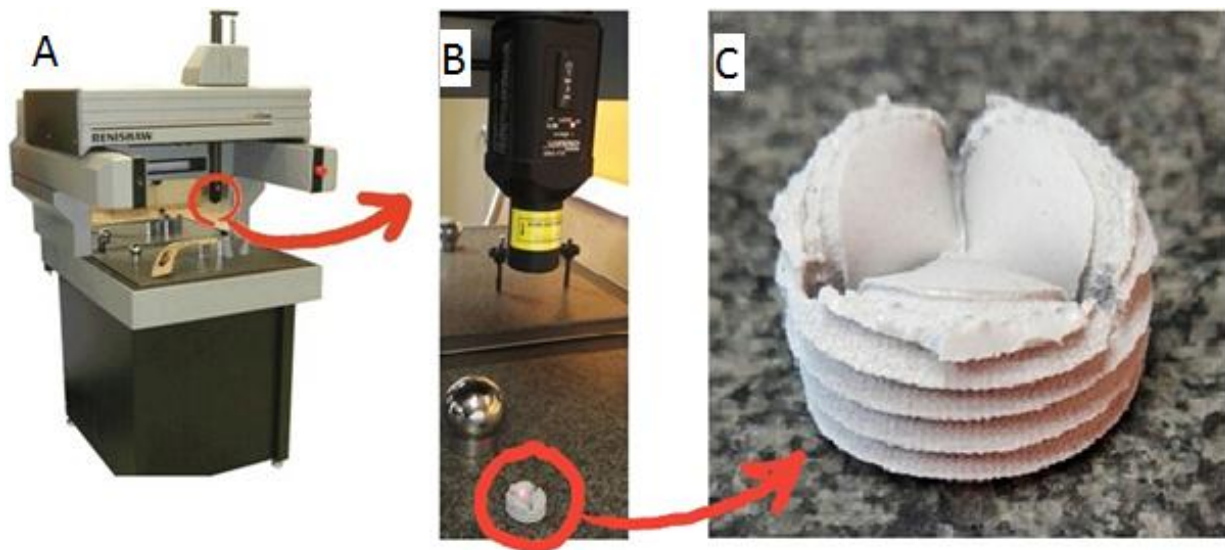


**Figure 3.18: Reverse-engineering process. (A): Renishaw Cyclone 2 scanner device, (B): Wolf and Beck OTM3M laser scanning unit on cyclone, (C): Negative silicone half of the heart valve.**



Scan data was obtained with a Wolf & Beck OTM3M optical laser scanner (shown in Figure 3.18 B) at a scanning rate of up to 400 points per second with a resolution of 0.1 mm and 5  $\mu$ m respectively. A cloud of points obtained from the scanned data was converted to a STL file using Trace Scan 24A software. The resultant mesh was cleaned up, smoothed and sculpted to the required shape with the use of Geomagic® Quality software. The final non-uniform rational base spline (NURBS) file was exported to CAD software to generate a solid model of the valve. Figure 3.19 shows an exploded view of the assembled dip moulding tool. From Figure 3.19, the complex geometry of the leaflets is revealed, with different curvatures in the circumferential direction (i.e. parallel to leaflet free edge), and radial direction (i.e. perpendicular to the circumferential direction).

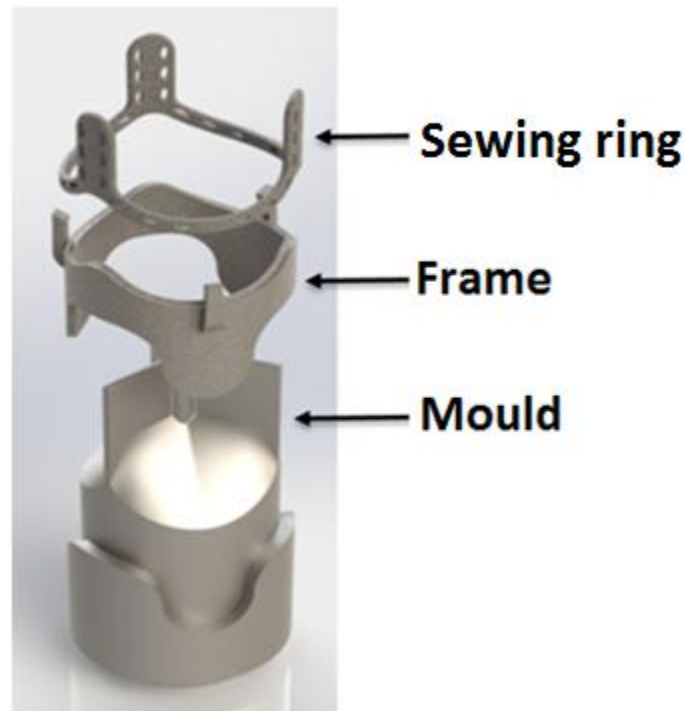


**Figure 3.19: Exploded view of the CAD tri-leaflet mould assembly.**

The CAD model of the tri-leaflet dip moulding tool (Figure 3.19) consists of the stent with three posts where the three PCU leaflets are attached, with an exterior diameter of

19 mm. The frame part was designed in such a way to lock the sewing ring onto three hooks. This design feature was implemented to locate the stent correctly and fix it to the mould assembly.

### 3.5.2. Additive Manufacturing of the mould assembly

AM was the most suitable manufacturing method to manufacture the tri-leaflet mould, frame and sewing ring. This manufacturing technique allows prototypes with complex and intricate shapes to be built. The mould assembly components were produced through the Direct Metal Laser Sintering (DMLS) process followed by a stress-relieving heat treatment. Ti6Al4V (ELI) was selected due to its high strength and fatigue resistance.

### 3.5.3. Surface finish of the tri-leaflet mould

Despite significant progress made in material flexibility and mechanical performance of AM, a relatively poor surface finish when compared to the surface finish of traditional fabrication methods, still presents a major limitation in all types of AM processes. The surface quality is greatly influenced by the “stair-step” effect, which is the stepped approximation of curved and inclined surfaces by the layered AM structure, as shown in Figure 3.20.

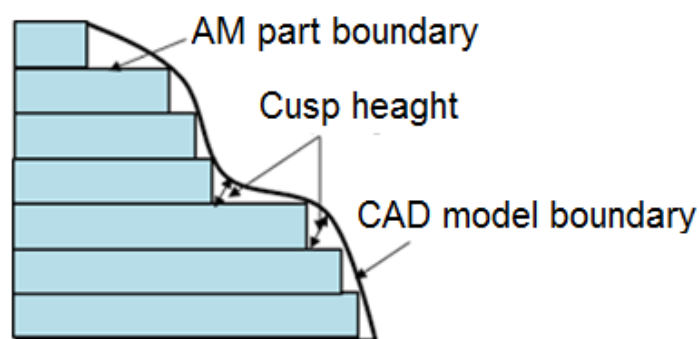


**Figure 3.20: Schematic illustration of the stair-step effect typical of the DMLS surface finish.**

For certain applications, surface finish improvement of AM parts after the building process is very necessary. The surface topography of the PCU heart valve leaflets can influence thrombus formation (clotting) in the blood. Therefore, a smooth finish on both surfaces of the dip moulded PCU leaflet was required. Obtaining a mirror-like surface on the mould would significantly influence the inside surface of the moulded leaflet, therefore, removal of stair-steps on the mould was necessary. Figure 3.21 shows the rough surface finish of the Ti6Al4V(ELI) tri-leaflet mould produced by the DMLS technique and application of Micro Machining Process.

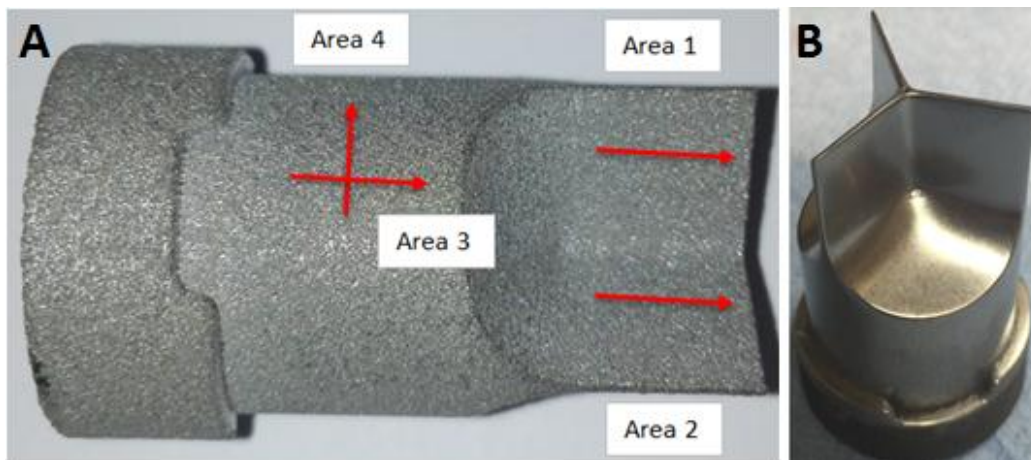


**Figure 3.21: Ti6Al4V(ELI) tri-leaflet mould manufactured with DMLS. (A): Showing the rough surface finish obtained in as-built state, (B): Showing mould after Micro Machining Process.**

An improvement of surface roughness was obtained through First Surface Oberflächentechnik®, a company based in Munich, Germany. Their adaptation of the Micro Machining Process technology is capable of selectively filtering out successive levels of roughness without changing the basic form of the surface, see Figure 3.21 B. Evaluation of the surface area between the actual profile obtained from DMLS and the Micro Machining Process technology was conducted. The arithmetic average of the absolute surface roughness, denoted by  $R_a$ , the root square average,  $R_z$  and the

maximum height of the profile,  $R_t$  were measured in the four areas, indicated in Figure 3.21 A.

### 3.5.4. Tri-leaflet mould assembly

A cylindrical mild steel rod consisting of two sections, 1 and 2, was manufactured. Section 1 (15 mm in diameter and 25 mm long) was designed to be press-fitted in the bottom hole of the mould, which is 12 mm deep. Section 2 (10 mm diameter and 30 mm long) served as the mounting section of the mould into the CNC machine collet. A cylindrical bush was used to allow for the vertical suspension of the mould assembly (Figure 3.22) on a supporting stand for the solvent to evaporate after the dipping process. A fixing grub screw was used to secure the bush onto section 1.

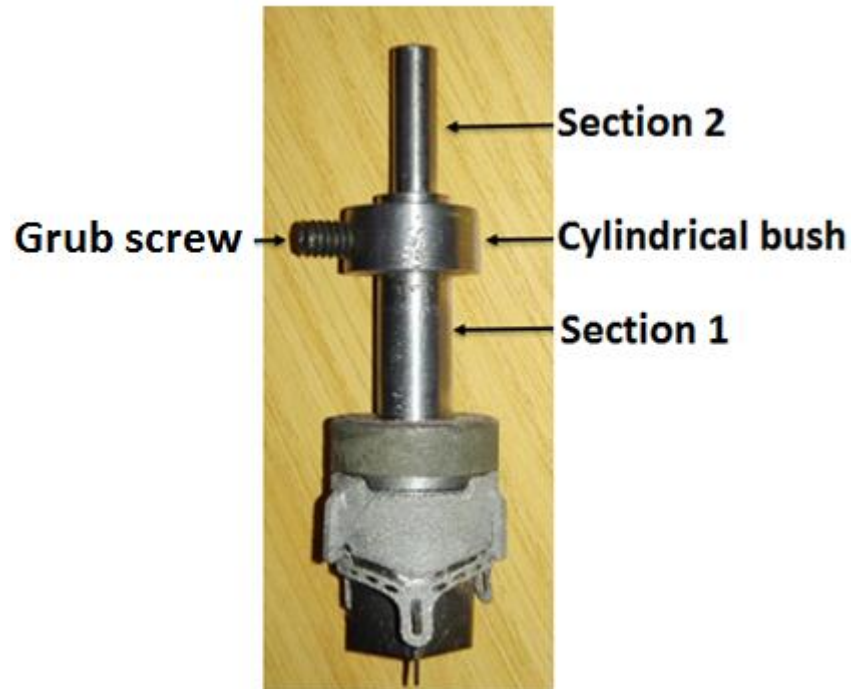


**Figure 3.22: Tri-leaflet mould assembly.**

The stent and frame assembly slide over the mounted mould into position. Slide fit tolerance was adopted on the tri-leaflet mould to secure the stent and frame to the mould.

### 3.5.5. Dip moulding of the PCU heart valve

The aim of Phase 3 was to produce a functional prototype of a polyurethane heart valve. Key parameters that had an influence on producing acceptable leaflets were established in Phase 2. These parameters include (i) the concentration of the polymer in the polymer-solvent solution, (ii) dipping and withdrawal speed of the mould, (iii) curing temperature and (iv) the number of dips. To manufacture a dip moulded polymer heart valve, a solution of polyurethane (PC3595A clear) was dissolved in a solvent (DMAc). A 20% w/w solution was prepared, as described in section 3.3.1. The tri-leaflet mould and PCU solution were placed into ovens for preheating. Thereafter, the respective temperatures were measured (refer to section 3.3.4). When the correct temperatures were reached, they were removed from ovens. The mould assembly was then mounted in a collet of the CNC machine and lowered at a controlled speed into the concentrated PCU solution. This technique reduces the formation of air bubbles which can result in fatigue failure of the finished product and ensures a more even polymer thickness distribution across the leaflets.

After the dipping process, the mould, with a thin polymer coating, was removed from the CNC machine. After each dipping, excess polymer solution was allowed to drain. The mould was then placed vertically (see Figure 3.22) with the free edges of the mould (shown in Figure 3.23) facing downwards in an air circulating oven at 25°C for an hour to remove the excess DMAc solvent from the solution. The leaflet formed as the solvent evaporated and a thin layer of polymer remained on the mould. This process was repeated until the required leaflet thickness was obtained. Upon removal of the dip moulded leaflets from the mould, the leaflet edges were trimmed by hand to separate the individual leaflets from one another and to dispose of the thick ridge of PCU which formed along the free edges during the dipping and drying process.

### 3.6. Characterization of Dip Moulded Prototype Heart Valves

The thickness and surface finish of the moulded leaflets were measured. Dip moulding parameters were assessed and updated. A detailed surface topography of the prototype PCU heart valve leaflets was studied through SEM. The prototype PCU heart valves, with the required leaflet thickness and structural integrity, were tested in the valve pulse duplicator testing system (ViVitro Labs Model Left Heart) at the UFS to determine the performance characteristics and estimated functional lifespan of the manufactured PCU valves.

#### 3.6.1. Thickness measurement of PCU heart valve

A thick area close to the free edges of the valve (Figure 3.23) is likely to limit the opening of the leaflets.

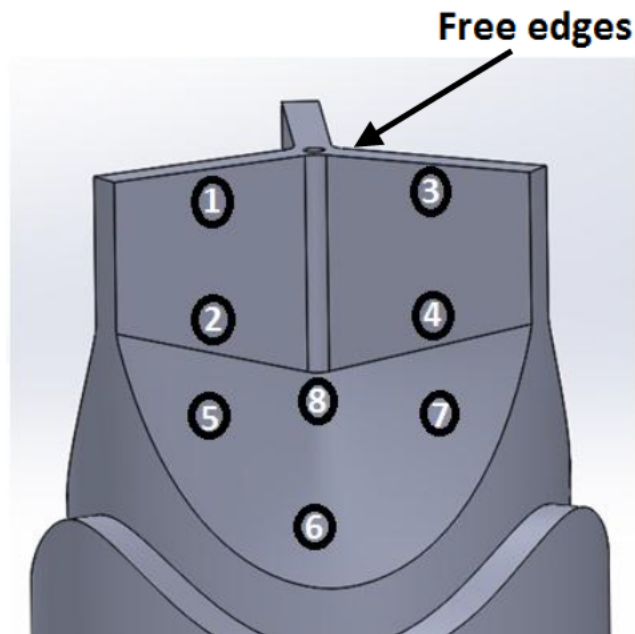


**Figure 3.23: Representation of the thickness measurement sites across a single leaflet.**

The thickness of the dip moulded heart valve leaflets were measured at different locations on the leaflets, as indicated in Figure 3.23. These eight locations were identified as critical areas in each leaflet, influencing the hydrodynamic behaviour of the valve [34][9]. A Fisher Dual Scope FMP40 with FD10 probe based on an Eddy current measurement principle was used for the thickness measurements. The influence of the dip moulding parameters was determined by comparing the layer thickness of the valve leaflets.

### **3.6.2. Surface topography of the PCU heart valve**

It is desirable that both sides (the side facing the mould and the side facing away from the mould) of the leaflets have very similar surface topography. The mould used to produce the heart valves has six vertical flat- (see Figure 3.23 number 1 and 3) and three upper curved surfaces (see Figure 3.23 number 5, 6, 7 and 8). The vertical flat and bottom curved surfaces of the prototype valve were cut from the valve leaflets and inspected with SEM. Refer to section 3.4.4 for the preparation of the specimens, and section 3.4.4 for the machine parameters used.

### **3.6.3. Testing of prototype PCU valve in pulse duplicator**

To obtain detailed information about the functioning of the prototype heart valves, they were subjected to tests in the pulse duplication system of the UFS. The pulse duplication test assesses heart valve function under simulated cardiac conditions. The ViVitro Labs Model Left Heart system (Figure 3.24), operated by UFS simulates the function of the heart's ventricle which generates pulsatile flow through a prosthetic heart valve. The setup consisted of a reservoir, a volumetric pumping system and a valve housing unit designed according to the guidelines of the ISO 5840 Standard. The pressure ports and flow measuring locations allow for data collection from the aortic or mitral sites. The ViVitest software controls the system while simultaneously collecting and analysing physiological flow and pressure data.





**Figure 3.24: The ViVITRO Labs Model Left Heart pulse duplicator machine.**

Before the pulse duplication can commence, the valve needs to be prepared. Woven Dacron, rolled up into a doughnut shape, is stitched around the outside of the sewing ring of the valve. The attachment is high enough to reduce paravalvular leaks, however, taking care not to impede the movement of the leaflets. A custom-made plastic fitting is fitted around the outside of the sewing ring. The plastic fitting is then inserted into a silicone rubber which has been manufactured to fit the pulse duplicator exactly. The silicone rubber ensures that the valve seats securely within the pulse duplicator and that there is no leakage between the upper and lower halves of the pulse duplicator.

The following results were obtained from the pulse duplicator:

- Average pressure drop
- Effective orifice area (EOA)
- Closing volume
- Leakage volume
- Total regurgitation



To meet testing requirements, each valve was tested at the following conditions:

- 60 Beats per minute (BPM) and 60 ml Stroke Volume (SV)
- 70 BPM and 70 SV
- 80 BPM and 80 SV
- 100 BPM and 80 SV
- 120 BPM and 80 SV

The total regurgitation was divided between closing and leakage volume, as the difference in the value of each relates to the functioning of the valve. Test 1, 2 and 3 were performed with valve 1, valve 2 and valve 3 respectively. Continuous and pulsatile flow tests were performed using distilled water at room temperature (25°C).

## CHAPTER 4: RESULTS AND DISCUSSION

### 4.1. Introduction

The polyurethane heart valves were manufactured from PC3595A granules dissolved in DMAc as solvent. The valve has a 3D-printed Ti6Al4V (ELI) frame with dip moulded polyurethane leaflets. Key parameters to be considered in the design and production of such a polymer heart valve are the valve geometry, the material properties, the manufacturing parameters and the resultant thickness and surface topography of the leaflets.

### 4.2. Presentation and Discussion of Phase 2 Results

#### 4.2.1. Surface roughness measurement of the experimental square mould

The surface roughness of the experimental square mould, manufactured through CNC milling, was measured at three positions on the flat faces shown in Figure 3.5, as described in section 3.3.3, before and after application of oil stone surface polishing. The results of these measurements are shown in Table 4.1.

**Table 4.1: Measurements of surface finish of the square mould flat faces**

	Surface finish $R_a$ ( $\mu\text{m}$ )					
	After CNC machining			After polishing		
	Positions					
Face	A	B	C	A	B	C
1	0.853	0.933	1.15	0.075	0.158	0.434
2	1.050	1.246	1.411	0.303	0.303	0.100
3	0.952	1.030	0.968	0.099	0.130	0.968
4	0.897	0.925	1.010	0.180	0.201	0.299
<b>Average</b>	0.938	1.034	1.135	0.164	0.198	0.450
<b>Standard Deviation</b>	0.085	0.149	0.200	0.103	0.076	0.373

A graphical representation of the surface roughness of the square mould is shown in Figure 4.1.

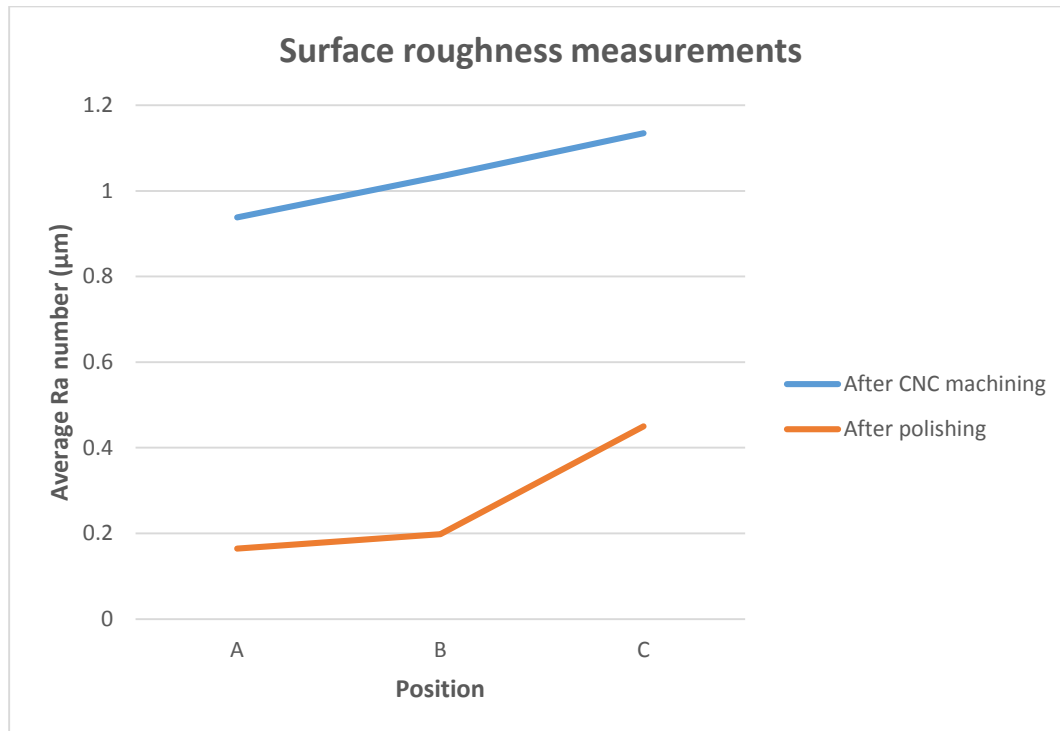


**Figure 4.1: Surface roughness measurements on square moulds before and after polishing.**

The left, middle and right side of the flat surface face on the mould were referred to as position A, B and C respectively (see Figure 3.5). From Table 4.1, the surface finish  $R_a$  of Face 1 of the mould after CNC machining, was observed to gradually vary from  $0.853 \mu\text{m}$  on position A to  $1.15 \mu\text{m}$  on the right side (position C). Despite the inconsistent surface roughness on 3 different positions on one face of the mould, each measured position showed consistence surface finish across the same position on four faces of the mould. However, this rough surface topography quantified by the high  $R_a$  numbers will result in rough surfaces of the heart valve leaflets, which will influence thrombus formation in the blood. Therefore, an improvement of the surface finish across all surfaces of the mould was necessary.

An improved surface finish was obtained by using an oil stone polishing technique subsequent to the CNC milling. This is evident from the improved average  $R_a$  numbers obtained after this treatment, as shown in Table 4.1. However, the standard deviations for the averages in Table 4.1 demonstrate the inconsistent surface finish from one face of the mould to another. From this it became clear that an automated surface polish technique would have to be applied on the tri-leaflet mould to improve the consistency of surface finish across all the surfaces of the mould.

#### 4.2.2. Film thickness measurement

In Table 4.2, thickness measurements of the films at different points and faces of the moulds are shown and are graphically presented in Figure 4.2.

**Table 4.2: Results of the thickness measurements of the PCU films at the different points on the four faces of the mould dipped in a 15% PCU solution.**

15% solution first dip ( $\mu\text{m}$ )						
Measured Point	Face 1	Face 2	Face 3	Face 4	Average	Standard deviation
1	35	52	73	38	50	17
2	15	10	12	12	12	2
3	12	8	10	9	10	2
4	8	6	7	7	7	1
5	2	3	2	3	2	1

A graphical representation of the results in Table 4.2 is shown in Figure 4.2.

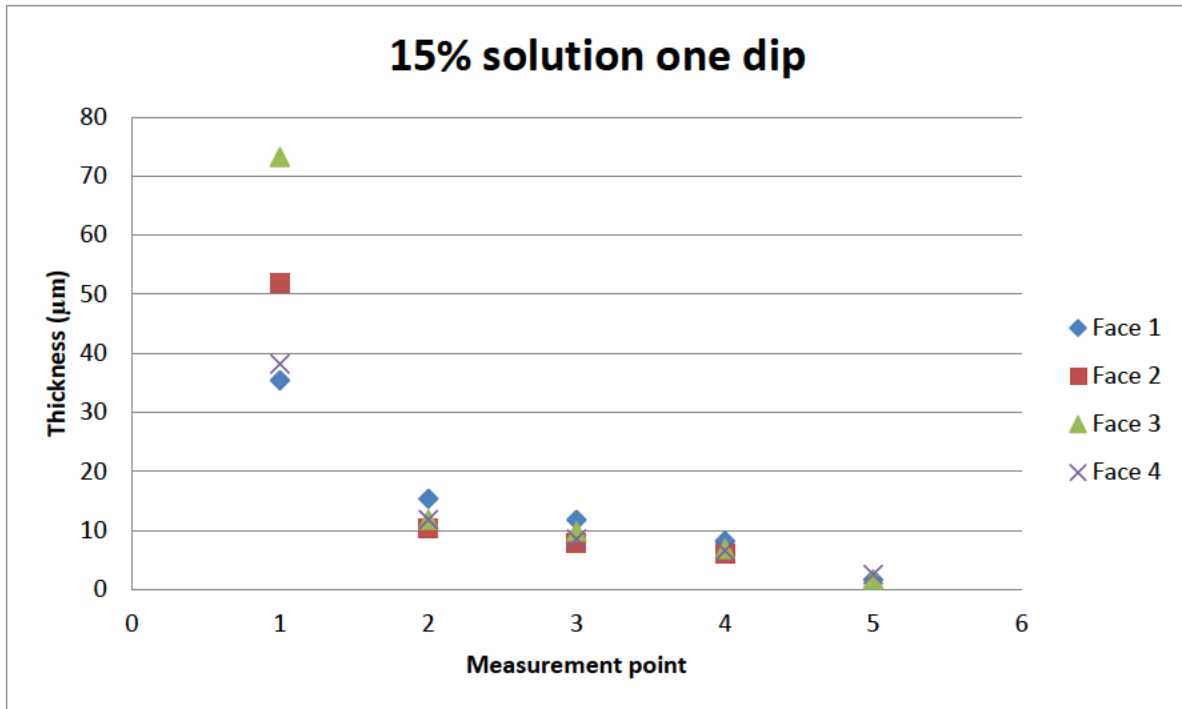


**Figure 4.2: Variation of the PCU film thickness for the different measurement points on each face of the mould dipped once in a 15% PCU solution.**

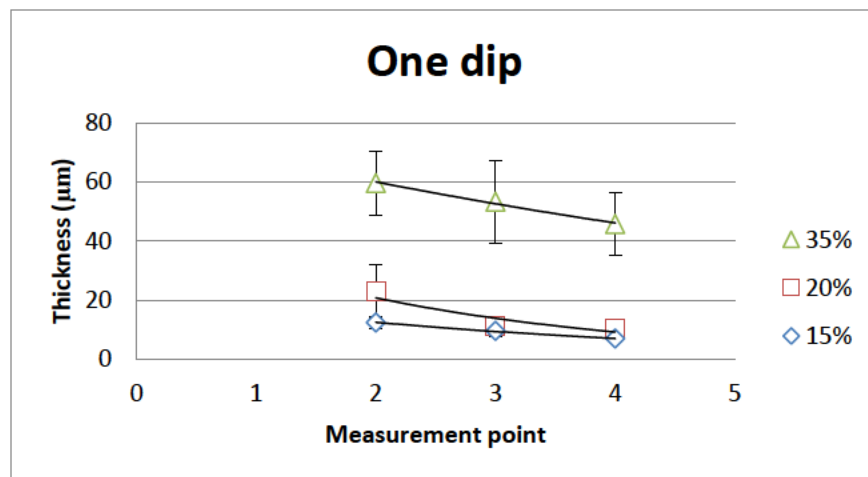
From Figure 4.2 it is evident that the thickness of the PCU films formed at point 1 on the four faces of the mould varies from 35 µm to 73 µm while at point 5 the thickness only varies from 2 µm to 3 µm. The drastic change in thickness from point 1 to point 5 is due to the non-uniform flow of the PCU liquid solution under gravity along the vertical direction of each face of the mould. Consequently, less solution remained on the upper part of the mould, while it tended to accumulate at the lowest part of the mould. This accumulation also resulted in much larger variation in film thickness on the four faces of the mould. The material of point 5, 6 and 7 remained on the actual mould after the frame was removed, whereas the material of point 1 and 3 was trimmed before the assessment of the heart valve functionality. Taking into consideration this spread of film thickness, it was decided to use only points 2, 3 and 4 for comparing the relative effects of different parameter sets on the film thickness.

For each measurement point of the 15% solution concentration, the thicknesses of the films did not change significantly between the different faces of the mould. This is confirmed by the small standard deviations of 2  $\mu\text{m}$  for points 2 and 3 and 1  $\mu\text{m}$  for point 4 (see Table 4.2). Furthermore, the thicknesses of these films increased almost linearly from point 4 to 2. In Table 4.3, the thicknesses at points 2, 3 and 4 of the PCU films after one, two and three dips in the three different solutions are given.

**Table 4.3: The recorded thicknesses of the PCU films at the different points on the moulds dipped in the different PCU solutions and for different numbers of dips.**

Point	15% solution ( $\mu\text{m}$ )			20% solution ( $\mu\text{m}$ )			35% solution ( $\mu\text{m}$ )		
	2	3	4	2	3	4	2	3	4
1 dip	12 $\pm$ 2	10 $\pm$ 2	7 $\pm$ 1	23 $\pm$ 9	11 $\pm$ 1	10 $\pm$ 3	60 $\pm$ 11	53 $\pm$ 14	46 $\pm$ 11
2 dips	46 $\pm$ 4	37 $\pm$ 3	27 $\pm$ 3	75 $\pm$ 5	63 $\pm$ 11	49 $\pm$ 2	296 $\pm$ 108	234 $\pm$ 95	167 $\pm$ 79
3 dips	92 $\pm$ 8	70 $\pm$ 7	53 $\pm$ 4	153 $\pm$ 7	109 $\pm$ 14	92 $\pm$ 6			

For the 35% solution, only one and two dips were done, because two dips already provided sufficient thickness for heart valve leaflets. Graphical representations of the results in Table 4.3 are shown in Figure 4.3.



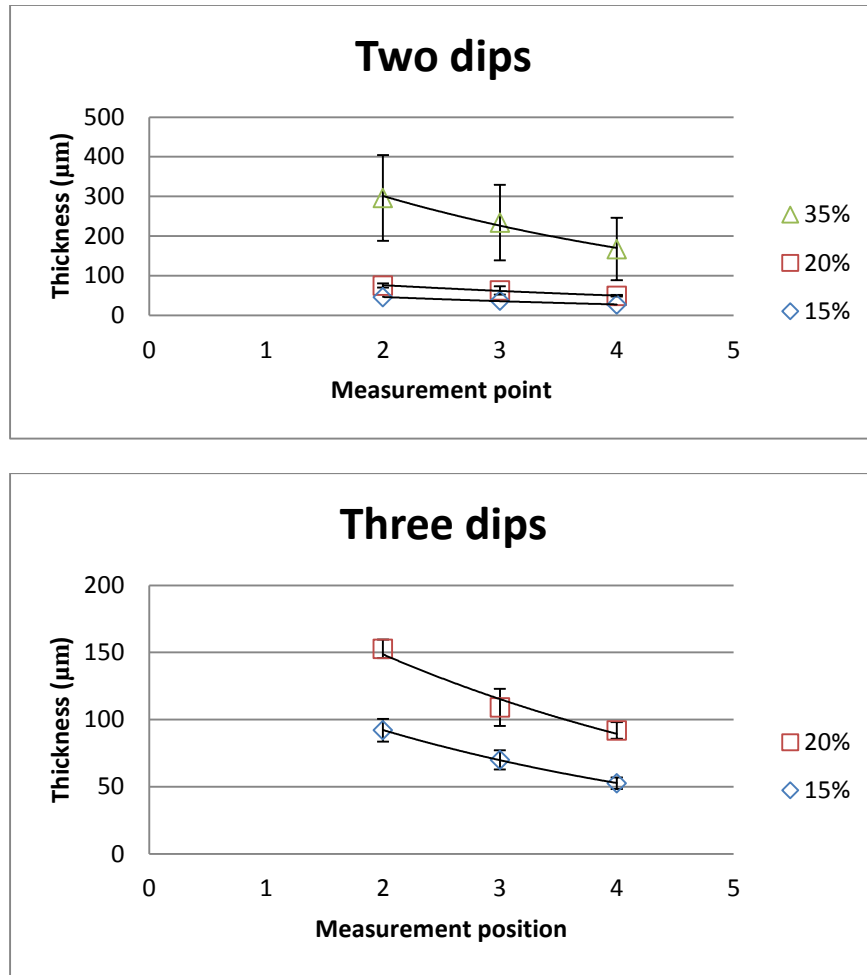


**Figure 4.3: Variation of the PCU film thickness along the measurement points after one, two and three dips in the 15%, 20% and 35% PCU solutions.**

From Figure 4.3 it is clear that the thickness of the films produced through dip moulding increases with increasing concentration of the PCU solution. Furthermore, the thickness of the films increases from the first dip to the second dip, and from the second dip to the third dip. In Figure 4.3 it can be seen that for point 2, which is located at 20 mm from the bottom, with a solution concentration of 15%, the thickness is 12 µm for the first dip, 46 µm after the second dip and 92 µm after the third dip. This trend was also recorded for the 20% solution.

A benchmark for acceptable heart valve leaflet thickness is indicated in a study of in vivo fatigue testing that found good durability for polyurethane valves with leaflet thicknesses of 100 to 300  $\mu\text{m}$  [20]. From Figure 4.3 it is evident that this thickness range is not achieved with any of the three solution concentrations after only a single dip. After two dips in the 15% and 20% concentrations the minimum thickness of 100  $\mu\text{m}$  was still not obtained. Only 75  $\mu\text{m}$  could be achieved with the 20% solution at position 2. However, after two dips in the 35% concentration solution the desired thickness range was obtained. A thickness of 296  $\mu\text{m}$  was obtained at point 2, 234  $\mu\text{m}$  at point 3 and 167  $\mu\text{m}$  at point 4.

From Table 4.3 it is clear that even after three dips the required minimum film thickness could not be obtained. With a concentration of 20%, the required range is almost achieved (92 to 153  $\mu\text{m}$  from point 4 to point 2). However, due to the time consumption between consecutive dips (approximately 24 hours), it is evidently necessary to limit the number of dips. Therefore, it was concluded that a solution of 35% concentration and two dips would be the optimal solution to obtain the thickness required for the heart valve leaflets.

#### **4.2.3. Optical microscopy observations**

Figure 4.4 gives representative images of the first moulded film surface facing towards the square mould as well as away from the mould. It is clear that the mould surface finish left an irregular striated structure on the surfaces of the films that had faced towards the moulds, see Figure 4.4 A. Considering the detrimental effects of rough surfaces with regard to possible blood clotting, this observation indicated that greater care had to be taken in polishing the mould surfaces.



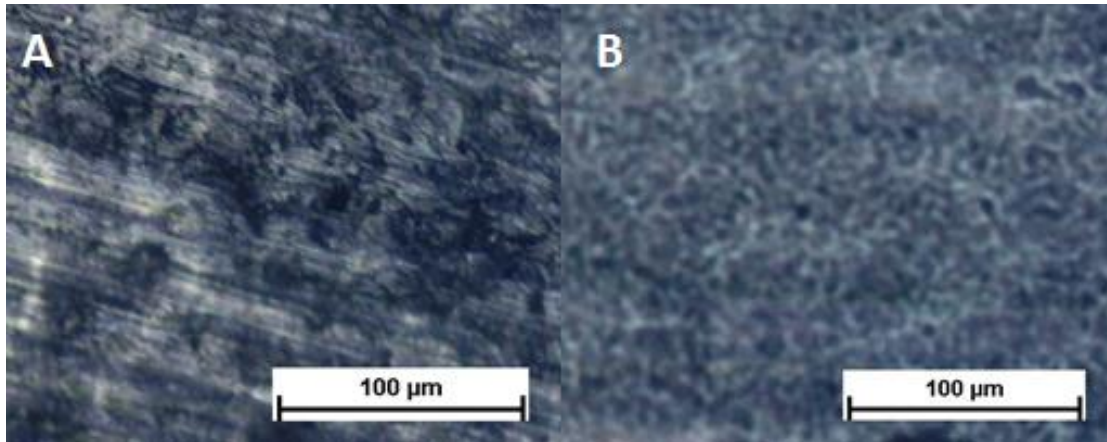


**Figure 4.4: Optical micrographs of surface structural features on the films produced by a CNC finished experimental mould. (A): Surface facing towards the mould (B): Surface facing away from the mould.**

An observation at a higher resolution in a SEM provided more evidence of localised damage introduced on the surfaces of the polyurethane films during peel-off. After this early detection, further investigations were conducted with a hand-polished experimental square mould.

#### **4.2.4. Scanning electron microscopy**

Figure 4.5 shows the surface topography of the polyurethane films produced with the three different PCU solutions for surfaces facing the mould and surfaces facing away from the mould. In all cases, the topography of the film surfaces facing away from the mould was smoother than the topography of the surfaces facing towards the mould. The topography of the surfaces facing the mould was clearly determined by the roughness of the mould surfaces. Although the surface finish of the experimental square moulds used to produce the films shown in Figure 4.5 D to E were similar, the film produced from the 35% PCU liquid solution had a rougher surface than the films produced from the other two solutions. It appeared as if this solution, with its higher viscosity than the other two, did not produce a film that replicated the topography of the experimental mould surface

as effectively as the other two solutions. This indicated that the 20% PCU solution would be preferred above the 35% solution for producing heart valve leaflets of the required thickness.

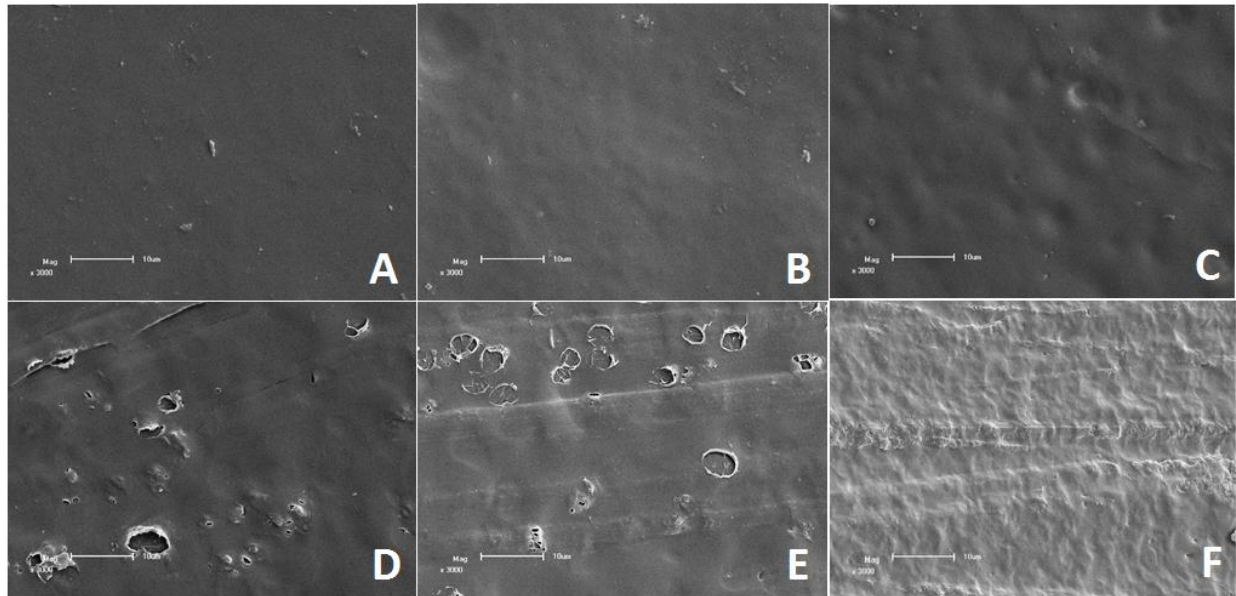


**Figure 4.5: SEM micrographs of the polyurethane film surface topography for the different PCU solutions at sense of scale 10 µm. (A): 15% solution, film surface facing away from the mould, (B): 20% solution, film surface facing away from the mould, (C): 35% solution, film surface facing away from the mould, (D): 15% solution, film surface facing towards the mould, (E): 20% solution, film surface facing towards the mould, (F): 35% solution, film surface facing towards the mould.**

The surface topography of the polyurethane heart valve leaflets can influence thrombus formation (clotting) of the blood. Therefore, a smooth finish on both surfaces of the dip-moulded polyurethane film should be produced. Figure 4.6 shows the surface finish of polyurethane films produced with three dips in the 20% PCU solution, using two moulds with surface finish values of  $R_a = 0.853 \mu\text{m}$  and  $R_a = 0.158 \mu\text{m}$ , respectively.

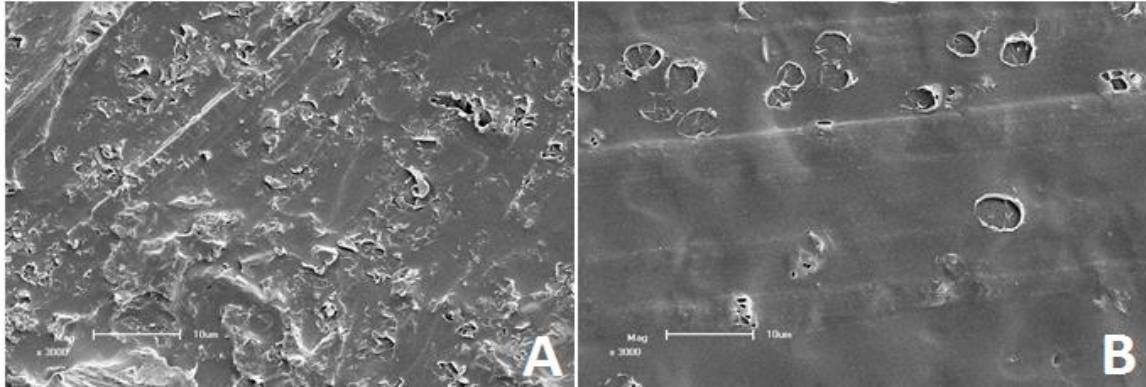


**Figure 4.6: SEM micrographs showing the variation of the surface topography of polyurethane films produced with two moulds of differing surface finish values (sense of scale 10 µm). (A):  $R_a = 0.853 \mu\text{m}$ , (B):  $R_a = 0.158 \mu\text{m}$**

It is clear from Figure 4.6 that there is a significant difference in the surface topography of the polyurethane films resulting from the different surface finishes of the two moulds. A mould with a surface finish better than  $R_a = 0.158 \mu\text{m}$  delivers films with satisfactory surface topography. However, as seen in Figure 4.6 B, some areas of the produced films still contained air bubbles. To avoid the formation of these air bubbles, the travelling speed of the mould during dip moulding must be properly controlled. Figure 4.7 shows the fracture surfaces of the polyurethane films produced with the three different PCU solutions as observed in the SEM.

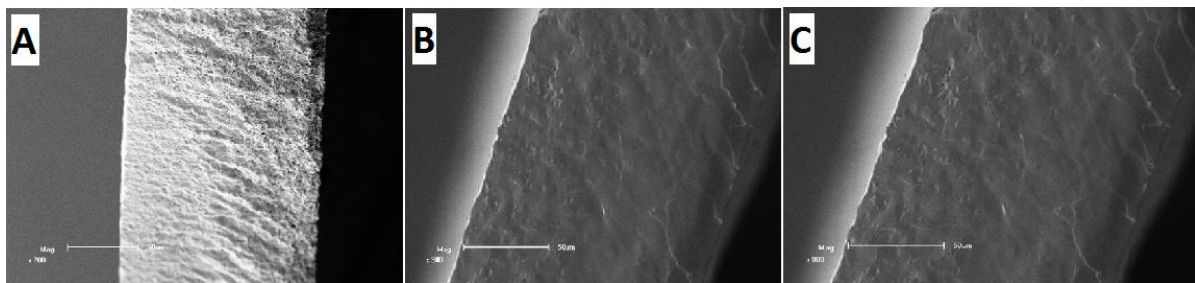


**Figure 4.7: SEM micrographs of the fracture surfaces of films produced with the three different PCU solutions at sense of scale 50 µm. (A): 35% solution, two dips, (B): 20% solution, three dips, (C): 15% solution, three dips.**

In Figure 4.7, no boundaries between layers formed through two or three repetitions of the dip-moulding process can be distinguished. This indicates a very thorough fusing of each new layer of polyurethane with the existing underlying layer. Multiple dipping to achieve required film thicknesses is therefore an acceptable practice. However, the fracture surface in Figure 4.7 A clearly differs from the other two and it was found to be due to porosity in this film. This resulted from air bubbles entrapped in the film during the dip moulding process. However, by increasing the temperature of the solution from 25 to 90°C, the air bubbles were completely eliminated.

#### 4.2.5. Mechanical properties of PCU film samples

The mechanical properties of the moulded PCU material were determined from the various film samples and are given in Table 4.4.

**Table 4.4: Mechanical properties determined for the films produced with the different PCU solutions and different numbers of dips.**

Type of sample	Thickness (µm)	Young's modulus (MPa)	Tensile strength (MPa)	Elongation (%)
35% solution 2 dips	167±79	12±1	10±2	862±276
35% solution 1 dip	46±11	37±9	37±5	417±23
20% solution 3 dips	92±6	29±5	18±4	662±226
20% solution 2 dips	49±2	35±4	37±8	341±110
15% solution 3 dips	53±4	30±4	35±7	699±102
15% solution 2 dips	27±3	28±8	19±5	307±138

It was expected that all the polyurethane film samples would break at their thinnest cross-sections, therefore the measured thickness values at point 4 (see Figure 3.5) were used

for all films as thicknesses for determining the mechanical properties of the samples. Among other factors, the physical performance of an artificial heart valve is assessed by the Young's modulus of the material used to produce it. The average Young's modulus of the film from three dips in the 20% solution is  $29 \pm 5$  MPa, which is below the value of 33 MPa that is the acceptable maximum Young's modulus for useful prosthetic heart valve leaflets [8]. The 35% solution was found to obtain a fairly lower average Young's modulus of 12 MPa.

#### **4.2.6. Recommended dip-moulding parameter set**

From the film thickness, topography, internal integrity and mechanical property results obtained in this study, it became apparent that a 20% PCU solution has the potential to provide polyurethane film properties that would be acceptable for producing heart valve leaflets. With this solution it appeared to be possible to obtain the required leaflet thickness with three, or at most, four dips during dip moulding.

### **4.3. Observation and Analysis of Phase 3 Results**

#### **4.3.1. Surface roughness measurement of the tri-leaflet mould**

The surface roughness of the tri-leaflet mould was measured after DMLS on the as-built surface and after application of the MMP technology on the mould surface areas shown in Figure 3.21. The application of the MMP technology displayed a smooth surface finish with an average  $R_a$  number of  $0.204 \mu\text{m}$ , compared to as-built DMLS surface with  $R_a$  number of  $11.34 \mu\text{m}$ , see Table 4.1.



**Table 4.5: Surface roughness of tri-leaflet mould after CNC machining and after MMP technique applied.**

Location	DMLS (as-built)			After MMP		
	R <sub>a</sub> (µm)	R <sub>t</sub> (µm)	R <sub>z</sub> (µm)	R <sub>a</sub> (µm)	R <sub>t</sub> (µm)	R <sub>z</sub> (µm)
Area 1	11.520	74.298	62.093	0.139	2.223	1.282
Area 2	10.335	71.453	58.890	0.165	4.794	2.389
Area 3	11.345	78.057	62.530	0.176	2.884	1.629
Area 4	12.58	75.741	67.181	0.337	10.088	3.078
Average	11.315	74.887	62.674	0.204	4.997	2.095
Standard deviation	0.720	2.763	3.415	0.09	3.564	0.802

In Figure 4.8 a graphical presentation of the measured surface roughness of the tri-leaflets mould is shown.

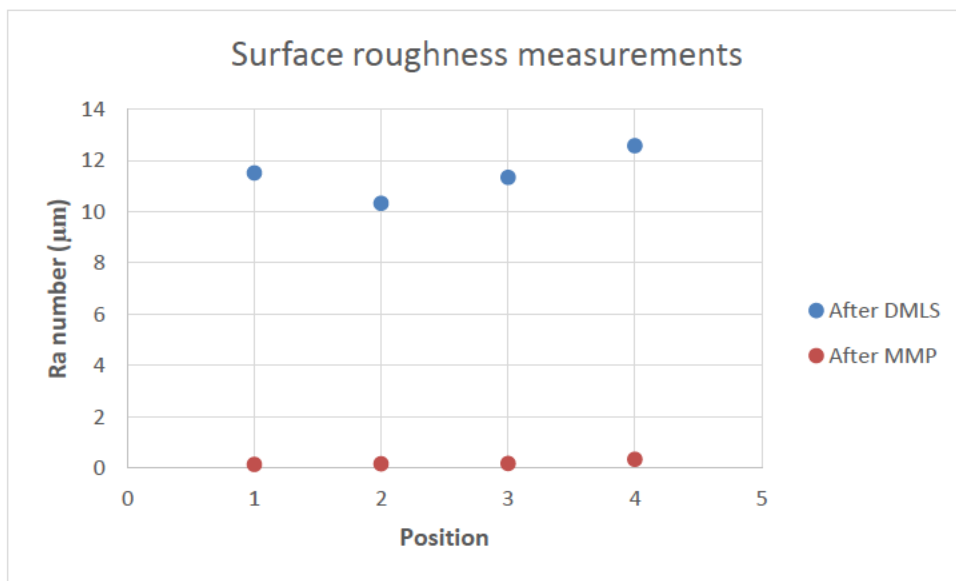


**Figure 4.8: Surface roughness measurements R<sub>a</sub> on tri-leaflet mould after DMLS (as-built) and MMP technology**

From Figure 4.8, a clear improvement of surface finish across all the surfaces was observed. The areas 1 and 2 are the most critical locations on the mould because the leaflets will form around them (refer to Figure 3.21). The average R<sub>a</sub> numbers at areas 1

and 2 are  $0.139\ \mu\text{m}$  and  $0.165\ \mu\text{m}$ , respectively (see Table 4.5), indicating a good surface finish produced from one surface to another. The Micro Machining Process technology demonstrated a consistent surface finish across all surfaces of the mould produced.

#### 4.3.2. Optimisation of dip moulding process parameters

Key parameters that have an influence on producing acceptable heart valve leaflets were assessed. These parameters included:

- The concentration of the polymer in the polymer-solvent solution,
- Dipping and withdrawal speed of the mould,
- Curing temperature,
- The number of dips.

Figure 4.9 shows the influence of each parameter on producing acceptable PCU heart valves. With three dips, the dipping speed was varied from 2 to 79 mm/min. The highest dipping speed was found to display a higher number of air bubbles (Figure 4.9 A) which consequently will lead to early failure of the valve. The lowest possible dipping speed (2 mm/min) resulted in significant elimination of air bubbles (Figure 4.9 C) for the first dip, however that speed did not completely eliminate them when a second or third dip was performed (see Figure 4.9 D and E). Figure 4.9 F shows a valve produced from a single dip with no air bubbles entrapped.

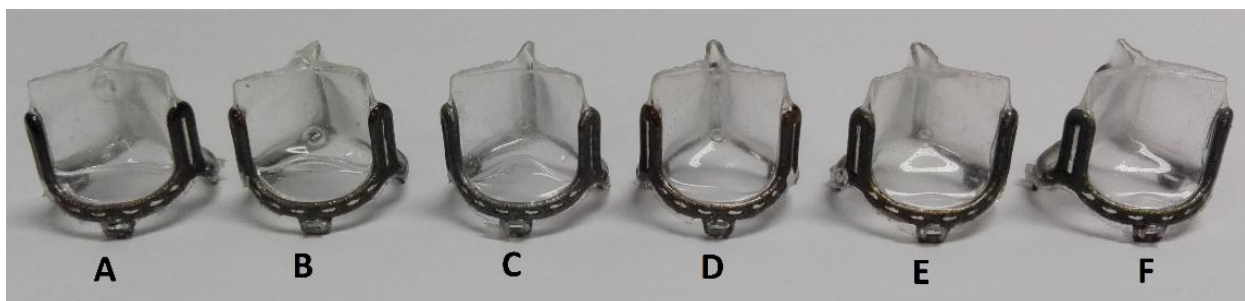


**Figure 4.9: Samples of the valves produced with different dip mould parameters.**

At room temperature, PC3595A granules were found partially dissolved in the DMAc solvent. When the temperature of both the mould and polymer solution was raised to 90°C, it was observed that a homogeneous solution was obtained. However, the preheating process of the mould and the solution resulted in about a 15% decrease of the resultant thickness of the heart valve leaflets, which was less than the minimum acceptable heart valve leaflet thickness.

To increase the thickness, the withdrawal speed was raised from 20 to 790 mm/min. This effect was also seen by other researchers [54][65]. Figure 4.10 shows a valve produced with a higher concentration of polymer-solution, when the mould and polymer solution were preheated at 90°C with a single dip at a lower dipping speed and a higher withdrawal speed.

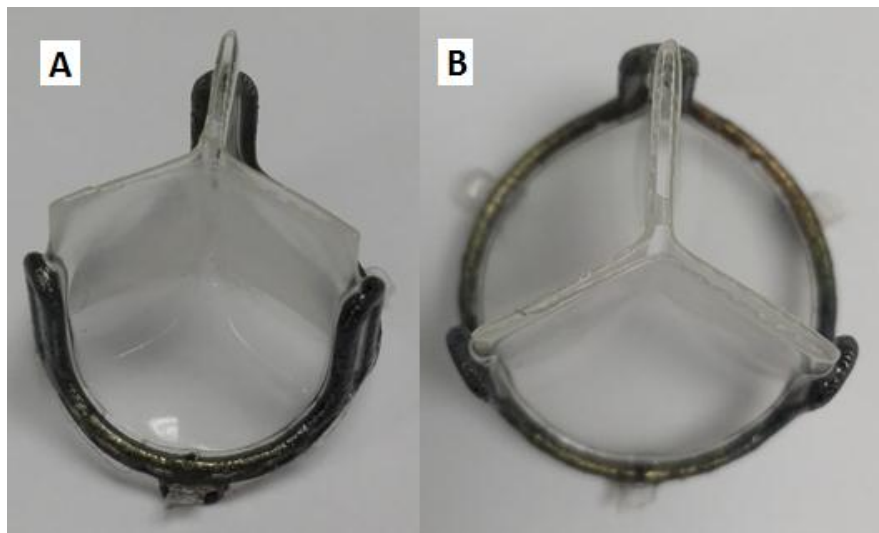


**Figure 4.10: Tri-leaflet PCU valve produced through the dip-moulding process without final trimming. (A): Side view of the valve, (B): Top view of the valve.**



### 4.3.3. Measurement of valve leaflet thickness

The thickness of the heart valve leaflets was measured at different locations on the leaflets, as indicated in Figure 3.23. These measured thicknesses are given in Table 4.6.

**Table 4.6: Thicknesses of the polyurethane leaflets in a high concentration polymer solvent solution.**

Measured location	1	3	2	4	5	7	6	8
Thickness ( $\mu\text{m}$ )	198 $\pm$ 16	173 $\pm$ 16	82 $\pm$ 9	89 $\pm$ 4	91 $\pm$ 20	95 $\pm$ 23	98 $\pm$ 6	85 $\pm$ 8

The ideal was to obtain thicknesses at locations 2 and 4 as well as at locations 5 and 7, with differences between each pair of not more than 10  $\mu\text{m}$ . From Table 4.6, it can be seen that this objective has been achieved. However, the measured thicknesses are less than 100  $\mu\text{m}$ , which is the minimum thickness required for durability of heart valve leaflets.

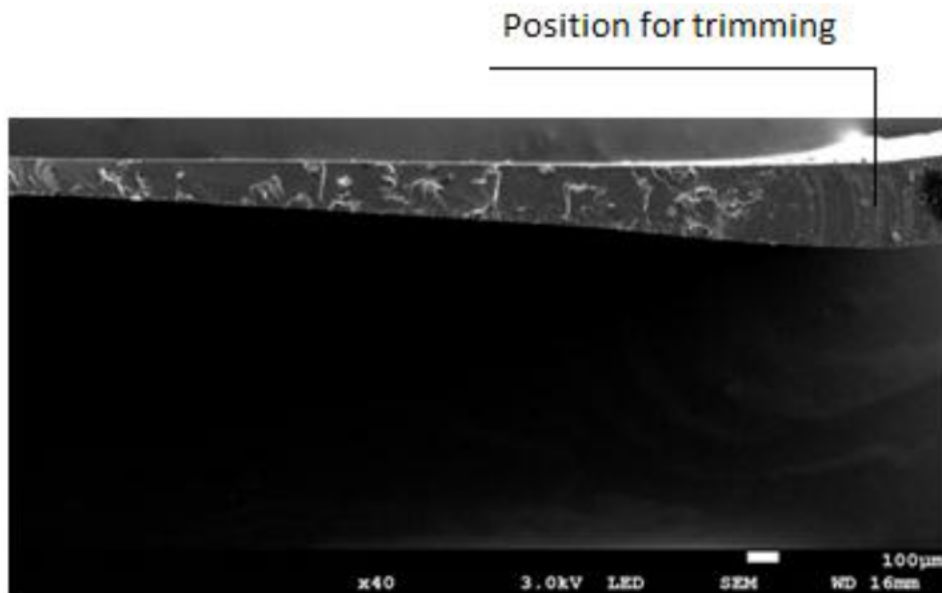


**Figure 4.11: A SEM micrograph of the leaflet fracture surface.**

Furthermore, the thickness measurements taken at locations 1 and 3 on the upper area of the tri-leaflet valve were greater than 150  $\mu\text{m}$ , which is the maximum thickness for good hydraulic functioning of the heart valve leaflets. However, in practice this area is eliminated by trimming it from the operational parts of the heart valve leaflets. The SEM was used to assess the variation of the thickness in the vertical direction (see Figure 4.11). The minimum thickness was found to be 76  $\mu\text{m}$  at the lowest edge of the heart valve leaflet while the maximum value was 249  $\mu\text{m}$  at the upper edge of the heart valve leaflet. This correlates with the previous findings where it was mentioned that the thickness varied linearly from lower edge with a minimum value to the upper edge with the maximum thickness.

#### **4.3.4. Surface topography of the valve leaflet**

It is desirable that both sides (the side facing the mould and the side facing away from the mould) of the leaflets have more or less the same surface topography. The mould that was used had six vertical flat- and three upper curved surfaces (Figure 3.23). It was observed that for all vertical flat- and curved surfaces, the leaflet sides facing away from the mould displayed more or less the same surface topography, see Figure 4.12 A & C. The same trend was also observed for the sides facing towards the mould (Figure 4.12 B & D). This indicated that the polishing technique of the flat vertical- and the curved surfaces produced the same quality of surface finish. However, the sides facing away from the mould (Figure 4.12 A & C) still displayed smoother surface topography than the sides facing towards the mould (Figure 4.12 B & D).

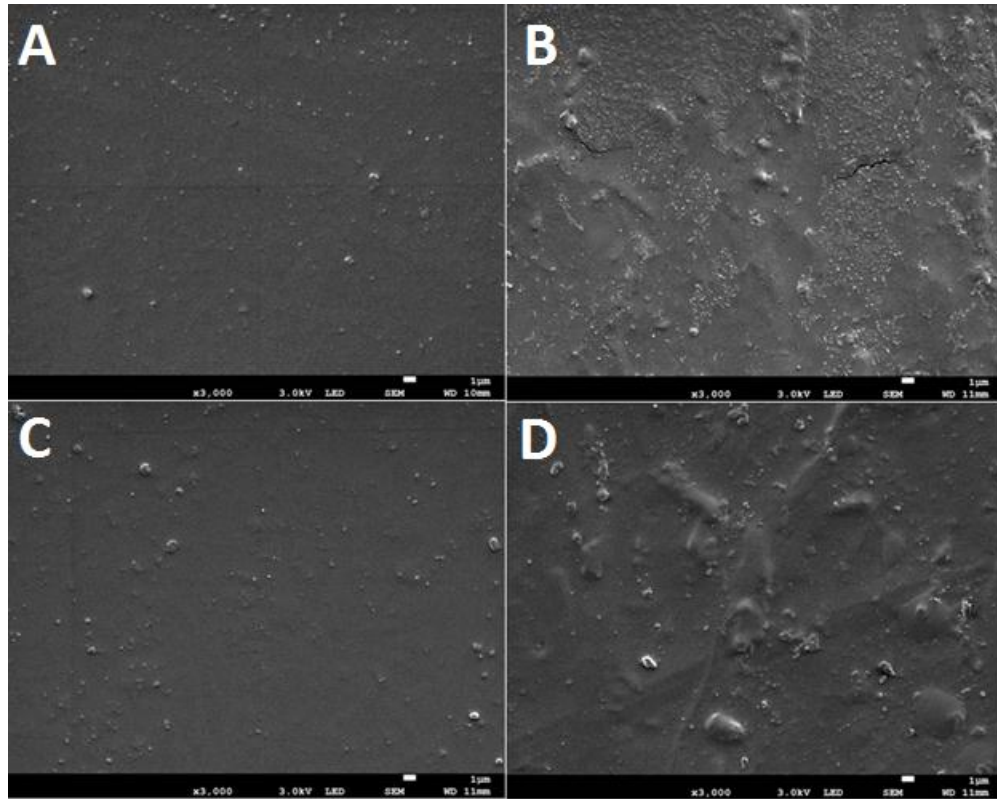


**Figure 4.12: SEM micrographs of the polyurethane leaflet surface topography for different mould faces. (A): Flat surface of the mould facing away from the mould, (B): Flat surface of the mould facing towards the mould, (C): Curved surface of the mould facing away from the mould, (D): Curved surface of the mould facing towards the mould.**

A cross-section of solidified typical polyurethane leaflet formed with the dip moulding method is shown in Figure 4.13. It can be observed that the high temperature of the solution (90°C) during the preheating stage of the dip moulding process, resulted in eliminating the air bubbles on the heart valve leaflets.

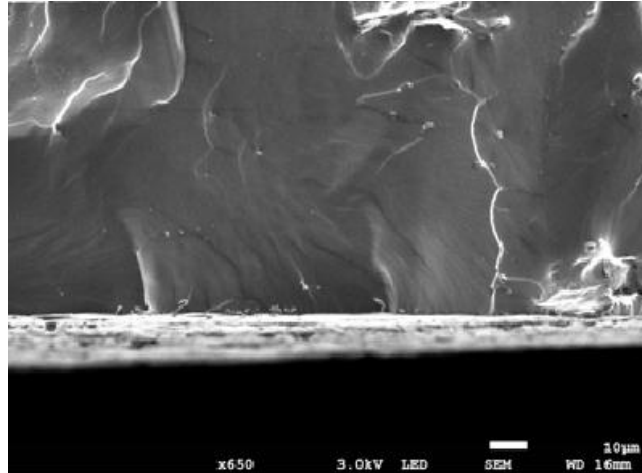


**Figure 4.13: SEM micrograph of the fracture surface of a leaflet produced with a single dip PCU solution.**

#### **4.3.5. Assessment of prototype PCU heart valves in a pulse duplicator machine**

Pulsatile hydrodynamic tests were performed in a pulse duplicator to acquire visual information and quantitative indicators of the fluid mechanical behaviour of the first prototype PCU valves manufactured through the dip moulding process. A video camera was used to capture the operational performance of the valve. Figure 4.14 shows a tri-leaflet polyurethane valve displaying the functionality of the valve during testing inside the pulse duplicator machine.

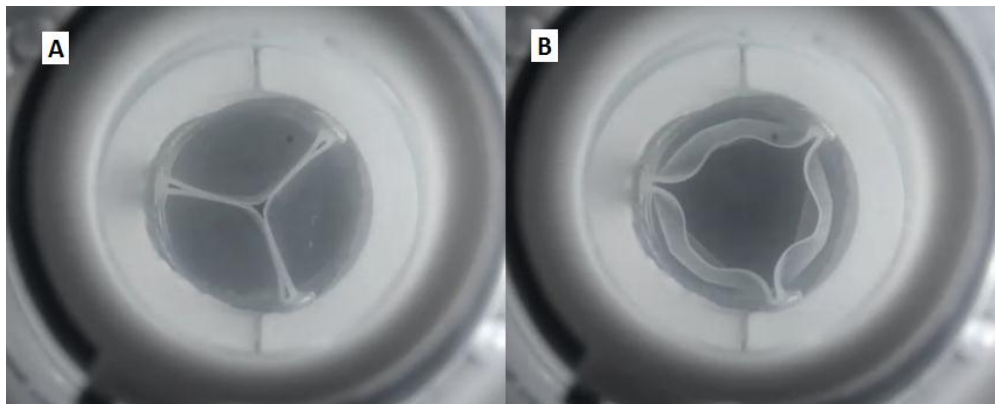


**Figure 4.14: Functioning of the polyurethane heart valve as captured on the pulse duplicator video, (A): Valve fully closed, (B): Valve fully opened.**

Table 4.7 gives a summary of the average pressure drop ( $\Delta P$ ), effective orifice area (EOA) which relates to the root mean square of the flow rate ( $Q_{rms}$ ) to pressure drop and the percentage regurgitation (reverse flow of fluid through the valve when closed) at a variety of conditions, ranging from 60 beats per minute (BPM) to 120 BPM, whilst varying the flow rate.

**Table 4.7: Pulse duplicator results obtained at different test conditions from three sets of PCU heart valves.**

Valve	Test Condition	BPM				
		60	70	80	100	120
1	$\Delta P$ (mmHg)	25.919	29.892	38.835	58.118	74.406
	EOA (cm <sup>2</sup> )	0.816	0.997	1.171	1.186	1.169
	Closing (nl)	-3.255	-4.979	-5.898	-5.419	-0.325
	Leakage (ml)	-22.578	-26.939	-24.845	-22.645	-28.487
	Regurgitation (%)	-43.2	-45.6	-38.4	-35.1	-36.2
2	$\Delta P$ (mmHg)	32.879	35.134	45.795	58.789	65.197
	EOA (cm <sup>2</sup> )	0.737	0.861	1.166	1.263	1.363
	Closing (nl)	-1.553	-3.395	-4.097	-4.283	-2.097
	Leakage (mℓ)	-3.528	-2.461	-2.104	-1.699	-3.077
	Regurgitation (%)	-8.5	-8.4	-7.8	-7.5	-6.5
3	$\Delta P$ (mmHg)	29.553	38.453	48.377	59.257	65.126
	EOA (cm <sup>2</sup> )	0.881	1.013	1.131	1.251	1.365
	Closing (nl)	-3.701	-4.969	-5.103	-4.627	-2.278
	Leakage (mℓ)	-1.166	-1.042	-0.816	-1.117	-2.046
	Regurgitation (%)	-8.1	-8.6	-7.4	-7.2	-5.41

From the high leakage volume data shown in Table 4.7, it is clear that there was an excessive gap between the frame and the sewing ring in valve 1. This gap allowed fluid to flow back while the valve was fully closed. The leakage volume of valve 2 is higher than valve 3, however both are extremely low. These effects were observed to have a direct impact on the percentage regurgitation (see Figure 4.15).

In order for blood to flow through a heart valve, there must be a force propelling the blood through the valve. This force is the difference in blood pressure across the valve (the pressure drop). At any given pressure drop, the flow rate is determined by the resistance to that flow. However, the percentage regurgitation is a good indicator of the functionality of the prototype heart valves. The percentage regurgitation across valve 1, 2 and 3 at different BPM in mmHg is shown in Figure 4.15. This is the combination of the closing and leakage volume expressed as a percentage of the stroke volume.

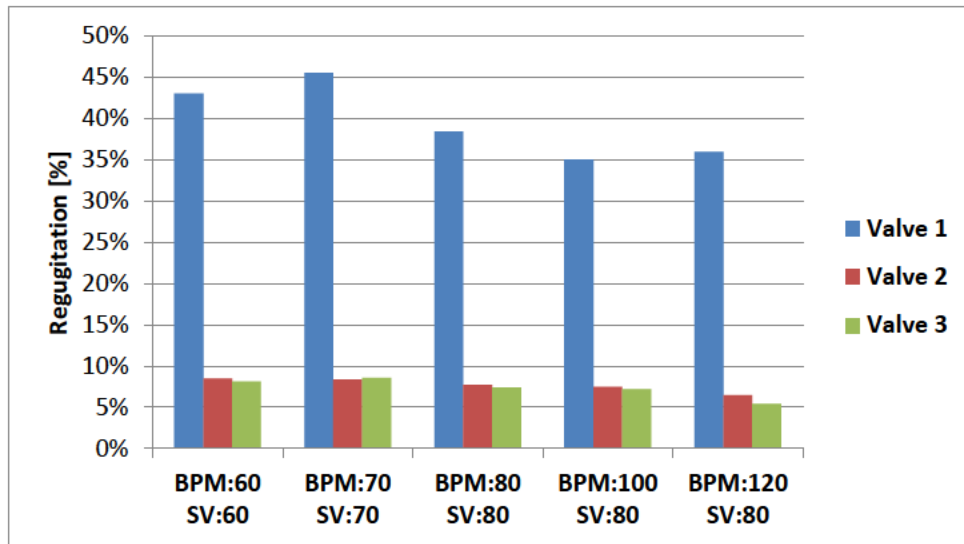


**Figure 4.15: Percentage regurgitation of three prototypes valves for different beats per minute.**

The low percentage regurgitation from valve 2 and valve 3 indicates both valves were completely closed, not allowing the liquid to flow back through the valve. The marginally small difference between these two could be due to the (i) slightly different position of the sewing ring, (ii) tightness of the stitching and (iii) amount of material placed around the sewing ring in the fitting to reduce leakage. However, according to the requirements of the ISO 5840 standard, the percentage regurgitation must be below 10%, which is met by both valve 2 and valve 3.

EOA, which incorporates both flow rate and pressure drop data, is defined by the Gorlin equation as [66]:

$$EOA = \frac{Q_{rms}}{51.6 * \sqrt{\frac{\Delta P}{\rho}}}$$

which shows the relationship between the root mean square ( $Q_{rms}$ ) of the flow rate and pressure drop. Figure 4.16 shows the comparison of the EOA for valve 1, valve 2 and valve 3 at five different BPM. From the pulse duplicator data it became apparent that a significant gap around the valve 1 frame and sewing ring affected the results of the  $Q_{rms}$ , which had an impact on the measured EOA values of valve 1. The comparison of valve 2 with valve 3 gave unexpected EOA results, because valve 2 performed worse than valve 3 for the first two testing conditions, while valve 3 performed better than valve 2 for the last three testing conditions. It was expected that valve 2 would outperform valve 3 on the EOA due to its slightly thinner leaflets that should allow easier opening of the valve. For this study, the long- term project plan was followed until Phase 3; however, preliminary performance data of the first prototypes were obtained. This anomaly should be further investigated leading to Phase 4 of this long-term project (see Figure 3.1).

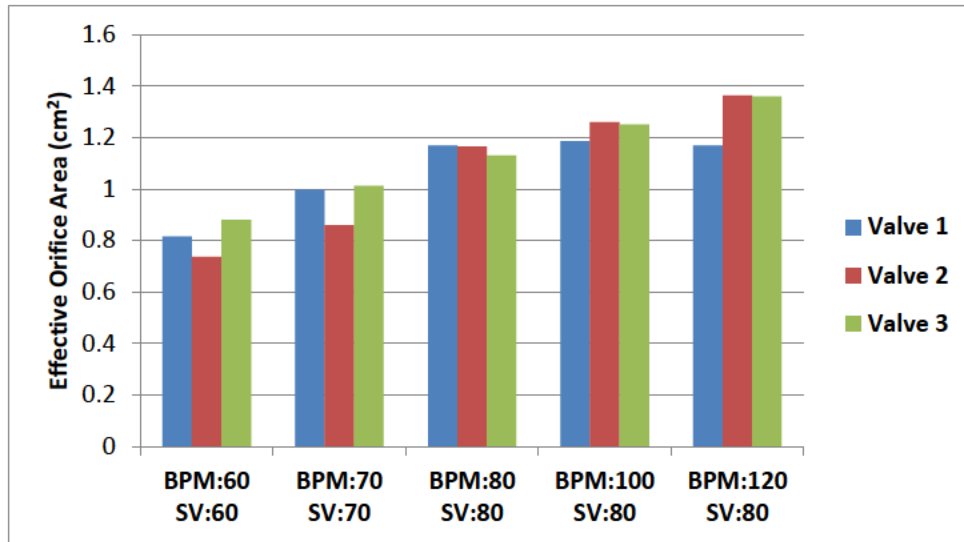


**Figure 4.16: Effective Orifice Area.**

For the valve size that was tested, the minimum EOA needs to be 0.85 cm<sup>2</sup> according to ISO Standard 5840. As observed in Figure 4.16, there are some conditions for which the valves do not meet this criterion. However, since these were only the first prototype valves produced through the process developed in this study, their performance was quite satisfactory with a correlation of 80% or more compared to ISO standard.



## CHAPTER 5: CONCLUSIONS AND FUTURE WORK

---

### 5.1. Conclusions

An optimally designed and manufactured polymer heart valve that would ideally be free from calcification, require no anticoagulation, function silently with a longevity that exceeds the biological valves is in high demand in cardiology. Medical grade segmented polyurethane has been successfully applied in various cardiovascular devices. However, more research has been performed on PCU which has shown the potential of manufacturing heart valves with excellent mechanical properties and biostability.

Experimental equipment and facilities to determine the dip moulding process variables that resulted in producing controllable and reproducible polyurethane films were successfully established. Through application of a reverse engineering technique, existing human heart valve leaflet geometry was converted to a CAD model. The complex leaflet mould with different curvatures in the circumferential and radial directions was manufactured through additive manufacturing in Ti6Al4V (ELI), a high strength, fatigue-resistant, biocompatible alloy.

A set of dip moulding parameters and a procedure which resulted in the successful production of prototype polymer heart valves was obtained through this research. From the results obtained, it was demonstrated that valves meeting the thickness requirements and also showing excellent surface topography without air bubbles could be produced by a relatively low dipping speed with a uniformly polished mould. It was shown that with a polyurethane solution concentration varying between 20 and 30%, a single dip could produce a tri-leaflet heart valve with leaflet thickness varying from 76 to 249  $\mu\text{m}$  in different locations on the heart valve leaflet.

The valves displayed good opening and closing performance, mimicking the behaviour of natural valves in pulse duplicator tests. Measured against the ISO 5840 standard, certain valves exceeded the minimum EOA performance requirements by obtaining values larger than  $0.85 \text{ cm}^2$  for corresponding pulsatile-flow conditions of 70, 80, 100 and 120 BPM. Altogether, the hydrodynamic assessment presented in this study indicates that tri-leaflet heart valves produced through dip moulding would make an attractive alternative to the tissue and mechanical heart valves currently used.

The correlation between the PCU tri-leaflet valve performance and ISO standard requirements was found to be 80% or even better. Therefore, this study has confirmed that the long-term goal of producing a fully functional, durable, and cost-effective heart valve, capable of regulating the one-way flow of blood through the heart valve, is indeed achievable. It has also gone a long way towards establishing a joint competence between CUT's CRPM and UFS's Robert WM Frater Cardiovascular Research Centre to produce affordable polyurethane heart valves suitable for the populations of emerging and developing countries.

## **5.2. Future Work**

Future work should focus on Phase 4 shown in Figure 3.1. This would entail pulse duplicator and fatigue tests of additional prototype polyurethane heart valves to obtain data that would confirm acceptable hemodynamic and life performance in conformance with regulatory authorities.

During Phase 4, the design of the PCU valve should be further improved. These design changes would improve the performance of the valve further, which would require further pulse duplicator tests to confirm the improvement.

Once the valve performance has been optimised, biological trials in animals will follow. If these are successful, the valve can be used in clinical trials.

## LIST OF REFERENCES

---

- [1] G. D. Baura, "Heart Valves," *Med. Device Technol. A Syst. based Overv. Using Eng. Stand.*, pp. 121–145, 2012.
- [2] H. Dean, "Development of Biopoly<sup>®</sup> materials for use in prosthetic heart valve replacements," 2012.
- [3] T. Korakianitis and Y. Shi, "Numerical simulation of cardiovascular dynamics with healthy and diseased heart valves," *J. Biomech.*, vol. 39, pp. 1964–1982, 2006.
- [4] D. Williams, David, Wheatley, "(12) United States Patent," vol. 1, no. 12, 2001.
- [5] D. Bezuidenhout, D. F. Williams, and P. Zilla, "Biomaterials polymeric heart valves for surgical implantation, catheter-based technologies and heart assist devices," *Biomaterials*, vol. 36, pp. 6–25, 2015.
- [6] M. S. Sacks, W. D. Merryman, and D. E. Schmidt, "On the biomechanics of heart valve function," *J. Biomech.*, vol. 42, no. 12, pp. 1804–1824, 2009.
- [7] H. Mohammadi and K. Mequanint, "Prosthetic aortic heart valves: Modeling and design," *Med. Eng. Phys.*, vol. 33, no. 2, pp. 131–147, 2011.
- [8] G. M. Bernacca, B. O'Connor, D. F. Williams, and D. J. Wheatley, "Hydrodynamic function of polyurethane prosthetic heart valves: Influences of Young's modulus and leaflet thickness," *Biomaterials*, vol. 23, pp. 45–50, 2002.
- [9] H. Leo, H. Simon, J. Carberry, S. Lee and A. Yoganathan, "A comparison of flow field structures of two tri-leaflet polymeric heart valves," vol. 33, no. 4, pp. 429–443, 2005.
- [10] T. Watch, "Heart valves, structural heart and endograft technologies Table of Contents," *J. Am. Coll. Cardiol.*, vol. 1, pp. 1–28, 2017.
- [11] M. Helmus and C. Cunanan, "Mechanical and bioprosthetic heart valves: anticoagulant therapy," *Biomater. Artif. Organs*, pp. 2–4, 2015.
- [12] M. S. Sacks and A. P. Yoganathan, "Heart valve function: a biomechanical perspective," *Philos. Trans. R. Soc. Lond. B. Biol. Sci.*, vol. 362, no. 1484, pp. 1369–91, 2007.
- [13] M.J. Blaha, S.E. Chiuwe, M. Cushman, R. Deo, D.M. Lloyd-Jones, E. J. Benjamin, J. D. Berry, "Heart Disease and Stroke Statistics," *Circulation*, vol. 125, pp. e2--e225, 2017.

- [14] C. American Heart Association Statistics, *Heart Disease and Stroke Statistics 2009 Update: A Report from the American Heart Association Statistics Committee and Stroke Statistics Subcommittee*, vol. 119, no. 71, 2009.
- [15] D. Bezuidenhout, D. F. Williams, and P. Zilla, "Polymeric heart valves for surgical implantation, catheter-based technologies and heart assist devices," *Biomaterials*, vol. 36, pp. 6–25, 2015.
- [16] A. Kheradvar, E. M. Groves, L. P. Dasi, H. S. Alavi, R. Tranquillo, J. K. Grande-Allen, C. A. Simmons, B. Griffith, A. Falahatpisheh, J. Georgen, M. Mafrad, F. Baaijens, S. H. Little, and S. Cain, "Emerging trends in heart valve engineering: Part 1. Solution for future," *Ann. Biomed. Eng.* 43(4), vol. 28, pp. 63–86, 2014.
- [17] V. Tarzia, T. Bottio, L. Testolin, and G. Gerosa, "Extended (31 years) durability of a Starr-Edwards prosthesis in mitral position," *Interact. Cardiovasc. Thorac. Surg.*, vol. 6, pp. 570–571, 2007.
- [18] P. Pibarot and J. G. Dumesnil, "Prosthetic heart valves: Selection of the optimal prosthesis and long-term management," *Circulation*, vol. 119, no. C, pp. 1034–1048, 2009.
- [19] J. H. Chesebro, P. C. Adams, and V. Fuster, "Antithrombotic therapy in patients with valvular heart disease and prosthetic heart valves," *J. Am. Coll. Cardiol.*, vol. 8, no. 6, p. 41B–56B, 1986.
- [20] P. Pibarot and J. G. Dumesnil, "Prosthetic heart valves: Selection of the optimal prosthesis and long-term management," *Circulation*, vol. 119, no. 7, pp. 1034–1048, 2009.
- [21] R. O. Bonow, B. A. Carabello, K. Chatterjee, A. C. de Leon, D. P. Faxon, M. D. Freed, W. H. Gaasch, B. W. Lytle, R. A. Nishimura, P. T. O’Gara, R. A. O’Rourke, C. M. Otto, P. M. Shah, J. S. Shanewise, S. C. Smith, A. K. Jacobs, C. D. Adams, J. L. Anderson, E. M. Antman, V. Fuster, J. L. Halperin, L. F. Hiratzka, S. A. Hunt, B. W. Lytle, R. Nishimura, R. L. Page and B. Riegel, "ACC/AHA 2006 Guidelines for the management of patients with valvular heart disease," *J. Am. Coll. Cardiol.*, vol. 48, no. 3, pp. e1–e148, 2006.
- [22] A. Vahanian, O. Alfieri, F. Andreotti, M.J. Antunes, G. Barón-Esquivias, H. Baumgartner, M.A. Borger, T.P. Carrel, M. De Bonis, A. Evangelista, V. Falk, B. Lung, P. Lancellotti, L. Pierard, S. Price, H.J. Schäfers, G. Schuler, J. Stepinska, K. Swedberg, U.O. Von Oppell, S. Windecker and J.L. Zamorano, "Guidelines on the management of valvular heart disease (version 2012)," *Circulation*, no. version, pp. 0–1, 2013.
- [23] M. M. Miller, R. Hipp, and M. E. Matsumura, "Freedom from complications related to dual ball-and-cage mechanical valve prostheses despite thirty years without

- anticoagulation," *Interact. Cardiovasc. Thorac. Surg.*, vol. 7, no. 6, pp. 1167–9, 2008.
- [24] F. J. Schoen and R. J. Levy, "Tissue heart valves: current challenges and future research perspectives," *Found.'s Award, 25th Annu. Meet. Soc. Biomater., Provid., RI, April 28 – May 2, 1999*, pp. 439–465, 1999.
- [25] M. Heras, J. H. Chesebro, V. Fuster, W. J. Penny, D. E. Grill, K. R. Bailey, G. K. Danielson, T. A. Orszulak, J. R. Pluth, F. J. Puga, H. V. Schaff, and J. J. Larsonkeller, "High risk of thromboemboli early after bioprosthetic cardiac valve replacement," *J. Am. Coll. Cardiol.*, vol. 25, no. 5, pp. 1111–1119, 1995.
- [26] J. H. Chesebro, P. C. Adams, and V. Fuster, "Antithrombotic therapy in patients with valvular heart disease and prosthetic heart valves," *J. Am. Coll. Cardiol.*, vol. 8, no. 6, p. 41B–56B, 1986.
- [27] N. Piazza, S. Bleiziffer, G. Brockmann, R. Hendrick, M. A. Deutsch, A. Opitz, D. Mazzitelli, P. Tassani-Prell, C. Schreiber, and R. Lange, "transcatheter aortic valve implantation for failing surgical aortic bioprosthetic valve: From concept to clinical application and evaluation (Part 1)," *JACC Cardiovasc. Interv.*, vol. 4, no. 7, pp. 721–732, 2011.
- [28] M. S. Bettadapur, B. P. Griffin, and C. R. Asher, "Caring for patients with prosthetic heart valves," *Cleve. Clin. J. Med.*, vol. 69, no. 1, pp. 75–87, 2002.
- [29] F. J. Schoen and R. J. Levy, "Calcification of tissue heart valve substitutes: Progress toward understanding and prevention," *Ann. Thorac. Surg.*, vol. 79, no. 3, pp. 1072–1080, 2005.
- [30] J. Chikwe, Y. P. Chiang, N. N. Egorova, S. Itagaki, and D. H. Adams, "Survival and outcomes following bioprosthetic vs mechanical mitral valve replacement in patients aged 50 to 69 years," *Jama*, vol. 313, no. 14, p. 1435, 2015.
- [31] P. Stassano, L. Di Tommaso, M. Monaco, F. Iorio, P. Pepino, N. Spampinato, and C. Vosa, "Aortic valve replacement. A prospective randomized evaluation of mechanical versus biological valves in patients ages 55 to 70 years," *J. Am. Coll. Cardiol.*, vol. 54, no. 20, pp. 1862–1868, 2009.
- [32] C. Otto, J. Kuusisto, D. Reichenbach, A Gown, and K. Obrien, "Characterization of the early lesion of degenerative valvular aortic-stenosis – histological and immunohistochemical studies," *Circulation*, vol. 90, pp. 844–853, 1994.
- [33] C.J. Haug, M.P. Kieny, and B. Murgue, "The New England Journal of Medicine," *Perspective*, vol. 363, no. 1, pp. 1–3, 2010.
- [34] B. Rahmani, S. Tzamtzis, H. Ghanbari, G. Burriesci, and A. M. Seifalian, "Manufacturing and hydrodynamic assessment of a novel aortic valve made of a new nanocomposite

- polymer,” *J. Biomech.*, vol. 45, no. 7, pp. 1205–1211, 2012.
- [35] S.H. Daebritz, J.S. Sachweh, B. Hermanns, B. Fausten, F. Andreas, J. Groetzner, B. Klosterhalfen and B.J.Messmer, “Introduction of a flexible polymeric heart valve prosthesis with special design for mitral position,” *Circulation*, vol. 108, p. 134II–139, 2003.
- [36] G. M. Bernacca, T. G. Mackay, R. Wilkinson, and D. J. Wheatley, “Calcification and fatigue failure in a polyurethane heart valve,” *Biomaterials*, vol. 16, no. 4, pp. 279–285, 1995.
- [37] M. Rozeik, D. Wheatley, and T. Gourlay, “The aortic valve: structure, complications and implications for transcatheter aortic valve replacement,” *Perfusion*, vol. 29, pp. 285–300, 2014.
- [38] E. Di Martino, R. Pietrabissa, and S. Mantero, “The computational approach applied to the design and structural verification of a trileaflet polymeric heart valve,” *Adv. Eng. Softw.*, vol. 28, no. 6, pp. 341–346, 1997.
- [39] G. M. Bernacca, B. O. Connor, D. F. Williams, and D. J. Wheatley, “Hydrodynamic function of polyurethane prosthetic heart valves: influences of Young ’s modulus and leaflet thickness,” *Biomaterials*, vol. 23, pp. 45–50, 2002.
- [40] H. Ghanbari, H. Viatge, A. G. Kidane, G. Burriesci, M. Tavakoli, and A. M. Seifalian, “Polymeric heart valves: new materials, emerging hopes,” *Trends Biotechnol.*, vol. 27, no. May, pp. 359–367, 2009.
- [41] M. Kütting, J. Roggenkamp, U. Urban, T. Schmitz-Rode, and U. Steinseifer, “Polyurethane heart valves: past, present and future,” *Expert Rev. Med. Devices*, vol. 8, no. 2, pp. 227–233, 2011.
- [42] S. H. Daebritz, “Introduction of a flexible polymeric heart valve prosthesis with special design for mitral position,” *Circulation*, vol. 108, no. 90101, p. 134-139, 2003.
- [43] F. De Gaetano, M. Serrani, P. Bagnoli, J. Brubert, J. Stasiak, G. D. Moggridge, and M. L. Costantino, “Fluid dynamic characterization of a polymeric heart valve prototype (Poli-Valve) tested under continuous and pulsatile flow conditions,” *Int. J. Artif. Organs*, vol. 38, no. 11, pp. 600–606, 2015.
- [44] D. J. Wheatley, J. Fisher and D. Williams, “(12) United States Patent,” vol. 1, no. 12, 2001.
- [45] S.-J. Liu, *Manufacturing techniques for polymer matrix composites (PMCs)*. Woodhead Publishing Limited, 2012.
- [46] J. George and P. E. D. Vargot, “Method and apparatus for injection-compression & ejecting paired thermoplastic spectacle lens suited for fully automated dip hardcoating,”

- 1998.
- [47] S. A. Ashter, “*Thermoforming of Single and Multilayer Laminates*,” Hanser Verlag, 2014.
- [48] P. D. Yee Han Kuan, “Division of Bioengineering, National University of Singapore  
Department of Mechanical Engineering, Colorado State University Wallace H. Coulter  
Department of Biomedical Engineering, Georgia Institute of Technology,” 2008.
- [59] K. R. M. Mackey, J. J. Morris, F. M. M. Morel, and S. A. Kranz, “Previously published works  
UC Irvine,” *Oceanography*, vol. 28, pp. 63–86, 2012.
- [50] T. G. Mackay, D. J. Wheatley, G. M. Bernacca, A. C. Fisher, and C. S. Hindle, “New  
polyurethane heart valve prosthesis: Design, manufacturing and evaluation,”  
*Biomaterials*, vol. 17, no. 19, pp. 1857–1863, 1996.
- [51] C. Strobel, A. Kadow-Romacker, T. Witascheck, G. Schmidmaier, and B. Wildemann,  
“Evaluation of process parameter of an automated dip-coating,” *Mater. Lett.*, vol. 65, no.  
23–24, pp. 3621–3624, 2011.
- [52] C. Jones, I. D. MacKnight, M. Hujar and B. Steere, “Dip molding,” Tool and Manufacturing  
Engineers Handbook knowledge base, Chapter 15, pp 554-664, 1998.
- [53] S. Aydemir, “Effects of withdrawal speed on the microstructural and optical properties of  
sol-gel grown ZnO:Al thin films,” *Vacuum*, vol. 120, pp. 51–58, 2015.
- [54] H. Jiang, G. Campbell, D. Boughner, W. K. Wan, and M. Quantz, “Design and manufacture  
of a polyvinyl alcohol (PVA) cryogel tri-leaflet heart valve prosthesis,” *Med. Eng. Phys.*,  
vol. 26, pp. 269–277, 2004.
- [55] M. Ando and Y. Takahashi, “Trileaflet polytetrafluoroethylene valved conduit for  
pulmonary reconstruction,” *Oper. Tech. Thorac. Cardiovasc. Surg.*, vol. 16, no. 3, pp. 168–  
178, 2011.
- [56] M. R. Labrosse, C. J. Beller, F. Robicsek, and M. J. Thubrikar, “Geometric modeling of  
functional trileaflet aortic valves: Development and clinical applications,” *J. Biomech.*,  
vol. 39, no. 14, pp. 2665–2672, 2006.
- [57] M. Shellabear and O. Nyrrhilä, “DMLS – Development history and state of the art,” *Lane  
2004*, pp. 1–12, 2004.
- [58] Royal Academy of Engineering, “Additive Manufacturing: Opportunities and Constraints,”  
*R. Acad. Eng.*, no. May 2013, p. 21, 2013.
- [59] W. Gao, Y. Zhang, D. Ramanujan, K. Ramani, Y. Chen, C. B. Williams, C. C. L. Wang, Y. C.  
Shin, S. Zhang, and P. D. Zavattieri, “The status, challenges, and future of additive



- manufacturing in engineering,” *Comput. Des.*, vol. 69, pp. 65–89, 2015.
- [60] S. Mellor, L. Hao, and D. Zhang, “Additive manufacturing: A framework for implementation,” *Int. J. Prod. Econ.*, vol. 149, pp. 194–201, 2014.
- [61] M. Baumers, P. Dickens, C. Tuck, and R. Hague, “The cost of additive manufacturing: Machine productivity, economies of scale and technology-push,” *Technol. Forecast. Soc. Change*, vol. 102, pp. 193–201, 2016.
- [62] U. Karabiyik, M. Mao, S. K. Satija, and A. R. Esker, “Determination of thicknesses and refractive indices of polymer thin films by multiple incident media ellipsometry,” *Thin Solid Films*, vol. 565, pp. 72–78, 2014.
- [63] P. Lemoine, J. P. Quinn, P. D. Maguire, and J. A. D. Mclaughlin, “Measuring the thickness of ultra-thin diamond-like carbon films,” vol. 44, pp. 2617–2624, 2006.
- [64] J. Brinker and D. P. Birnie III, “Chemical solution deposition of functional oxide thin films,” *Chem. Solut. Depos.*, pp. 233–261, 2013.
- [65] N. Saikrishnan, C. H. Yap, S. Lerakis, G. Kumar, and A. P. Yoganathan, “Revisiting the Gorlin equation for aortic stenosis - Is it correctly used in clinical practice?,” *Int. J. Cardiol.*, vol. 168, no. 3, pp. 2881–2883, 2013.